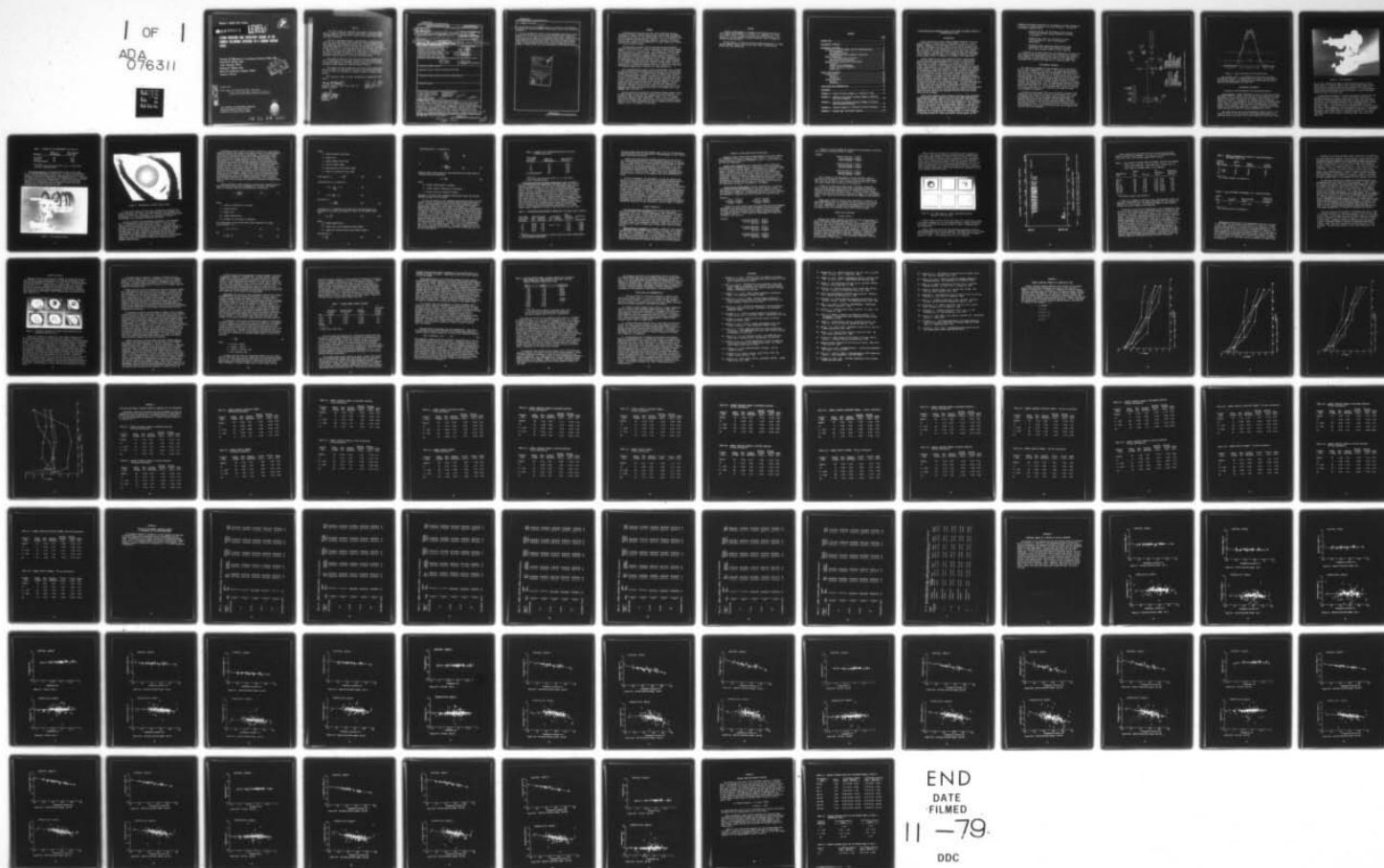


AD-A076 311

SCHOOL OF AEROSPACE MEDICINE BROOKS AFB TX
F/6 6/18
LESION DURATION AND CURVATURE CHANGE IN THE CORNEA FOLLOWING EX--ETC(U)
OCT 79 G W MIKESELL, E O RICHEY, J TABOADA
UNCLASSIFIED SAM-TR-79-26

NL

1 OF 1
ADA
076311



Report SAM-TR-79-26

A076311

LEVEL

PS.

**LESION DURATION AND CURVATURE CHANGE IN THE
CORNEA FOLLOWING EXPOSURE TO A CARBON DIOXIDE
LASER**

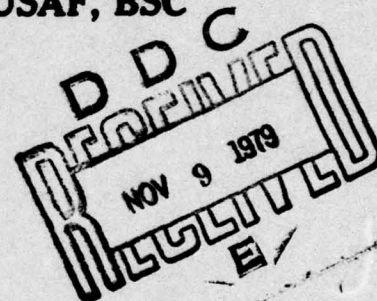
**George W. Mikesell, Jr., Lieutenant Colonel, USAF, BSC
Everett O. Richey, M.S.**

John Taboada, Ph.D.

Richard C. McNee, M.S.

Bruce R. Anderson, Captain, USAF

James L. Bower



DDC FILE COPY

October 1979

Final Report for Period July 1976 - June 1978

Approved for public release; distribution unlimited.

**USAF SCHOOL OF AEROSPACE MEDICINE
Aerospace Medical Division (AFSC)
Brooks Air Force Base, Texas 78235**



79 11 08 020

NOTICES


This final report was submitted by personnel of the Laser Effects Branch, Radiation Sciences Division, USAF School of Aerospace Medicine, Aerospace Medical Division, AFSC, Brooks Air Force Base, Texas, under job order 7757-02-52.

When U.S. Government drawings, specifications, or other data are used for any purpose other than a definitely related Government procurement operation, the Government thereby incurs no responsibility nor any obligation whatsoever; and the fact that the Government may have formulated, furnished, or in any way supplied the said drawings, specifications, or other data is not to be regarded by implication or otherwise, as in any manner licensing the holder or any other person or corporation, or conveying any rights or permission to manufacture, use or sell any patented invention that may in any way be related thereto.

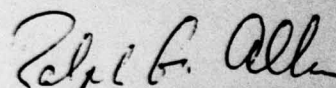
The animals involved in this study were procured, maintained, and used in accordance with the Animal Welfare Act of 1970 and the "Guide for the Care and Use of Laboratory Animals" prepared by the Institute of Laboratory Animal Resources - National Research Council.

This report has been reviewed by the Office of Public Affairs (PA) and is releasable to the National Technical Information Service (NTIS). At NTIS, it will be available to the general public, including foreign nations.

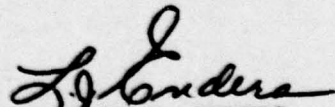
This technical report has been reviewed and is approved for publication.



GEORGE W. MIKESELL, JR., Lt Col, USAF, BSC
Project Scientist



RALPH G. ALLEN, Ph.D.
Supervisor



LAWRENCE J. ENDERS
Colonel, USAF, MC
Commander

UNCLASSIFIED

SECURITY CLASSIFICATION OF THIS PAGE (When Data Entered)

REPORT DOCUMENTATION PAGE		READ INSTRUCTIONS BEFORE COMPLETING FORM
1. REPORT NUMBER 14 SAM-TR-79-26	2. GOVT ACCESSION NO.	3. RECIPIENT'S CATALOG NUMBER
4. TITLE (and Subtitle) 6 LESION DURATION AND CURVATURE CHANGE IN THE CORNEA FOLLOWING EXPOSURE TO A CARBON DIOXIDE LASER	5. TYPE OF REPORT & PERIOD COVERED 9 Final Report July 1976 - June 1978	
7. AUTHOR(s) 10 George W. Mikesell, Jr., Lt Col, USAF, DSC; Everett O. Richey, Jr.; John Taboada, PhD; Richard C. McNee, MS; Dr. R. Anderson, Capt, USAF; J. Bower	8. CONTRACT OR GRANT NUMBER(s) McNee Bruce R. Anderson	
9. PERFORMING ORGANIZATION NAME AND ADDRESS USAF School of Aerospace Medicine (RZL) Aerospace Medical Division (AFSC) Brooks Air Force Base, Texas 78235	10. PROGRAM ELEMENT, PROJECT, TASK AREA & WORK UNIT NUMBERS 62202F 16 7757487-52	
11. CONTROLLING OFFICE NAME AND ADDRESS USAF School of Aerospace Medicine (RZL) Aerospace Medical Division (AFSC) Brooks Air Force Base, Texas 78235	12. REPORT DATE 11 October 1979	
14. MONITORING AGENCY NAME & ADDRESS (if different from Controlling Office) 12 93	13. NUMBER OF PAGES 89	
15. SECURITY CLASS. (of this report) Unclassified		15a. DECLASSIFICATION/DOWNGRADING SCHEDULE
16. DISTRIBUTION STATEMENT (of this Report) Approved for public release; distribution unlimited.		
17. DISTRIBUTION STATEMENT (of the abstract entered in Block 20, if different from Report)		
18. SUPPLEMENTARY NOTES		
19. KEY WORDS (Continue on reverse side if necessary and identify by block number) Corneal damage threshold Thermokeratoplasty Corneal injury assessments Orthokeratology Laser radiation Ophthalmology Laser safety standards <i>lambda</i> Carbon dioxide laser <i>sigma</i> <i>sgcm</i>		
20. ABSTRACT (Continue on reverse side if necessary and identify by block number) The corneas of Dutch belted rabbits were exposed for 0.5 sec to the radiation from a carbon dioxide laser ($\lambda = 10.6 \mu\text{m}$) emitting a Gaussian beam with a 1/e radius of $r = \sigma = 2.65 \text{ mm}$ at the corneal plane. The 1/e radiant exposure required for a 50% probability (ED_{50}) of producing a minimum visible lesion within 30 minutes postexposure was 4.71 J/cm^2 . The 1/e radiant exposure is the incident beam energy delivered in 0.5 sec divided by the area of a circle of radius $r = 2.65 \text{ mm}$, the beam radius at the 1/e point. Corneas with lesions resulting from suprathreshold exposures were examined at specified intervals for		

DD FORM 1 JAN 73 1473 EDITION OF 1 NOV 65 IS OBSOLETE

UNCLASSIFIED

SECURITY CLASSIFICATION OF THIS PAGE (When Data Entered)

ED 50 327 000

yB

UNCLASSIFIED

SECURITY CLASSIFICATION OF THIS PAGE(When Data Entered)

20. ABSTRACT (Continued)

ED 50

1 year postexposure and the ED₅₀ determined as a function of lesion duration. Two methods for assessing permanent corneal damage clinically are discussed and compared.

Pre- and postexposure corneal curvature measurements made during a year of observations show that the curvature of the irradiated corneas decreased by a factor of 2 to 3 over those in a nonirradiated control group. Randomly recurring postexposure edema in many irradiated corneas caused curvature increases which tended to mask the decrease expected from corneal collagen shrinkage. Mechanisms which could affect the results of this and other studies are presented. Parallels between induced corneal curvature changes and resulting changes in refractive error and visual performance are presented and evaluated.

Accession For	
NTIS GRA&I	<input checked="checked" type="checkbox"/>
DDC TAB	<input type="checkbox"/>
Unannounced	<input type="checkbox"/>
Justification	
By	
Distribution/	
Availability Codes	
Dist.	Avail and/or special
A	

UNCLASSIFIED

SECURITY CLASSIFICATION OF THIS PAGE(When Data Entered)

SUMMARY

A multiple pulse CO₂ laser has been used to determine the ED₅₀ required to produce a minimum visible corneal lesion within 30 minutes postexposure. Using a 0.5 sec exposure time, and a 5.3 mm diameter beam at the 1/e point, the ED₅₀ was 4.71 J/cm²(1/e). This is a factor of 12 above the MPE set forth in the ANSI standard. The lowest 1/e radiant exposure that resulted in the formation of a visible lesion was a factor of 10 above the ANSI standard.

The durations of corneal lesions resulting from suprathreshold exposures were observed for 1 year and analyzed in terms of the exposure (Tables 4, 5, 6, E-1, E-2, and E-3). The criterion for permanent damage was the presence of a visible lesion 1 year postexposure. It was found that objective assessment of corneal damage in the living eye by slit lamp examination should be augmented by other objective procedures. A more sensitive test involves examination of the corneal homogeneity by an ophthalmoscopic light reflex from the fundus. Use of this procedure in the present study indicated that permanent corneal changes occurred at 1/e radiant exposures that were a factor of 18 above MPE. This is in comparison to 1/e radiation exposures that were a factor of 56 above MPE for permanent damage found by routine slit lamp examinations.

Pre- and postexposure corneal curvature measurements were performed by both keratometry and photokeratoscopy during the year of observations (Appendixes A through D). In general terms, the mean corneal curvatures of the irradiated groups decreased by a factor of 2 to 3 over those in the nonirradiated group. However, randomly recurring postexposure edema in many of the irradiated corneas caused curvature increases. This produced a great deal of variability in the data and tended to mask the decreased curvature expected from corneal collagen shrinkage. Possible mechanisms entering into the results of this and other studies are discussed. One model indicates that tension in the corneal wall of the average rhesus monkey may be only half that in the corneal wall of the average rabbit (see Table 7).

Current thinking concerning the relationship between induced corneal curvature change and the resultant refractive error is discussed. It is pointed out that a refractive error greater than 1.00 D. will produce undesirable symptoms in most individuals. Using a 1.00 D. refractive error as the criterion where serious effects to visual efficiency become apparent, it is shown (by equation 10) that an induced corneal curvature change of 0.50 D. or greater is significant.

PREFACE

Grateful acknowledgment is extended to the following persons for their advice and assistance: R. G. Allen, K. L. Schepler, R. D. Reed, C. W. Houser, and K. A. Toth, all of the Laser Effects Branch; R. J. Haines, Jr., of the Veterinary Sciences Division; and D. A. Mabry of the Data Sciences Division.

We also thank S. F. Kane of the Laser Effects Branch and M. E. Green of the Technical Services Division for their help in preparing and editing the final manuscript.

CONTENTS

	<u>Page</u>
INTRODUCTION.....	5
EXPERIMENTAL APPARATUS.....	6
EXPERIMENTAL PROCEDURES.....	8
Evaluation of the Keratometer and the Photokeratoscope.....	8
The Keratometer.....	8
The Photokeratoscope.....	10
Photokeratoscope and Keratometer Comparisons.....	15
Animal Preparation.....	16
Pre- and Postexposure Procedures.....	16
Administration of Anesthesia.....	16
Methods for Data Acquisition and Recording.....	17
Schedule.....	17
Corneal Lesion Experiments.....	17
Corneal Curvature Experiments.....	17
Group Sizes.....	18
RESULTS AND DISCUSSION	18
Corneal Lesions.....	18
Results.....	18
Discussion.....	22
Corneal Curvatures.....	24
Results.....	24
Discussion.....	26
CONCLUSIONS AND RECOMMENDATIONS.....	30
REFERENCES.....	31
APPENDIX A: Corneal Curvature Changes as a Function of Time.....	35
APPENDIX B: Statistics for Corneal Curvature Changes as Measured with the Keratometer.....	40
APPENDIX C: Statistics for Corneal Curvature Changes as Measured with the Photokeratoscope.....	54
APPENDIX D: Curvature Change as a Function of Initial Curvature.....	63
APPENDIX E: Average Power and Radiant Exposure.....	88

LESION DURATION AND CURVATURE CHANGE IN THE CORNEA FOLLOWING EXPOSURE TO A CARBON DIOXIDE LASER

INTRODUCTION

Carbon dioxide (CO_2) lasers produce coherent radiation in the far infrared region of the spectrum at a wavelength of $10.6\text{ }\mu\text{m}$. Electromagnetic radiation of this wavelength which is incident on the eye is partially reflected by the tear layer, and the rest is absorbed in the eye. More than 99% of the portion which is not reflected is absorbed in the tear layer and corneal epithelium as long as these layers retain their integrity. The absorbed radiant energy increases the temperature of the corneal epithelium, and if the biological tolerance is exceeded, corneal damage results in temporary or permanent visual impairment.

Corneas exposed to CO_2 laser radiation at doses slightly above threshold typically develop greyish-white lesions or opacifications which normally disappear completely in a few days, but exposure to higher doses may result in permanent scarring of the cornea (1-10). A pilot study conducted in this laboratory (6) demonstrated that corneal changes produced by CO_2 laser radiation include, in addition to thermal lesion damage, a significant decrease in corneal curvature which persists for several months after the initial lesion has healed and disappeared. It was reported that corneal opacification cleared entirely within 1 week postexposure, but corneal curvatures measured 1-week postexposure were approximately 19 diopters (D.) less than the preexposure curvatures. Corneal curvatures measured 2 months postexposure indicated that 3 D. of curvature decrease was still present, but by 1 year postexposure the curvature had returned to the preexposure value. This persistent decrease in dioptric power was attributed to hydrothermal shrinkage of corneal collagen fibers that normally make up about 90% of the corneal bulk. The reported degree of change in corneal power is surprising and indicates that exposure of the cornea to the CO_2 laser must produce a profound effect on visual function that apparently persists long after corneal opacification disappears.

Laser safety standards evolve primarily from ED_{50} values determined in experimental animals, augmented by predictions from biomathematical models when experimental data is sparse or unavailable. Only recently, however, has theoretical modeling of corneal exposures to laser radiation considered criteria other than visible lesion damage (4). The startling results of the corneal curvature measurements reported in reference 6 indicated the need for more information concerning the ocular effects of the CO_2 laser. The present experiment was undertaken to: (1) test the adequacy of the existing CO_2 laser safety standard; (2) provide additional data and a broader base of information for use in the validation of theoretical models for predicting corneal thermal damage; and (3)

determine the degree and duration of the changes in corneal curvature as a function of corneal exposure to CO₂ laser radiation. The specific experimental objectives were:

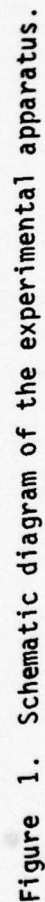
- Determine the ED₅₀ for the minimum visible corneal lesion using the same exposure parameters described in reference 6.
- Determine ED₅₀ values as a function of visible lesion duration for 1 year of postexposure observations.
- Determine corneal curvature changes during 1 year postexposure and relate these changes to exposure and to their probable effects on visual function.

In addition to the above objectives, the temperatures of normal and laser-injured corneas were measured in order to provide more accurate input parameters for mathematical models used to predict the effects of corneal exposure to laser radiation. The results of the temperature measurements were compiled and submitted in a separate report (11).

EXPERIMENTAL APPARATUS

The laboratory arrangement of the equipment used in the present study is shown schematically in Figure 1. The source for the corneal exposures was a pulsed CO₂ laser (Perkin-Elmer Model 2600 Molecular Gas laser) emitting a collimated beam at a wavelength of 10.6 μ m and 120 pulses per second with a 50% duty cycle. The gold-plated mirror normally reflected the beam into a power meter (CRL Model 201) for monitoring and cross adjustments. The mirror was removed from the beam for corneal exposures and calibration, and a shutter (Compur Electronic 3) was used to control the exposure time. The iris diaphragm was adjusted to provide Gaussian beam configuration with a 1/e beam diameter of 5.3 mm at the plane of the cornea (Fig. 2). A helium-neon laser, aligned to coincide with the CO₂ laser beam, was used to position the animal to insure proper placement for exposure.

A thermopile (Hadron Model 100) with calibration traceable to NBS standards was used to measure the power in the CO₂ beam at the cornea. The thermopile was placed at the corneal exposure position and its output measured with a microvolt-ammeter (Keithley Model 150B). A thermopile (Hadron Model 101) driving a microvolt-ammeter (Keithley Model 150A) received a fraction of the beam energy reflected from a germanium beam splitter. This thermopile was cross-calibrated with the primary thermopile at the corneal position and was used to measure the beam power during each exposure.



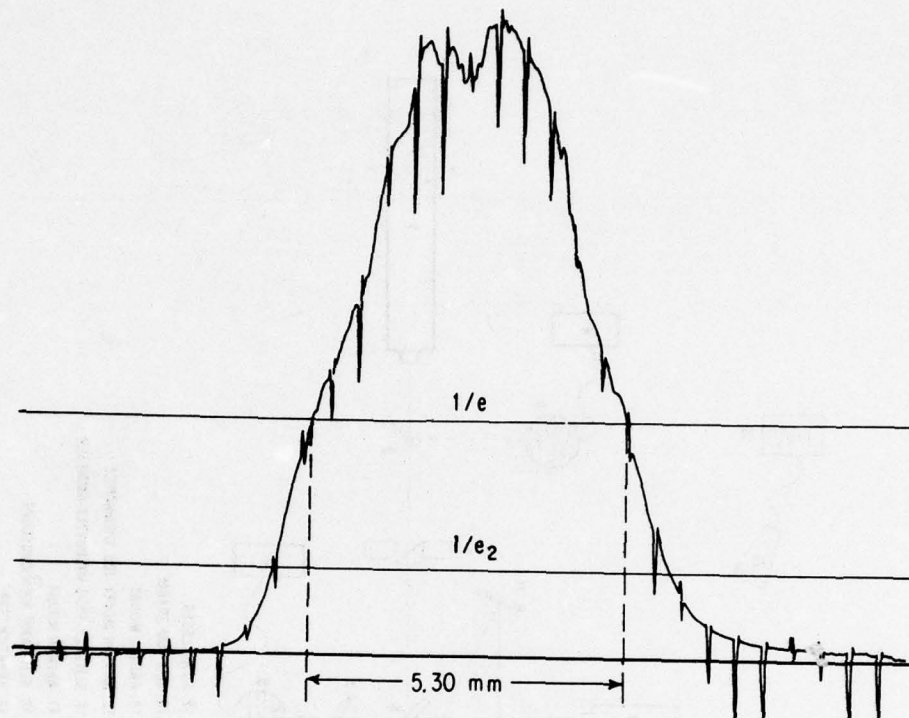


Figure 2. Spatial beam scan at the corneal plane.

The equipment used for eye examinations and corneal curvature measurements included: a standard Nikon slit lamp, a standard Bausch and Lomb keratometer, and a photokeratoscope constructed and modified from a design promulgated by El Hage (12).

EXPERIMENTAL PROCEDURES

Evaluation of the Keratometer and the Photokeratoscope

The Keratometer-- Modern keratometers, such as the one used in this experiment (Fig. 3), provide, with only one setting, quick and accurate measurements of the central corneal curvature in two meridians at right angles to each other. Although it was invented over a century ago (Helmholtz, 1854), the keratometer has probably gained its widest contemporary usage in the measurement of corneal curvatures for the fitting of contact lenses to humans. Applications of the keratometer, including details of its theory and operation, are generally well covered in texts under keratometry or under the synonym ophthalmometry (13-21).

The normal design range of the keratometer extends from 36 D. (36 diopters) to 52 D., but the range can be extended approximately 6 D. above and below those points by the simple addition of auxiliary lenses

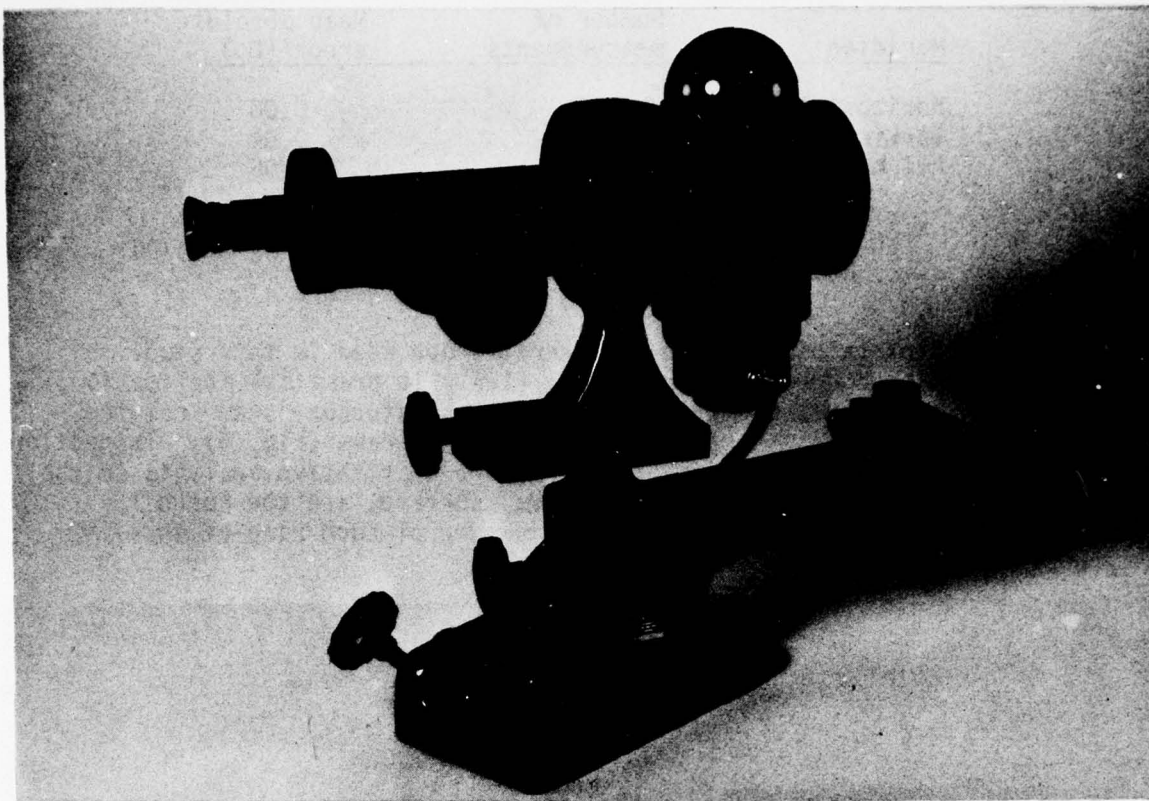


Figure 3. The keratometer.

(6, 18, 22). Because the range of corneal curvature found in normal mature rabbits is about the same as that found in normal human corneas, the corneas of the rabbits used in this experiment could usually be measured without amplifying the instrument range. In a few postexposure corneas where laser-induced curvatures exceeded the normal measurement range, auxiliary lenses were used.

To determine the degree of accuracy that might be expected from the instrument used in this study, a series of horizontal and vertical meridian measurements were made using spherical steel balls with known curvatures. Each measurement was made from a random instrument setting and was carried out without reference to the instrument scale or to the ball being used. The absolute value of each measurement error was recorded. Table 1 shows the mean of the absolute errors for each meridian and for all the measurements. The mean absolute error for all measurements was 0.05 D. An average cornea has a curvature of about 44 D.; thus the keratometer used in this study is accurate to about 0.1%. The largest error was 0.25 D. with a 42.50 D. calibration ball, an error of less than 0.6%.

TABLE 1. ACCURACY OF THE KERATOMETER (steel balls)

Meridian	Number of measurements	Mean absolute error (D.)
Horizontal	90	0.06
Vertical	90	0.04
All measurements ^a	180	0.05

^aThe worst case error was 0.25 D. (i.e., < 0.6%) using a 42.50 D. calibration ball.

The Photokeratoscope--The photokeratoscope used in this study (Fig. 4) has been described previously (12). In practical application, corneal curvature measurements made by photokeratoscopy stem from the instrument's Placido disc photographs or keratograms (Fig. 5). Inspection of a keratogram of the eye readily permits a qualitative analysis of the regularity or irregularity of the corneal surface, and the corneal curvature can be calculated from the diameter of each ring of the keratogram when certain conditions are met.

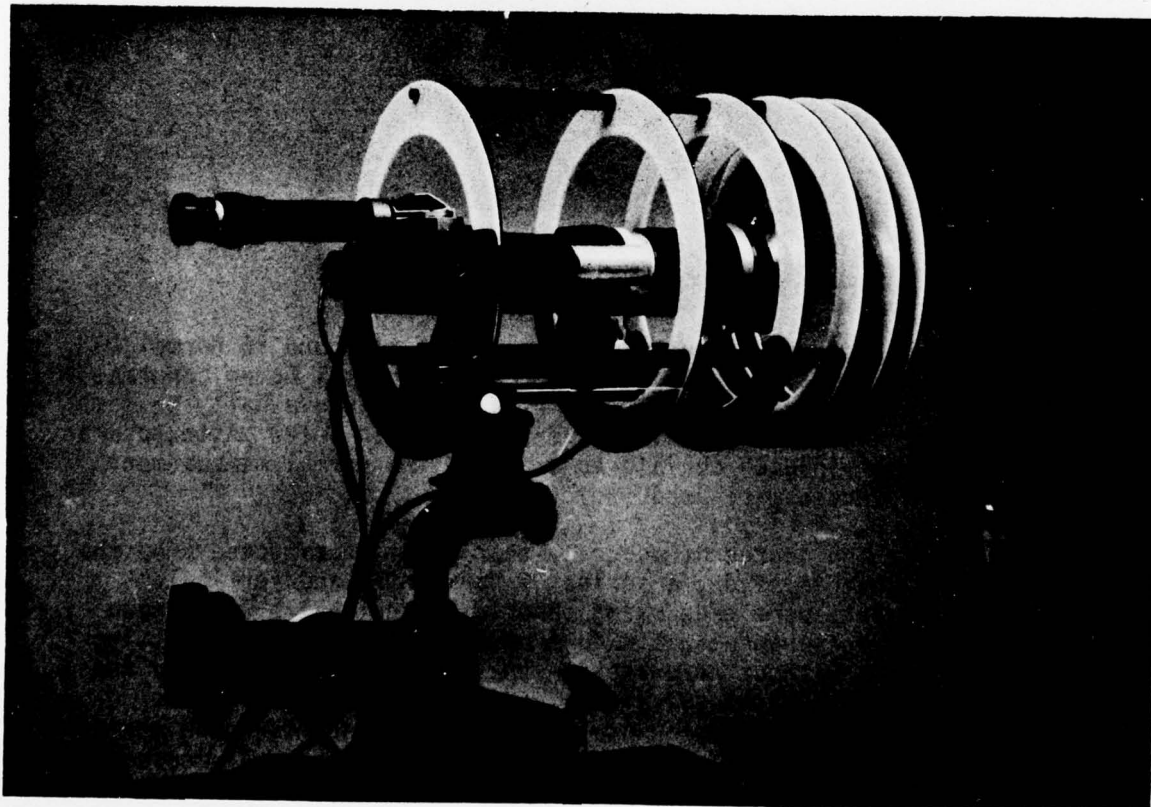


Figure 4. The photokeratoscope.



Figure 5. Keratogram of a normal rabbit cornea.

In the present study, the film used to produce the keratograms was a black and white, fine grain, high speed (ASA 400) film, packaged in 20 exposure 135 magazines. After each roll of film was exposed and developed, the negatives, i.e., the keratograms, were separated and mounted in slide holders for convenience in handling and filing.

In order to measure the keratogram ring diameters, the keratogram was first centered on a motor-driven table where it could be viewed under a binocular microscope fitted with a reticle. The table was connected to an Aerotech digitizer that provided a continuous display of the table position, or table position change, in increments of 0.0001 in. The motor drive was then activated to scan across any given ring of the keratogram as viewed through the microscope, and the digitizer simultaneously provided a readout of the distance traveled across a given ring. This information was automatically fed into a 9810-A Hewlett-Packard calculator and recorded in meters (m) on paper tape and/or magnetic tape cassettes.

Keratograms used for corneal curvature calculations or quantitative comparisons require that object size, object distance, and camera magnification be held constant during the photography. As used here, object size refers to the physical dimensions of the photokeratoscope rings, which of course were always constant in size. Object distance, i.e., the distance of any photokeratoscope ring from the corneal plane, was controlled by triangulation projectors mounted on the photokeratoscope and double checked just prior to the photographic exposure by observing, through the camera, the focus of the ring images reflected from the corneal surface. Observation through the camera was facilitated by a 5X telescope mounted to the camera eyepiece. Magnification of the camera was held constant by retaining the same position and adjustment of the camera for all photographs. Magnification of the system was determined by photographing a linear millimeter scale through the photokeratoscope and measuring the scale on the negative with the digitizer using the same procedures described for scanning keratograms. This provided the ratio of object size to image size required to determine the magnification constant.

With the setting of these constants, and with image diameter measurements obtained by the scan of a keratogram of a cornea, the corneal radius of curvature could be calculated by the relationship

$$r = \frac{2uh''}{hM_c - h''} \quad (m) \quad (1)$$

where

r = radius of curvature of the cornea

u = object distance

h = object size

M_c = camera magnification

h'' = diameter of ring image on keratogram

This relationship can be derived from classic equations for simple curved surfaces, i.e.,

$$-1/u + 1/v = \frac{2}{r} \quad (m) \quad (2)$$

and

$$M = \frac{h'}{h} = \frac{v}{u} \quad (m) \quad (3)$$

where

u = object distance from cornea

h = object size

v = image distance from cornea

h' = size of corneal image

M = magnification of the corneal image

r = radius of curvature of the cornea

From Equation 3,
$$v = \frac{h'u}{h} \quad (m) \quad (4)$$

Substituting for v in Equation 2,

$$-1/u + \frac{1}{\frac{h'u}{h}} = 2/r \quad (m)$$

or

$$-1/u + \frac{h}{h'u} = 2/r \quad (m)$$

Solving for r ,

$$r = \frac{2h'u}{h-h'} \quad (m) \quad (5)$$

In Equation 5, h' represents the image size of the keratoscope ring reflected by the cornea and becomes the object for the camera system. Thus

$$M_c = \frac{h''}{h'} \quad (m) \quad (6)$$

where

M_c = camera magnification

h'' = image size on the keratogram (camera image)

h' = image size reflected from cornea (camera object)

From Equation 6,

$$h' = \frac{h''}{M_c} \quad (m) \quad (7)$$

Substituting for h' in Equation 5,

$$r = \frac{\frac{2h''}{M_c} u}{h - \frac{h''}{M_c}} \quad (m) \quad (1)$$

or

$$r = \frac{2uh''}{hM_c - h''} \quad (m) \quad (1)$$

Dioptric power of the cornea was calculated from the corneal radius of curvature using the expression

$$D = \frac{n-1}{r} \quad (8)$$

where

D = corneal surface power in diopters

n = 1.3375, index of refraction of the cornea

r = corneal radius of curvature in meters.

Equation 8 is found in most textbooks dealing with optics and has been derived by others (13, 20, 23-26).

To test the accuracy of the combined photokeratoscope/data retrieval system, a series of keratograms were made using the steel calibration balls. Each keratogram of a steel ball was made independently keeping constant only those factors which should be constant, i.e., camera magnification, object size, and distance. By convention, the 5 concentric rings on each keratogram (Fig. 5) were identified by roman numerals with the smaller inner ring being I, and each successively larger ring labeled II through V. The curvature in diopters was calculated for the horizontal meridian of each of the 5 rings in 44 keratograms. Errors were recorded as the absolute values of the differences between the calculated dioptric power and the actual dioptric power of the steel balls. Table 2 presents the mean of the absolute errors for each of the 5 rings and for all of the ring measurements combined. The mean for all of the measurements was 0.12 D. For an average cornea of 44 D., this error would be less than 0.3% of the total corneal power. The largest single error for the 220 ring measurements was 0.46 D. using a 47.25 D. calibration ball--an error of less than 1%.

TABLE 2. ACCURACY OF THE PHOTOKERATOSCOPE/DATA RETRIEVAL SYSTEM (steel balls)

Ring number (horizontal meridian)	Number of measurements	Mean absolute error (D.)
I	44	0.22
II	44	0.10
III	44	0.09
IV	44	0.14
V	44	0.08
All measurements ^a	220	0.12

^aThe worst case error was 0.46 D. (i.e., <1%) using a 47.25 D. calibration ball.

Photokeratoscope and Keratometer Comparisons--Steel calibration balls are spherical; thus comparison may be made between the radius of curvature as determined by the single ring keratometer method and the radius determined from any of the 5 rings of the photokeratoscope (Tables 1 and 2). In addition, the radii determined from the different rings of the ideal photokeratoscope should be identical if the sphere being measured were perfect. In contrast to a steel calibration ball, however, the normal cornea, rather than being spherical, is somewhat conical and tends to decrease in curvature toward the periphery. Therefore, where the eye is concerned, comparison of these 2 instruments must take into account that the single ring of the keratometer reflecting from a given cornea will probably have only one close counterpart within the ring cluster of the photokeratoscope reflecting from that same cornea. Photokeratoscope and keratometer measurements of 20 normal rabbit corneas, summarized in Table 3, show this to be the case. Note

TABLE 3. PHOTOKERATOSCOPE/KERATOMETER COMPARISONS (20 normal rabbit corneas)

Ring number (horizontal meridian)	Photokeratoscope		Keratometer		Mean absolute difference (D.)	Coefficient of correlation
	Mean (D.)	Standard deviation	Mean (D.)	Standard deviation		
I	45.80	1.60			0.31	0.981
II ^a	45.54	1.58	45.54	1.59	0.19	0.989
III	45.37	1.59			0.26	0.985
IV	45.31	1.52			0.27	0.987
V	45.17	1.57			0.40	0.983

^aPhotokeratoscope measurements at Ring II were the closest approximation of the keratometer measurements.

the mean corneal power decrease between rings I and V of the photokeratoscope measurements and the similarity of the measurements of the 2 instruments at the ring II position.

Table 3 also shows the mean absolute difference for each ring of the photokeratoscope compared to the keratometer readings of the same 20 eyes. The mean absolute difference between photokeratoscope and keratometer was lowest at the ring II position with a value of 0.19 D. The coefficients of correlation between each ring measurement of the photokeratoscope and the keratometer readings also are listed in Table 3. The correlation coefficient for measurements by the 2 instruments was excellent, i.e., 0.981 or better. Ring II data of the photokeratoscope had the highest correlation to keratometer data with a coefficient of 0.989.

Of the 2 instruments, the keratometer is by far the quickest and easiest to use. The large physical bulk of the photokeratoscope makes it difficult to manipulate and to align properly without at least some cooperation from the subject. In addition, photokeratoscopy requires many more procedures than keratometry. Instrument calibration, photography, film processing, keratogram scanning, and curvature calculations are arduous, time consuming, and expensive, particularly when large quantities of data must be processed. A key disadvantage of photokeratoscopy found in the present study was the lack of instant feedback that a satisfactory keratogram had been achieved. In contrast, the keratometer provided on-the-spot curvature measurements whenever there was sufficient specular reflection from the cornea. In terms of accuracy of measurement, both instruments are excellent, and they augment each other where comprehensive information concerning corneal curvatures or surface changes is required.

Animal Preparation

Pre- and Postexposure Procedures--Mature Dutch belted rabbits were used in this study. Pre- and postexposure slit lamp examinations, photography, and corneal curvature measurements were carried out without anesthesia since no pain is associated with these procedures. At such times, sufficient cooperation was achieved by confining each animal in a standard rabbit restraining box with only the head exposed. The box, in turn, was placed upon an adjustable animal mount which was mated to the adjustment range of the examination equipment. Normal saline solution was used as an irrigant to remove hair or other debris from the corneal surface.

Administration of Anesthesia--To prepare a rabbit for laser exposure, a preanesthetic agent, ketamine hydrochloride (2.5 mg/kg), was injected into the rabbit's hindquarter. After 30 minutes for effect, the animal was placed in the restraining box, and the anesthetic, sodium thiopental (50 mg/kg), was administered using a syringe inserted into an ear vein. When satisfactorily anesthetized, an eye speculum was inserted for lid control, and the animal was promptly positioned for the laser exposure.

Methods for Data Acquisition and Recording

Schedule--Corneal observations and measurements of the laser effects were conducted on each eye in sequence over a period of 1 year at pre-exposure (baseline), 30 minutes postexposure, and 1, 7, 30, 90, 180, 270, and 365 days postexposure.

Corneal Lesion Experiments--The criterion for corneal injury was the appearance of a corneal lesion as determined by slit lamp examination within 30 minutes following exposure. The probability of permanent corneal damage is dependent upon the injury sustained during the exposure. Lightly injured corneas were expected to repair and regain their normal transparency within a few hours or days, while more seriously injured corneas were expected to require a longer recovery time or to be injured permanently. Therefore, slit lamp examinations were conducted for 1 year postexposure to provide a record of the duration of each lesion. This provided data for determining the ED_{50} for a minimum visible lesion and for determining the ED_{50} for the duration of the damage.

Corneal Curvature Experiments--Corneal curvatures were measured by both keratometry and photokeratoscopy at the times specified above. All measurements of corneal curvature were recorded in diopters of change from preexposure conditions. A postexposure decrease in corneal curvature was recorded as a negative value and an increase as a positive value.

Examples:

Day 7 = 42.50 D.
Baseline = 43.50 D.
Change = -1.00 D.

Day 30 = 44.00 D.
Baseline = 43.50 D.
Change = +0.50 D.

Corneas with toric surfaces were also quantified from the keratometer measurements by recording the dioptric difference of the two principal meridians, giving the resultant toricity value a positive sign when curvature was greater horizontally and a negative sign when curvature was greater vertically. Purely spherical (nonastigmatic) corneas were recorded as zero toricity.

Examples:

Horizontal Meridian = 45.00 D.
Vertical Meridian = 44.00 D.
Toricity = +1.00 D.

Horizontal Meridian = 45.75 D.
Vertical Meridian = 46.75 D.
Toricity = -1.00 D.

Horizontal Meridian = 44.50 D.
Vertical Meridian = 44.50 D.
Toricity = 0.00 D.

Changes in toricity between the preexposure and postexposure conditions were recorded as absolute values of change.

Examples:

$$\begin{array}{r} \text{Baseline Toricity} = +1.00 \text{ D.} \\ \text{Day 7 Toricity} = +2.00 \text{ D.} \\ \hline \text{Toricity Change} = 1.00 \text{ D.} \end{array}$$
$$\begin{array}{r} \text{Baseline Toricity} = +1.00 \text{ D.} \\ \text{Day 30 Toricity} = 0.00 \text{ D.} \\ \hline \text{Toricity Change} = 1.00 \text{ D.} \end{array}$$
$$\begin{array}{r} \text{Baseline Toricity} = +1.00 \text{ D.} \\ \text{Day 90 Toricity} = -1.00 \text{ D.} \\ \hline \text{Toricity Change} = 2.00 \text{ D.} \end{array}$$

This treatment of the measurements not only afforded a means of quantifying the curvature or toricity of a cornea for any given measurement, but also provided an index of changes occurring with time, using the initial normal value of each eye as its baseline.

Because it is known that rabbit corneal curvatures change with time, a control group of mature rabbits was established to undergo the handling and measurement procedures of the irradiated rabbits, except, of course, for the laser exposure itself. In this way, corneal curvature changes occurring with time could be compared to changes in a nonirradiated group, or the values occurring with time could be compared to the baseline values.

Group sizes--A total of 160 eyes were examined for irradiation, but some of the corneas were not acceptable and were rejected at the time of the initial examination. In some cases the subject did not survive the full year. Remaining for observation and measurement for a full year postexposure were 120 irradiated corneas and 32 control corneas.

RESULTS AND DISCUSSION

Corneal Lesions

Results--All corneal exposures are given in either average power in watts, the incident beam power averaged over time, or 1/e radiant exposure (dose) in J/cm^2 , the average power multiplied by the exposure time and divided by the area of a circle with a radius equal to the beam radius at the 1/e point. The exposure time was 0.5 sec, and the beam radius at the 1/e point was 2.65 mm for all corneal exposures. Typically, corneal lesions at 30 minutes postexposure were greyish-white in appearance with size and severity proportional to the dose. Frequently, at doses near threshold, there was only light stippling of the corneal epithelium visible at the exposure site. In this experiment epithelial stippling was considered a visible lesion.

Minor lesions of the superficial epithelial layer disappeared in 1 to 7 days. More serious injuries characteristically showed marked opacification and sloughing of necrotic tissue during the first week, but a new epithelial cover was usually complete by 7 days postexposure. After 7 days, stromal opacification, edema, and irregular thickness variations of the cornea persisted for varying periods of time. By the end of the year, nearly all of the corneas had stabilized in either a state of transparency or an apparently permanent condition of opacification. However, some corneas, even though transparent, appeared to have a poorly attached epithelial layer.

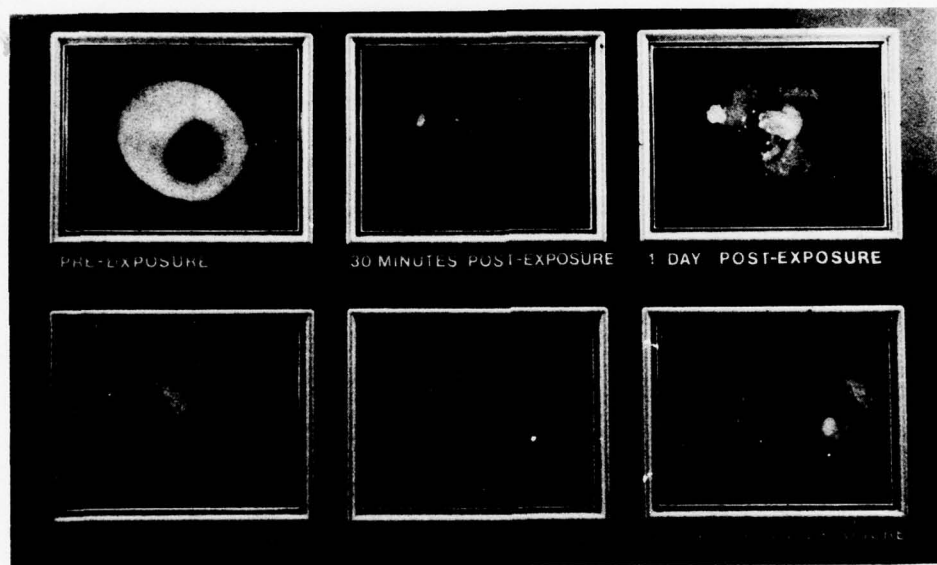


Figure 6. Slit lamp views of a rabbit eye before and after exposure to the CO_2 laser.

Figure 6 shows a series of slit lamp photos of a cornea that received a $1/e$ radiant exposure of 17.0 J/cm^2 that returned to normal transparency in 30 days. Note how the necrotic epithelial layer is sloughing away 1 day postexposure.

Figure 7 shows the results of the 30-minute postexposure lesion/no lesion evaluations for all of the exposures. The upper scale of Fig. 7 shows the average power in watts (W), and the lower scale shows the $1/e$ radiant exposure in J/cm^2 . All exposures were 0.5 sec in duration.

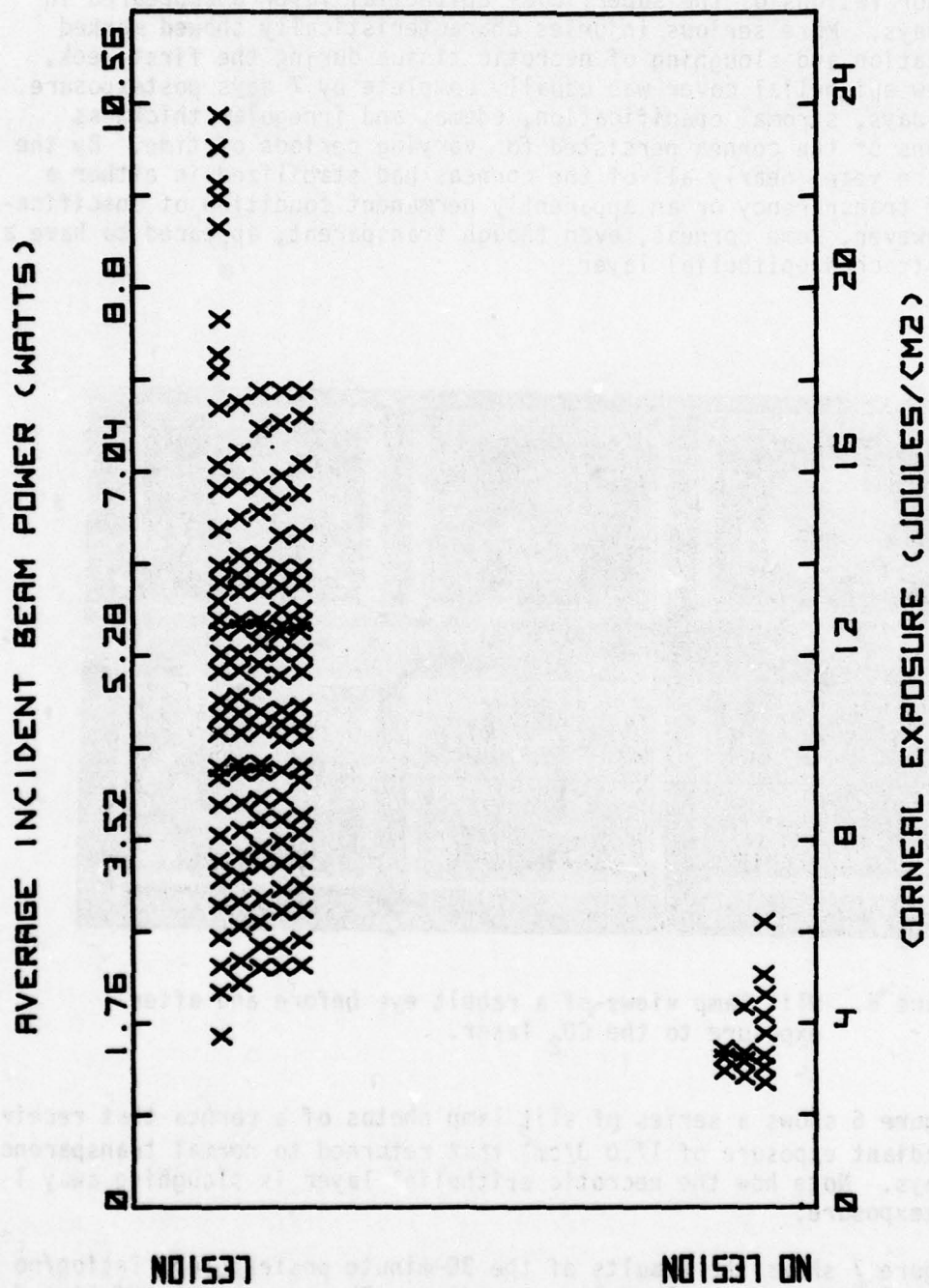


Figure 7. The array of CO₂ laser exposures ($t = 0.5$ sec) showing lesion/no lesion responses of the cornea within 30 min postexposure.

Probit analysis was performed using the log dose transformation normally used for ED_{50} estimates. The ED_{50} for the 30-minute minimum lesion was 2.08 W, a 1/e radiant exposure of 4.71 J/cm^2 .

TABLE 4. ED_{50} VALUES OF AVERAGE POWER FOR CORNEAL LESIONS AFTER EXPOSURE TO CO_2 LASER RADIATION. BEAM RADIUS WAS 2.65 MM AT THE 1/e POINT, AND ALL EXPOSURES WERE 0.5-SEC DURATION.

Postexposure time	Number of eyes	ED_{50} (W) ^a	95% confidence limits	Regression coefficient estimate
30 min.	144	2.08	1.79 - 2.32	13.05
Day 1	138	2.30	1.91 - 2.60	7.41
Day 7	138	2.77	2.27 - 3.17	5.07
Day 30	134	4.85	4.20 - 5.62	4.00
Day 90	132	8.58	6.83 - 15.23	3.15
Day 180	131	11.06	8.18 - 32.02	3.31
Day 270	127	11.13	8.18 - 34.01	3.23
Day 365	120	9.90	7.73 - 21.30	3.79

^aFor radiant exposure see Appendix E.

Table 4 is a summary of the ED_{50} values, 95% confidence limits, and regression coefficients for each time of evaluation for the presence or absence of a visible lesion. The decreasing number of eyes examined reflects the loss of animals during the year.

On the day of the final eye examination (1 year postexposure), each cornea was also evaluated with a hand ophthalmoscope, although this was not part of the original experimental plan. Using a +6 D. lens in the instrument's lens-disc, the eye was examined from a distance of about 15 inches. Light from an ophthalmoscope directed into the eye in this way produces an orange glow (the fundus reflex) which, in a normal eye, appears homogeneous to the observer. Opacities or heterogeneous indices of refraction within the cornea or lens produce black obstructions or mottled areas within the glow of the fundus reflex. The location (i.e., corneal or lenticular) of an opacity or heterogeneity can easily be determined by parallax (14, 18, 27). This examination technique is a more sensitive indicator of corneal heterogeneity than the slit lamp examination. The results of this examination are summarized in Table 5 with the data grouped according to exposure. It was obvious that the number of positive findings increased with average power, and an ED_{50} for this effect was calculated and found to be 3.2 W (Table 6).

TABLE 5. CORNEAL HETEROGENEITIES DETECTED 1 YEAR POSTEXPOSURE BY THE FUNDUS REFLEX TEST

Average power (W) (t=0.5 sec) ^a	Number of corneas	Number positive	Percent positive
<2	8	0	0
2 - 3.99	35	16	46
4 - 5.99	41	34	83
≥6	35	34	97

^aFor radiant exposure see Appendix E.

TABLE 6. ED₅₀ FOR CORNEAL HETEROGENEITY AT 1 YEAR POSTEXPOSURE

Number of eyes	ED ₅₀ (W) ^a	95% confidence limits	Regression coefficient estimate
120	3.2	2.02 - 4.03	5.27

^aFor radiant exposure see Appendix E.

Discussion--Achieving two of the experimental objectives set forth in this study, the data enable determination of the ED₅₀ for a minimum visible lesion appearing in 30 minutes and provide comprehensive information concerning the lesion duration of suprathreshold exposures. The data also provide a basis for assessing the adequacy of current laser safety standards for the exposure parameters used in this experiment and for estimating the operational impact of personnel exposure. The data may also be useful for reference in clinical or medicolegal assessments in cases of injury or claims where exposure parameters are known or can be determined.

The ED_{50} for the 30-min minimum visible lesion was $4.71 \text{ J/cm}^2 (1/e)$. The lowest dose which produced a lesion (see Fig. 7) was $3.94 \text{ J/cm}^2 (1/e)$. The American National Standards Institute (ANSI) standard (28) maximum permissible exposure (MPE) to laser radiation with these parameters ($\lambda = 10.6 \mu\text{m}$, exposure time = 0.5 sec, duty cycle = 50%, pulse repetition frequency = 120 Hz) is 0.0066 J/cm^2 -pulse or a total radiant exposure of 0.396 J/cm^2 . This MPE is a factor of almost 12 lower than the ED_{50} found in this experiment and is a factor of almost 10 lower than the radiant exposure for producing a lesion. Since a factor of 10 between the safety standard and "threshold" is generally viewed as sufficient, the ANSI standard appears to be adequate for these exposure conditions.

It seems very unlikely that corneas still showing lesions 1 year postexposure would ever return to clinical normalcy. In fact, this may be true even for corneas with lesions persisting longer than a week. For example, the ED_{50} for 7-day and 30-day lesions (Table 4) was 2.77 and 4.85 W (6.28 and $11.0 \text{ J/cm}^2 (1/e)$) respectively. This compares closely to the ED_{50} of 3.2 W ($7.25 \text{ J/cm}^2 (1/e)$) found for permanent destruction of corneal homogeneity. This comparison assumes a 1-year point as the criterion for irreversible corneal damage. In our judgment, the ED_{50} of 9.90 W ($22.44 \text{ J/cm}^2 (1/e)$) for permanent damage determined by slit lamp examination (Table 4, day 365) is quite high, and the better assessment of permanent damage elicited by clinical means is that given by the examination for corneal heterogeneity. The ED_{50} of $22.44 \text{ J/cm}^2 (1/e)$ for permanent corneal damage as determined using the slit lamp is a factor of 56 greater than the MPE, while the ED_{50} of $7.25 \text{ J/cm}^2 (1/e)$ for permanent corneal damage as determined using the test for corneal heterogeneity is a factor of 18 greater than the MPE.

With the increasing utilization of high powered CO_2 lasers, there is increasing potential for inadvertent exposure to the invisible beam of this laser. In the event of such an accident, there is a high probability of exposure to levels above the ED_{50} for a reversible minimum visible lesion. Although histological studies can be used to define initial or permanent damage in the eyes of euthanized experimental animals, other criteria are required to evaluate the eyes of living personnel. The above data provide at least a preliminary basis for this.

Corneal Curvatures

Results--The data are expressed in diopters of change from the baseline for each of the variables measured, in the manner outlined in the section on "Experimental Procedures." The data for the irradiated corneas were divided into four exposure groups: average power <2 W, 2-3.99 W, 4-5.99 W, and ≥ 6 W. Although the curvatures of both the irradiated and control corneas were measured at the same predetermined intervals during the year of observations, measurements of many of the irradiated eyes, especially at the higher radiant exposures, were not possible until day 7 (see Fig. 8).

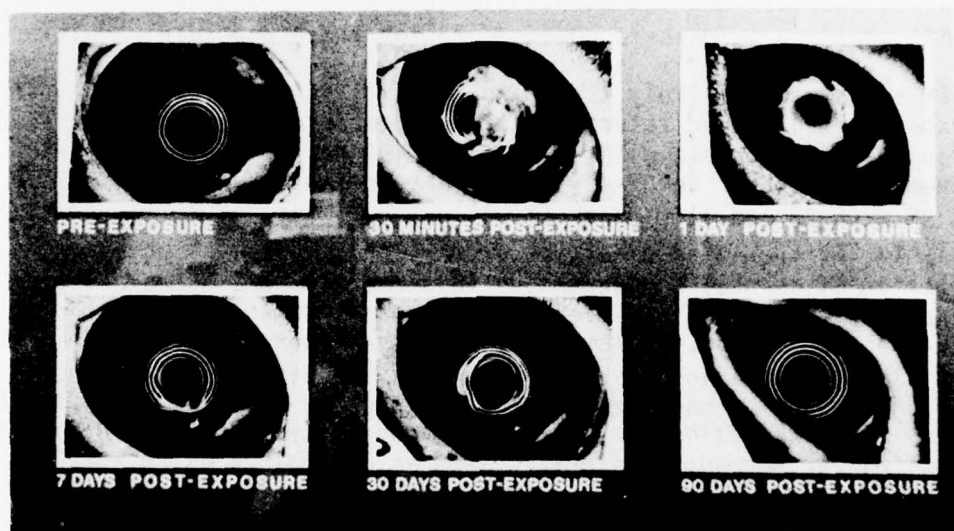


Figure 8. Keratogram sequence of a rabbit cornea before and after exposure to the CO_2 laser.

Figures A-1 through A-4, Appendix A, show dioptric changes vs. time for the horizontal meridian, vertical meridian, spherical equivalent, and toricity, respectively, for the control group and each of the irradiated groups. In these figures the curves for the control group are indicated by the letter C; the irradiated groups are indicated by numbers 1 through 4 in the same sequence as listed above, i.e., with the number 1 indicating the <2 W exposure group, 2 indicating the 2-3.99 W exposure group, etc. In Figures A-1 through A-3, positive changes indicate curvatures greater than baseline, and negative changes indicate curvatures less than baseline. In Figure A-4, positive values indicate toricity changes from baseline with the horizontal curvature greater than the vertical, and negative values indicate toricity changes from baseline with the vertical curvature greater than the horizontal. Because a few of the animals died during the year, estimates of the changes at each time were obtained from analyses of variances for each group in order to provide values corrected for the absent data. When looking at a trend, these are the appropriate estimates to use.

The trends shown in Figures A-1 through A-4 indicate the early postirradiation turmoil, especially through day 30, for the irradiated groups. This was followed by a decrease of curvature for all groups with time. In general terms, the change in the dioptric power of the irradiated corneas was approximately a factor of 2 to 3 greater than the change in the control group.

Summary statistics of the horizontal and vertical meridional changes and of the spherical equivalent and toricity changes, as measured with the keratometer, for both the control and irradiated groups during the year of observations, are given in Appendix B, Tables B-1 through B-28. Each of the tables lists the number of eyes (group size), mean change (D.), standard deviation, and the range of change. In addition, the tables for meridional and spherical equivalent changes show the maximum change, positive and negative, in each group for that measurement; similarly, the tables for toricity change show the minimum and maximum values of this topographical alteration for each group for that measurement. Since absolute values for toricity changes are used, minimal toricity changes are close to zero.

Postexposure variability and the range of changes in the irradiated corneas are quite evident in these data tables, and both of these features tend to increase as a function of dose. Postexposure variability was accentuated by the fact that curvature data for any given cornea, especially during the early postexposure stages, might show either random increase (edema) or decrease (collagen shrinkage), irrespective of dose or time of measurement. As an example, one irradiated cornea (52R) demonstrated spherical equivalent changes of -2.42 D., +0.48 D., and -5.96 D. respectively on days 7, 30, and 90. Over the next 6 months, this cornea appeared to be returning to normal; however, on day 365, edema was in evidence, and the spherical equivalent change from baseline had increased to +3.73 D. Corneas which reacted in such an unpredictable fashion tended to mask the overall trends shown by the group means. As a result, traditional tests for significance between means tended to bog down, even though other differences between the groups were apparent.

Summary statistics of the horizontal meridional changes shown by the rings of the keratograms taken on the same days as the keratometer measurements are given in Appendix C, Tables C-1 through C-7. The format of these tables follows that of the meridional tables of Appendix B, but the tables are expanded to include data from each of the photokeratoscope rings, providing an additional dimension of the surface topography. Variability evidenced by the standard deviations and the range of changes of the inner rings (e.g., rings I and II), particularly from 7 or more days postexposure, tends to be higher than for the outer rings. This corresponds to the area of the cornea receiving the greatest exposure from the Gaussian beam produced by the laser. However, there are no trends apparent in a comparison of the mean curvature change of the central rings and the peripheral rings. Data from ring II of the keratograms closely paralleled the keratometer data, and a summary of the mean changes found by these different measurement techniques for each of the days on which the curvature was measured is listed in Table C-8.

A final analysis of the postexposure curvature changes is provided in Appendix D, Figures D-1 through D-48. In these figures, curvature changes and toricity are plotted vs. preexposure values for both the control and irradiated groups and quadratic or linear curves fitted to the data. When a quadratic curve did not fit better than a linear, the linear was used, and when a linear curve did not fit better than a line with zero slope drawn through the mean value, the latter was used. These figures display the postexposure curvature change or toricity as a function of the initial curvature or toricity and a succinct view of the data spread for the two groups at each measurement.

Discussion--The results of these experiments indicate that collagen shrinkage is not the only dynamic factor causing curvature change in corneas following exposure to thermal radiation. Although there is adequate evidence to show that collagen shrinkage can produce a decrease in corneal curvature (6, 8, 29-33), epithelial edema and swelling within the injured stroma can produce an opposite or offsetting effect in a given cornea (3, 5, 8, 17, 29, 32, 34-36). For example, MacKeen et al. (8), in analyzing the histological results of eyes they had exposed to CO₂ laser radiation, state that collagen shrinkage would increase the corneal radius (to produce a decreased curvature); however, they also describe postirradiation corneal swelling and thickening and explain it with the observation that denatured collagen absorbs more water than natural collagen. In the present study, these two effects are very evident in the range of curvature change both above and below baseline.

In retrospect, other factors influencing the degree of postexposure curvature change in any given cornea may also be operative. For example, it may be important to consider the preexposure values for intraocular pressure, corneal thickness, and radius of curvature because of the relationship these factors have on the degree of tension existing in the corneal-scleral wall. Studies in the area of force mechanics (24, 34, 35, 37-39) have shown that the relation between pressure and circumferential tension in the wall of an inflated elastic sphere is given by the equation:

$$T = \frac{pr}{2t} \quad (9)$$

where

T = tension (g/cm²)
 p = pressure (g/cm²)
 r = radius of curvature (cm)
 t = wall thickness (cm)

In normal eyes the values for intraocular pressure and for corneal radius of curvature vary over wide ranges both within and between species (34, 35, 40). Such wide ranges and the interplay of possible variations produce eyes with different tensions in their corneal-scleral walls. These differences in tensions suggest that any given normal eye may

inherently possess a greater or lesser degree of resistance, or susceptibility, to collagen shrinkage or to other postexposure sequelae. Table 7 presents a summary of the average values for intraocular pressure, corneal radius of curvature, and corneal thickness in the human, the rabbit, and the rhesus monkey with corresponding literature references for each value. By substituting these values into the above equation, average normal tensions in the corneal walls of the different species can be approximated. The calculated tensions for the different corneas are also given in Table 7. Note that the tension in the average rhesus monkey cornea is only half that found in the rabbit cornea. Tension in the human cornea is about midway between those two.

TABLE 7. AVERAGE NORMAL CORNEAL TENSIONS

Eye	p Intraocular pressure (g/cm ²)	r Corneal radius of curvature (cm)	t Corneal thickness (cm)	T Calculated corneal tension (g/cm ²)
Human	20 ^a	0.785 ^a	0.052 ^b	151
Rabbit	24 ^b	0.740 ^c	0.040 ^b	222
Rhesus monkey	18 ^b	0.643 ^c	0.055 ^d	105

^a(34); ^b(35); ^c(6); ^d(41)

The pilot study (6) preceding this investigation reported that the corneas of a rhesus monkey decreased in curvature by approximately 19 D. in the horizontal meridian 1 week after exposure to CO₂ laser radiation, and 3 D. of curvature decrease was still present 2 months postexposure. In the present study, however, the maximum decreases in the corneal curvature were considerably less: 8.35 D. in the vertical meridian at 30 min postexposure, 5.9 D. in the horizontal meridian at 7 days postexposure, 5.87 D. in the horizontal meridian 30 days postexposure, 10.18 D. in the horizontal meridian 90 days and 180 days postexposure, 13.17 D. in the vertical meridian at 270 days postexposure, and 12.88 D. in the vertical meridian 365 days postexposure.

The average normal corneal tensions as shown in Table 7 may explain some of the differences between this investigation and the pilot study. The low tension in the cornea of the rhesus monkey may increase the susceptibility of this species to collagen shrinkage effects as compared to the rabbit. Probably of greater significance, however, is the fact that the monkey was under general anesthesia during the corneal curvature measurements while the rabbits were not. Blood pressure and intraocular

pressure decrease under general anesthesia, and this would result in a decrease of corneal curvature. Unfortunately, the pilot study reported on only one monkey.

Other studies (29, 30, 33), describing corneal curvature decrease by experimental thermokeratoplasty, have used a heated metal probe applied directly to the cornea. Application of the probe was described as "with gentle pressure." This procedure was followed by application of a Griffin bandage lens during the healing stage, and then a conventional contact lens was applied for optical improvement. Contact lenses acting as pressure bandages may control stromal edema and help sustain corneal flattening. A dramatic degree of corneal flattening by the heated probe method has also been reported in experiments using freshly enucleated pig and human eyes (29). The results are not surprising, since an enucleated eye is flaccid, and there would be little resistance to the hydrothermal shrinkage of the corneal collagen fibers. These differences in experimental approaches also must be considered in assessing the results of the present study.

It is obvious that any experimental or clinical procedure which alters the corneal radius of curvature also effectively alters the total refractive error of the eye. From a therapeutic point of view, it would be highly desirable to develop an acceptable technique that would eliminate the need for optical devices to correct ametropia or, at least, be effective in the reduction of high or malignant refractive errors. However, in the field of laser safety, interest is weighted more towards the prevention of personnel exposure and the potential operational impact when personnel with normal corneas are exposed to coherent thermal radiation. In either case, a common interest exists in terms of the change in corneal refraction caused by a change of corneal curvature after the exposure.

The most recent, and probably the most comprehensive, study (42) of this relationship found that refractive error change (ΔRE) produced by induced corneal curvature change (ΔK) is given by the regression equation

$$\Delta RE = (0.68)(\Delta K) + 0.72 \quad (D.) \quad (10)$$

This equation is based on the use of spherical equivalents and is derived from orthokeratologic data on 181 human eyes. Although the data used in deriving this equation includes corneal curvature changes only through a magnitude of about 2.62 D., it may be useful in estimating changes outside this range until further research can expand the range of the refractive-error/corneal-curvature relationship. Such estimates, however, must be used with extreme caution since equations of this type may produce large errors outside the range of the data used to determine the equation. With this limitation in mind, we have used the equation to prepare columns 1 and 2 of Table 8 so that at least an estimate of refractive error change can be made from the corneal curvature changes we have reported in spherical equivalents in Appendix B.

TABLE 8. RELATION BETWEEN CORNEAL CURVATURE CHANGE (ΔK), REFRACTIVE ERROR CHANGE (ΔRE), AND EXPECTED VISUAL ACUITY (VA) FOR ABSOLUTE REFRACTIVE ERROR GIVEN BY ΔRE .

1 $\Delta K(D.)$	2 $\Delta RE(D.)$	3 Expected VA
0.50	1.06	20/50
1.00	1.40	20/70
1.50	1.74	20/100
2.00	2.08	20/150
2.50	2.42	20/200
3.00 ^a	2.76	-
4.00	3.44	20/300
5.00	4.12	20/400
10.00	7.52	-
15.00	10.92	-
20.00	14.32	-

^aThe relationship between a ΔK greater than 2.62 D. and ΔRE has not yet been determined experimentally, and these estimates require caution in application.

The effect of refractive error change on visual acuity is influenced by several variables, e.g., age, type of refractive error (i.e., myopia or hyperopia), pupil size, amplitude of accommodation, etc. As an example, a change from emmetropia to 1.00 D. of myopia would probably drop visual acuity from 20/20 to 20/50; on the other hand, a change from emmetropia to 1.00 D. of hyperopia would produce no change from 20/20 whatsoever providing that the subject had sufficient amplitude of accommodation available to compensate for the refractive error change. However, the latter comparison is somewhat oversimplified because, as anyone who has tried to wear a 1.00 D. spectacle overcorrection can attest (thus producing a state of simulated hyperopia), ocular discomfort and general visual inefficiency are apparent in a very few moments. If one arbitrarily accepts a 1.00 D. change in refractive error as the point at which serious effects on visual efficiency or function begin to occur, then by equation 10 (and Table 8), even a 0.50 D. change in corneal radius of curvature becomes significant to the subject and his ability to carry out routine tasks, irrespective of the visual acuity outcome.

In combination with refractive error change, visual acuity data are important, however, particularly in the area of injury assessment. Column 3 of Table 8 provides estimates of visual acuities expected for given degrees of ametropia--i.e., simple myopia or simple uncompensated hyperopia. These estimates are a composite summary of an in-depth literature review by Borish (18) on this subject. Some of the acuities presented are modified slightly to fit the refractive error values stated in column 2 of the table.

The foregoing discussion of the experimental results illustrates the complex effects that can occur following exposure to IR laser radiation. The results demonstrate the importance of adequate protective measures for personnel who are subject to possible accidental (or hostile) exposure to infrared lasers. The data should also be of value to those clinicians faced with making medicolegal assessments and, in another vein, to those clinicians currently attempting to perfect thermokeratoplasty techniques for the treatment of keratoconus or malignant myopia.

CONCLUSIONS AND RECOMMENDATIONS

1. The ED₅₀ estimate of the 30-min postexposure minimum visible lesion found in this study is a factor of 12 above the MPE allowed in the current ANSI standard. A factor of 10 between the ED₅₀ and MPE is generally accepted as an adequate and necessary safety margin; therefore, the existing safety standard is considered satisfactory.

2. Corneal curvature changes and/or changes in corneal homogeneity resulting from CO₂ laser radiation frequently persist longer than lesions visible by slit lamp examination. Assessment of corneal injury from exposure of personnel to infrared laser radiation must consider these phenomena during the postexposure recovery phases. In evaluating these cases, it would be extremely helpful to have recent preexposure (i.e., preinjury) corneal curvature measurements on record in the personnel health folder for comparisons.

3. Lesions within the pupillary area of the cornea and persisting postlesion corneal curvature changes will have some impact on visual acuity. As a consequence, the visual evoked response (VER) should also manifest change from a normal baseline configuration. A follow-on experiment using the VER to quantify the functional vision effects and the changes that occur with time as a result of exposure to infrared laser radiation is recommended.

4. At the present time, treatment of keratoconus and malignant myopia by thermokeratoplasty is accomplished by means of a heated metal probe applied briefly to the corneal surface. Egbert and Maher (4) have pointed out that this clinical technique can be enhanced by the use of an infrared laser beam to heat the stroma. The results of the present study also indicate that laser thermokeratoplasty holds promise. However, considerably more effort is required to determine treatment parameters that are dependable and predictable with minimal side effects. The infrared laser wavelengths most applicable for successful thermokeratoplasty can be predicted using present mathematical models but must be verified by experimental data. It may also be necessary to quantify the relative importance of intraocular pressure, corneal radius of curvature, and corneal thickness in the pretreatment condition to obtain desired results. The somewhat nebulous role played by this triad may be a key factor in the prognosis expected with either thermokeratoplasty or orthokeratology.

REFERENCES

1. Borland, R. G., et al. Threshold levels for damage of the cornea following irradiation by a continuous wave carbon dioxide (10.6 μ m) laser. *Nature* 234:151-152 (1971).
2. Byer, H. H., et al. Determination of the thresholds of CO₂ laser corneal damage to owl monkeys, rhesus monkeys, and Dutch belted rabbits. Memorandum Report M72-3-1, Dept. of the Army, Frankford Arsenal, Philadelphia, Pa, Feb 1972.
3. Campbell, C. J., et al. Ocular effects produced by experimental lasers. *Am J Ophthalmol* 66:604-614 (1968).
4. Egbert, D. E., and E. F. Maher. Corneal damage thresholds for infrared laser exposure: Empirical data, model predictions, and safety standards. SAM-TR-77-29, Dec 1977.
5. Fine, B. S., et al. Preliminary observations on ocular effects of high-power continuous CO₂ laser irradiation. *Am J Ophthalmol* 64:209-222 (1967).
6. Gallagher, J. T. Corneal curvature changes due to exposure to a carbon dioxide laser: A preliminary report. SAM-TR-75-44, Dec 1975.
7. Gullberg, K., et al. Carbon dioxide laser hazards to the eye. *Nature* 215:857-858 (1967).
8. MacKeen, D., et al. Anterior chamber measurements on CO₂ laser corneal irradiation. *Invest Ophthalmol* 9:366-371 (1970).
9. Stuck, B. E. Corneal damage thresholds for carbon dioxide laser irradiation. Joint AMRDC-AMC Laser Safety Team, Frankford Arsenal, Philadelphia, Pa, June 1972.
10. Stuck, B. E. U.S. CO₂ literature review. Joint AMRDC-AMC Laser Safety Team, Frankford Arsenal, Philadelphia, Pa, June 1972.
11. Mikesell, G. W., Jr. Corneal temperatures: A study of normal and laser-injured corneas in the Dutch belted rabbit. *Am J Optom Physiol Optics* 55(2):108-115 (1978).
12. El Hage, S. G. A new photokeratoscopic technique. *Opt Eng* 15:308-311 (1976).
13. Fincham, W. H. A. *Optics*, 5th ed., pp.42, 83-84, 91-92, 127. London: Hatton Press Ltd., 1947.
14. Emsley, H. H. *Visual optics*, 4th ed., pp.236-237, 298-321. London: Hatton Press Ltd., 1948.

15. Mountcastle, V. B. Medical physiology, 12th ed., vol. II, pp.1547-1548. St. Louis: The C. V. Mosby Co., 1968.
16. Vaughn, D., et al. General ophthalmology, 5th ed., pp.27-28, 292-293. Los Altos, Calif.: Lange Medical Publications, 1968.
17. Davson, H. The physiology of the eye, 2d ed., pp.55-59, 454-456. Boston: Little, Brown and Co., 1963.
18. Borish, I. M. Clinical refraction, 3d ed., pp.361-367, 518-519, 617-657. Chicago: The Professional Press, Inc., 1970.
19. Bausch and Lomb Ophthalmic reference book, pp.93-120. Rochester, N.Y.: Bausch and Lomb Optical Co., 1947.
20. Atkinson, T. G. Oculo-refractive cyclopedia and dictionary, pp. 201-204, 242-250. Chicago: The Professional Press, Inc., 1944.
21. Ryer, E. L., and E. E. Hotaling. Ophthalmometry. Southbridge, Mass: American Optical Co., 1945.
22. Girard, L. J. Corneal contact lenses, pp.74-76. St. Louis: The C. V. Mosby Co., 1964.
23. Sinn, F. W. Manual of physical and geometrical optics, p. 72. Philadelphia: College Offset Press, Pennsylvania State College of Optometry, no date.
24. Schaum, D. College physics, 6th ed., pp.108-109, 222-225. New York, St. Louis, San Francisco: McGraw-Hill Book Co., 1961.
25. Emsley, H. H., and W. Swaine. Ophthalmic lenses, 5th ed., pp.12-13. London: Hatton Press Ltd., 1946.
26. Blaker, J. W. Focus on physics-optics I, pp.41-44, 51-52. New York: Barnes and Noble, Inc., 1969.
27. Perera, C. A. May's manual of the diseases of the eye, 19th ed., pp.29-31. Baltimore: Williams and Wilkins Co., 1947.
28. American national standard for the safe use of lasers. ANSI Z136.1-1976, New York, 1976.
29. Gasset, A. R., et al. Thermokeratoplasty. Trans Am Acad Ophthalmol Otolaryngol 77:441-454 (1973).
30. Shaw, E. L., and A. R. Gasset. Thermokeratoplasty (TKP) temperature profile. Invest Ophthalmol 13:181-186 (1974).
31. Stringer, H., and J. Parr. Shrinkage temperature of eye collagen. Nature 204:1307 (1964).

32. Gustavson, K. H. The chemistry and reactivity of collagen, pp.211-227. New York: Academic Press, 1956.
33. Fogle, J. A., et al. Damage to epithelial basement membrane by thermokeratoplasty. *Am J Ophthalmol* 83 (3):392-401 (1977).
34. Moses, R. A. Adler's physiology of the eye, 5th ed., pp.35-53, 262-265, 581-582. St. Louis: The C. V. Mosby Co., 1970.
35. Davson, H. The eye, 2d ed., vol. I, pp.205, 491, 512-522. New York and London: Academic Press, 1969.
36. Duke-Elder, S. The physiology of the eye and of vision, vol. IV, pp. 345-347. St. Louis: The C. V. Mosby Co., 1968.
37. Nash, W. A. Strength of materials, 2d ed., pp.40-45. New York, St. Louis, and San Francisco: McGraw-Hill Book Co., 1972.
38. Mountcastle, V. B. Medical physiology, 12th ed., vol. 1, pp.107-109. St. Louis: The C. V. Mosby Co., 1968.
39. Timoshenko, S. Strength of materials, 3d ed., pt. 2, p. 236. Princeton, N.J.: D. Van Nostrand Co., Inc., 1955.
40. Prince, J. H. The rabbit in eye research, pp.86-89, 155. Springfield: Charles C Thomas, 1964.
41. Gallagher, J. T. Ultrasound measurement of the rhesus monkey eye. Laser Effects Branch, USAF School of Aerospace Medicine, Brooks AFB, Tex. Unpublished data, 1975.
42. Erickson, P., and F. Thorn. Orthokeratology and refractive error. *Am J Optom Physiol Optics* 54(9):581-587 (1977).

APPENDIX A

CORNEAL CURVATURE CHANGES AS A FUNCTION OF TIME

Corneal curvature changes measured in the control and irradiated groups during 365 days postexposure are shown for each variable in Figures A-1 through A-4. In Figures A-1 through A-3, positive changes indicate curvatures greater than baseline, and negative changes indicate curvatures less than baseline. In Figure A-4, positive changes indicate toricity changes from baseline with horizontal curvature greater than the vertical, and negative values represent toricity changes from baseline with vertical curvature greater than the horizontal. The key indicating the average power, P , for the different exposure groups is the same for all figures in this Appendix, i.e.:

C: control

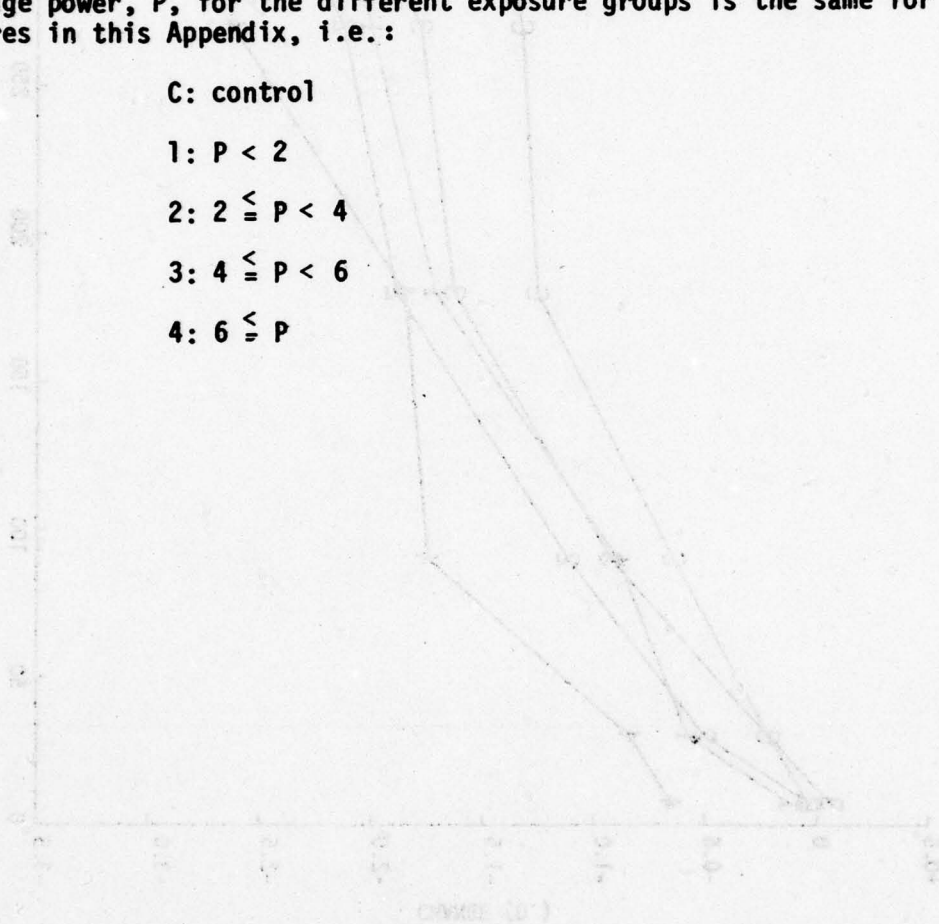
1: $P < 2$

2: $2 \leq P < 4$

3: $4 \leq P < 6$

4: $6 \leq P$

Figure A-1: Corneal curvature changes (D) (mm) (mm)



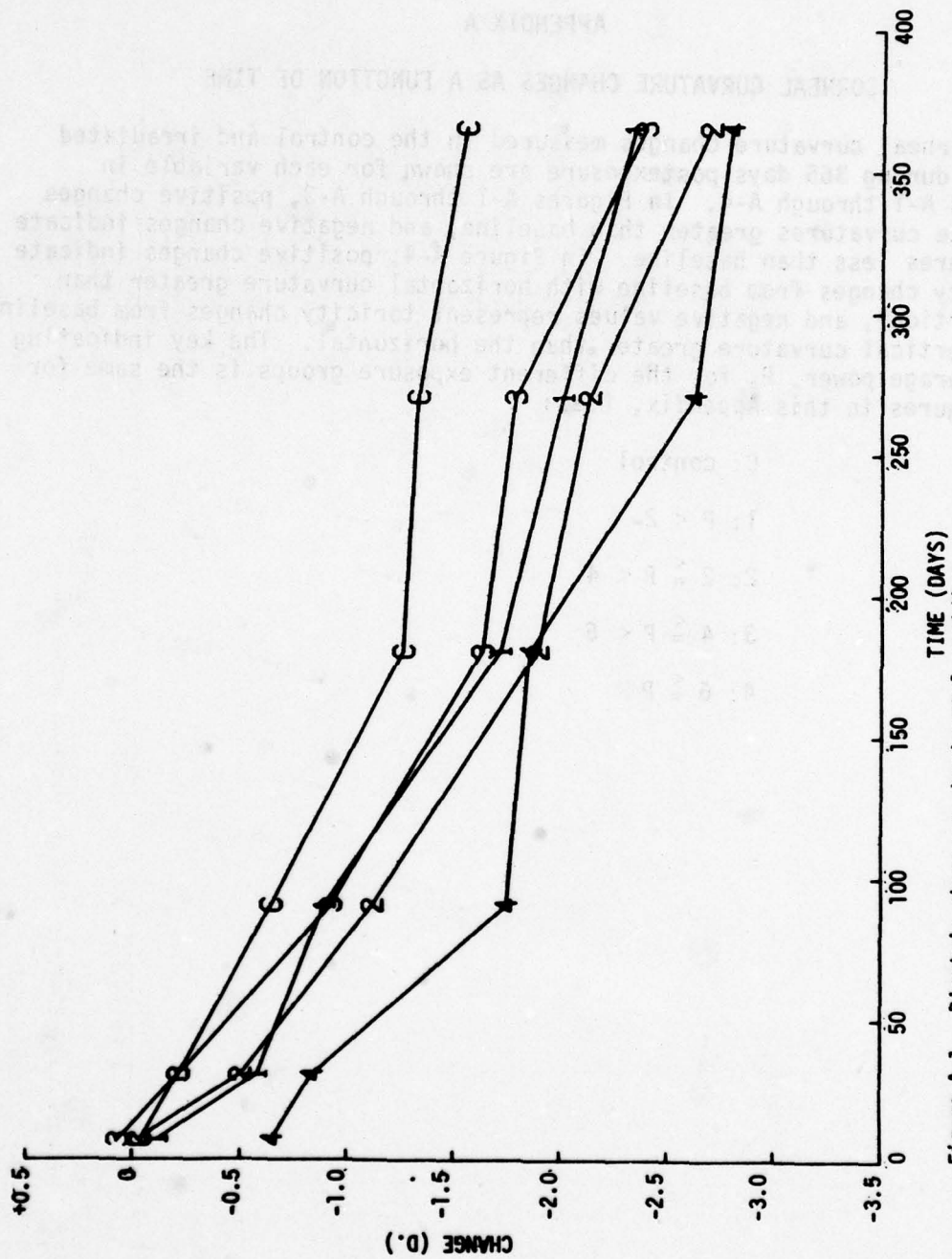


Figure A-1. Dioptric changes: horizontal meridian.

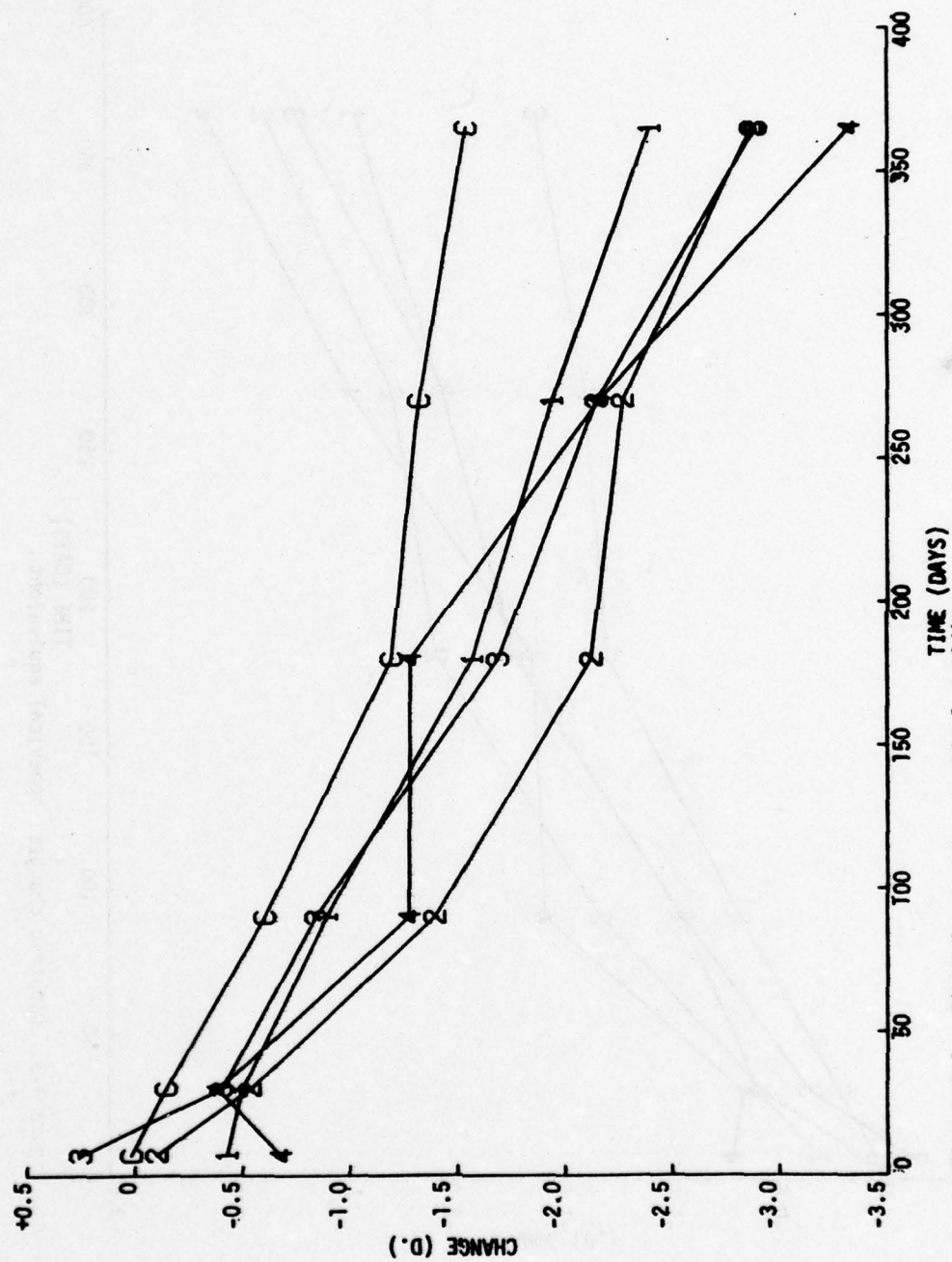


Figure A-2. Dioptric changes: vertical meridian.

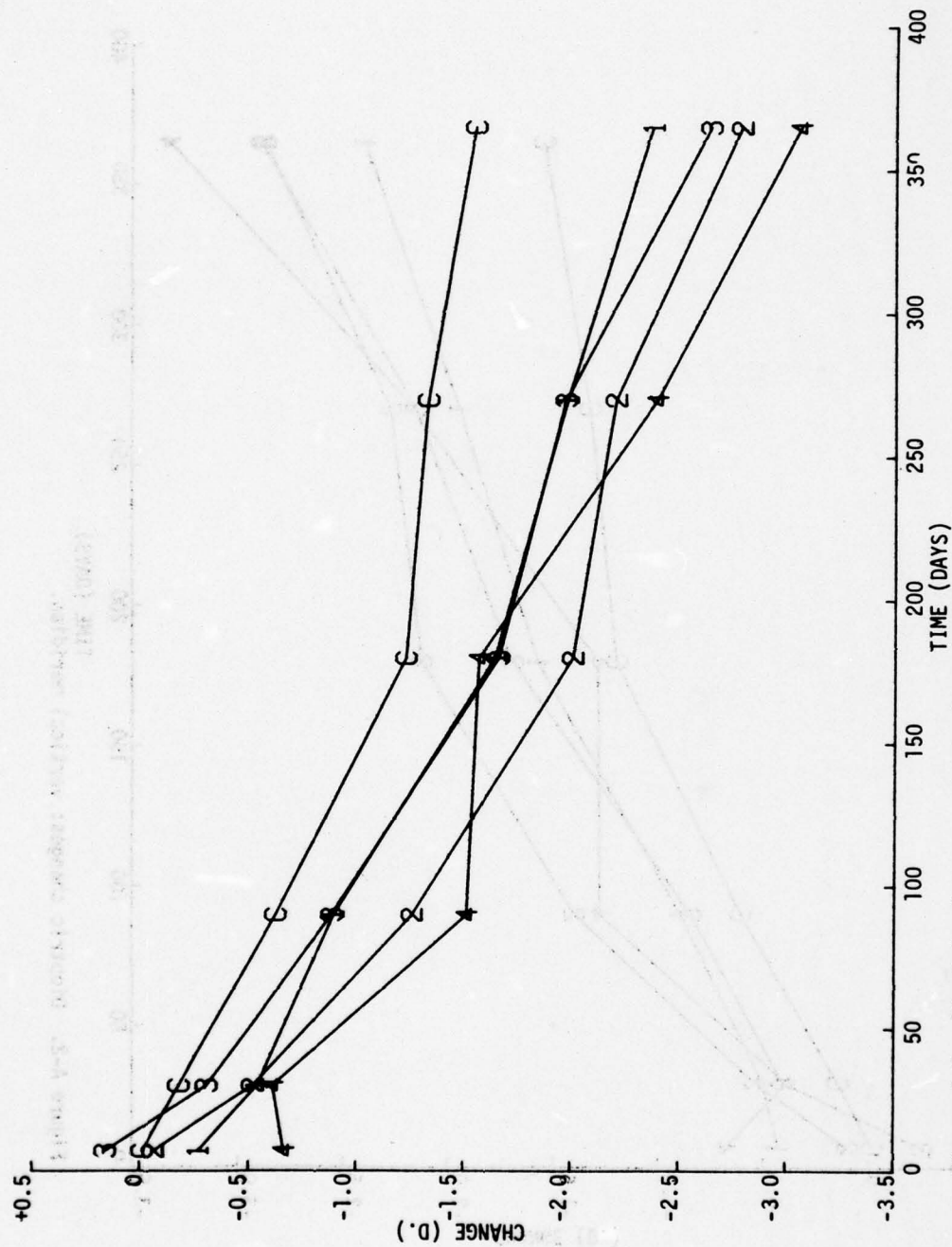


Figure A-3. Dioptric changes: spherical equivalent.

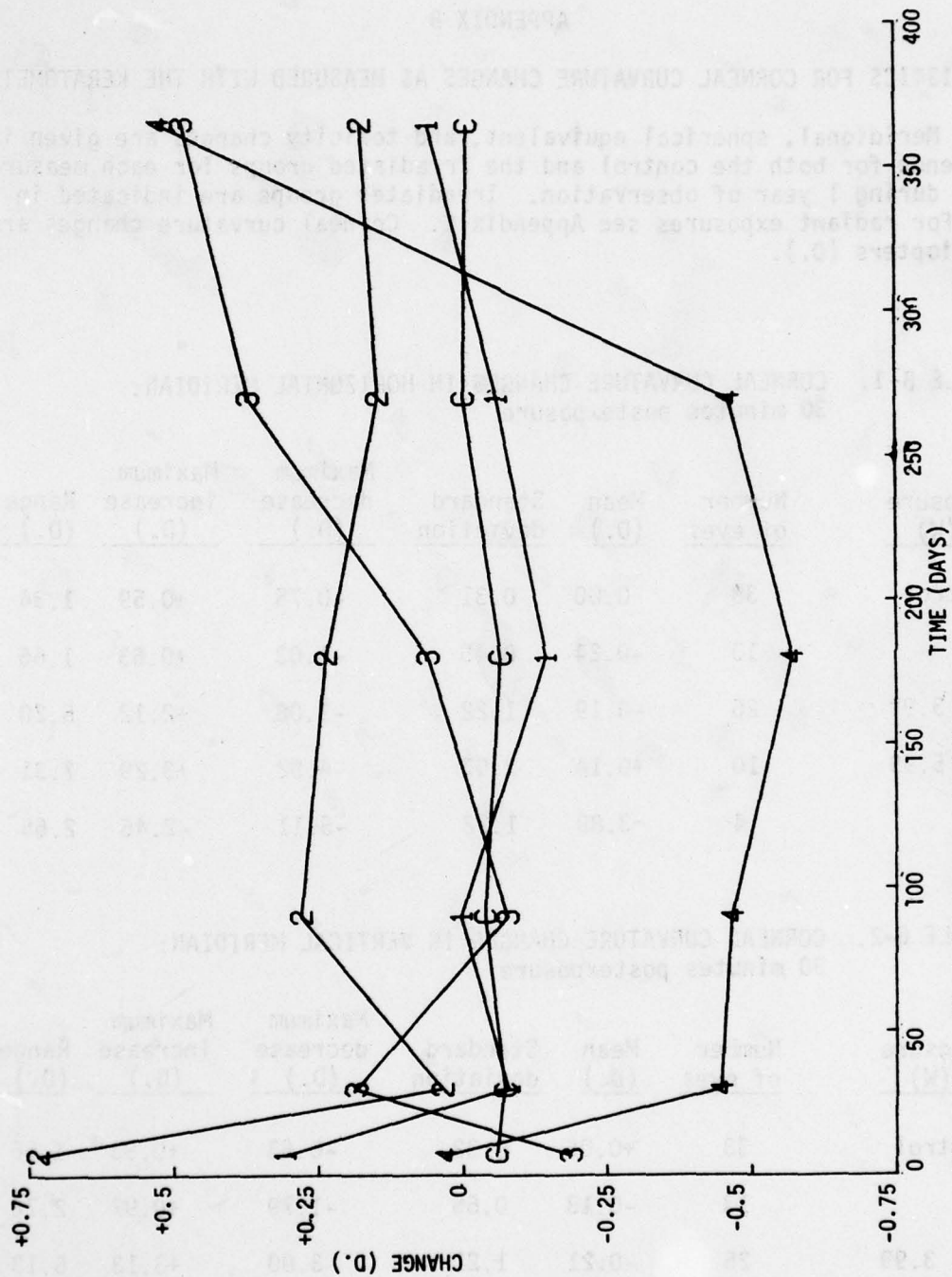


Figure A-4. Dioptric changes: toricity.

APPENDIX B

STATISTICS FOR CORNEAL CURVATURE CHANGES AS MEASURED WITH THE KERATOMETER

Meridional, spherical equivalent, and toricity changes are given in sequence for both the control and the irradiated groups for each measurement during 1 year of observation. Irradiated groups are indicated in W. For radiant exposures see Appendix E. Corneal curvature changes are in diopters (D.).

TABLE B-1. CORNEAL CURVATURE CHANGES IN HORIZONTAL MERIDIAN:
30 minutes postexposure

<u>Exposure (W)</u>	<u>Number of eyes</u>	<u>Mean (D.)</u>	<u>Standard deviation</u>	<u>Maximum decrease (D.)</u>	<u>Maximum increase (D.)</u>	<u>Range (D.)</u>
Control	38	0.00	0.31	-0.75	+0.59	1.34
<2	13	-0.24	0.45	-1.03	+0.63	1.66
2 - 3.99	26	-0.19	1.22	-3.08	+2.12	5.20
4 - 5.99	10	+0.14	2.07	-4.02	+3.29	7.31
<u>≥6</u>	4	-3.89	1.22	-5.11	-2.46	2.65

TABLE B-2. CORNEAL CURVATURE CHANGES IN VERTICAL MERIDIAN:
30 minutes postexposure

<u>Exposure (W)</u>	<u>Number of eyes</u>	<u>Mean (D.)</u>	<u>Standard deviation</u>	<u>Maximum decrease (D.)</u>	<u>Maximum increase (D.)</u>	<u>Range (D.)</u>
Control	38	+0.06	0.32	-0.63	+0.93	1.56
<2	13	-0.13	0.65	-1.79	+0.97	2.76
2 - 3.99	25	-0.21	1.21	-3.00	+3.13	6.13
4 - 5.99	10	-0.20	1.47	-2.97	+1.52	4.49
<u>≥6</u>	4	-5.26	2.57	-8.35	-2.08	6.27

TABLE B-3. CORNEAL SPHERICAL EQUIVALENT CHANGES:
30 minutes postexposure

Exposure (W)	Number of eyes	Mean (D.)	Standard deviation	Maximum decrease (D.)	Maximum increase (D.)	Range (D.)
Control	38	+0.03	0.21	-0.35	+0.44	0.79
<2	13	-0.18	0.38	-1.06	+0.50	1.56
2 - 3.99	25	-0.22	0.88	-2.89	+1.45	4.33
4 - 5.99	10	-0.03	1.39	-3.50	+1.17	4.67
≥6	4	-4.57	1.87	-6.73	-2.27	4.46

TABLE B-4. CORNEAL TORICITY CHANGES:
30 minutes postexposure

Exposure (W)	Number of eyes	Mean (D.)	Standard deviation	Minimum (D.)	Maximum (D.)	Range (D.)
Control	38	0.39	0.27	0.00	1.04	1.04
<2	13	0.64	0.47	0.02	1.47	1.45
2 - 3.99	25	0.97	1.37	0.01	5.17	5.16
4 - 5.99	10	1.42	1.73	0.02	5.49	5.47
≥6	4	1.56	1.25	0.38	3.24	2.86

TABLE B-5. CORNEAL CURVATURE CHANGES IN HORIZONTAL MERIDIAN:
7 days postexposure

<u>Exposure (W)</u>	<u>Number of eyes</u>	<u>Mean (D.)</u>	<u>Standard deviation</u>	<u>Maximum decrease (D.)</u>	<u>Maximum increase (D.)</u>	<u>Range (D.)</u>
Control	38	-0.04	0.33	-0.86	+0.70	1.56
<2	11	-0.12	0.38	-0.59	+0.78	1.37
2 - 3.99	39	-0.03	0.80	-1.85	+2.05	3.90
4 - 5.99	45	+0.04	1.57	-5.90	+4.97	10.87
≥6	39	-0.57	1.34	-3.28	+1.77	5.05

TABLE B-6. CORNEAL CURVATURE CHANGES IN VERTICAL MERIDIAN:
7 days postexposure

<u>Exposure (W)</u>	<u>Number of eyes</u>	<u>Mean (D.)</u>	<u>Standard deviation</u>	<u>Maximum decrease (D.)</u>	<u>Maximum increase (D.)</u>	<u>Range (D.)</u>
Control	38	+0.02	0.40	-0.72	+1.00	1.72
<2	11	-0.43	0.75	-1.94	+0.57	2.51
2 - 3.99	39	-0.10	0.82	-2.55	+2.60	5.15
4 - 5.99	45	+0.22	1.74	-3.55	+6.65	10.20
≥6	39	-0.55	1.63	-4.28	+2.70	6.98

TABLE B-7. CORNEAL SPHERICAL EQUIVALENT CHANGES:
7 days postexposure

<u>Exposure (W)</u>	<u>Number of eyes</u>	<u>Mean (D.)</u>	<u>Standard deviation</u>	<u>Maximum decrease (D.)</u>	<u>Maximum increase (D.)</u>	<u>Range (D.)</u>
Control	38	-0.01	0.30	-0.56	+0.83	1.39
<2	11	-0.27	0.40	-0.81	+0.39	1.20
2 - 3.99	39	-0.06	0.73	-2.18	+1.73	3.91
4 - 5.99	45	+0.13	1.37	-3.41	+4.21	7.62
≥6	39	-0.56	1.31	-3.69	+1.94	5.63

TABLE B-8. CORNEAL TORICITY CHANGES:
7 days postexposure

<u>Exposure (W)</u>	<u>Number of eyes</u>	<u>Mean (D.)</u>	<u>Standard deviation</u>	<u>Minimum (D.)</u>	<u>Maximum (D.)</u>	<u>Range (D.)</u>
Control	38	0.36	0.25	0.01	1.05	1.04
<2	11	0.51	0.78	0.01	2.72	2.71
2 - 3.99	39	0.55	0.40	0.03	2.13	2.10
4 - 5.99	45	1.05	1.55	0.01	8.38	8.37
≥6	39	1.04	0.98	0.04	3.53	3.49

TABLE B-9. CORNEAL CURVATURE CHANGES IN HORIZONTAL MERIDIAN:
30 days postexposure

<u>Exposure (W)</u>	<u>Number of eyes</u>	<u>Mean (D.)</u>	<u>Standard deviation</u>	<u>Maximum decrease (D.)</u>	<u>Maximum increase (D.)</u>	<u>Range (D.)</u>
Control	38	-0.22	0.43	-1.13	+1.00	2.13
<2	11	-0.58	0.44	-1.33	+0.09	1.42
2 - 3.99	39	-0.50	0.59	-1.53	+1.01	2.54
4 - 5.99	47	-0.22	1.23	-2.79	+4.50	7.29
<u>>6</u>	35	-0.59	1.54	-5.87	+3.26	9.13

TABLE B-10. CORNEAL CURVATURE CHANGES IN VERTICAL MERIDIAN:
30 days postexposure

<u>Exposure (W)</u>	<u>Number of eyes</u>	<u>Mean (D.)</u>	<u>Standard deviation</u>	<u>Maximum decrease (D.)</u>	<u>Maximum increase (D.)</u>	<u>Range (D.)</u>
Control	38	-0.15	0.41	-0.84	+1.15	1.99
<2	11	-0.50	0.40	-1.34	-0.10	1.24
2 - 3.99	39	-0.54	0.60	-1.75	+1.02	2.77
4 - 5.99	47	-0.40	1.48	-4.75	+5.67	10.42
<u>>6</u>	35	-0.37	1.78	-4.61	+4.59	9.20

TABLE B-11. CORNEAL SPHERICAL EQUIVALENT CHANGES:
30 days postexposure

<u>Exposure (W)</u>	<u>Number of eyes</u>	<u>Mean (D.)</u>	<u>Standard deviation</u>	<u>Maximum decrease (D.)</u>	<u>Maximum increase (D.)</u>	<u>Range (D.)</u>
Control	38	-0.18	0.33	-0.78	+1.08	1.86
<2	11	-0.54	0.32	-1.05	-0.10	0.96
2 - 3.99	39	-0.52	0.53	-1.43	+0.81	2.24
4 - 5.99	47	-0.31	1.08	-2.60	+3.21	5.81
≥6	35	-0.48	1.32	-5.24	+2.28	7.52

TABLE B-12. CORNEAL TORICITY CHANGES:
30 days postexposure

<u>Exposure (W)</u>	<u>Number of eyes</u>	<u>Mean (D.)</u>	<u>Standard deviation</u>	<u>Minimum (D.)</u>	<u>Maximum (D.)</u>	<u>Range (D.)</u>
Control	38	0.41	0.32	0.02	1.15	1.13
<2	11	0.44	0.28	0.06	1.15	1.09
2 - 3.99	39	0.43	0.32	0.04	1.13	1.09
4 - 5.99	47	1.03	1.27	0.03	5.21	5.18
≥6	35	1.33	1.53	0.14	7.37	7.23

TABLE B-13. CORNEAL CURVATURE CHANGES IN HORIZONTAL MERIDIAN:
90 days postexposure

<u>Exposure (W)</u>	<u>Number of eyes</u>	<u>Mean (D.)</u>	<u>Standard deviation</u>	<u>Maximum decrease (D.)</u>	<u>Maximum increase (D.)</u>	<u>Range (D.)</u>
Control	36	-0.65	0.71	-2.63	+0.93	3.56
<2	9	-0.90	0.57	-1.49	+0.37	1.86
2 - 3.99	39	-1.12	1.03	-5.05	+0.77	5.82
4 - 5.99	46	-0.93	1.08	-4.93	+1.41	6.34
≥6	37	-1.66	2.55	-10.18	+4.03	14.21

TABLE B-14. CORNEAL CURVATURE CHANGES IN VERTICAL MERIDIAN:
90 days postexposure

<u>Exposure (W)</u>	<u>Number of eyes</u>	<u>Mean (D.)</u>	<u>Standard deviation</u>	<u>Maximum decrease (D.)</u>	<u>Maximum increase (D.)</u>	<u>Range (D.)</u>
Control	36	-0.60	0.75	-1.98	+1.33	3.31
<2	9	-0.91	0.56	-1.91	-0.26	1.65
2 - 3.99	39	-1.40	0.91	-4.33	+1.14	5.47
4 - 5.99	46	-0.86	1.00	-3.86	+1.45	5.31
≥6	37	-1.31	1.78	-5.79	+2.44	8.23

TABLE B-15. CORNEAL SPHERICAL EQUIVALENT CHANGES: 90 days postexposure

<u>Exposure (W)</u>	<u>Number of eyes</u>	<u>Mean (D.)</u>	<u>Standard deviation</u>	<u>Maximum decrease (D.)</u>	<u>Maximum increase (D.)</u>	<u>Range (D.)</u>
Control	36	-0.63	0.67	-2.29	+1.13	3.42
<2	9	-0.91	0.52	-1.70	+0.02	1.72
2 - 3.99	39	-1.26	0.93	-4.69	+0.68	5.37
4 - 5.99	46	-0.90	0.90	-4.12	+0.65	4.77
≥6	37	-1.49	1.71	-6.07	+1.60	7.67

TABLE B-16. CORNEAL TORICITY CHANGES: 90 days postexposure

<u>Exposure (W)</u>	<u>Number of eyes</u>	<u>Mean (D.)</u>	<u>Standard deviation</u>	<u>Minimum (D.)</u>	<u>Maximum (D.)</u>	<u>Range (D.)</u>
Control	36	0.44	0.40	0.01	1.29	1.28
<2	9	0.36	0.22	0.06	0.71	0.65
2 - 3.99	39	0.44	0.43	0.01	1.93	1.92
4 - 5.99	46	0.72	0.76	0.01	3.73	3.72
≥6	37	1.53	2.32	0.03	9.37	9.34

TABLE B-17. CORNEAL CURVATURE CHANGES IN HORIZONTAL MERIDIAN:
180 days postexposure

<u>Exposure (W)</u>	<u>Number of eyes</u>	<u>Mean (D.)</u>	<u>Standard deviation</u>	<u>Maximum decrease (D.)</u>	<u>Maximum increase (D.)</u>	<u>Range (D.)</u>
Control	36	-1.27	0.96	-3.31	+0.50	3.81
<2	9	-1.72	0.45	-2.17	-1.01	1.16
2 - 3.99	39	-1.89	1.15	-5.73	-0.16	5.57
4 - 5.99	44	-1.66	1.19	-4.42	+0.82	5.24
≥6	35	-1.79	2.34	-10.18	+3.41	13.59

TABLE B-18. CORNEAL CURVATURE CHANGES IN VERTICAL MERIDIAN:
180 days postexposure

<u>Exposure (W)</u>	<u>Number of eyes</u>	<u>Mean (D.)</u>	<u>Standard deviation</u>	<u>Maximum decrease (D.)</u>	<u>Maximum increase (D.)</u>	<u>Range (D.)</u>
Control	36	-1.20	0.97	-2.95	+1.19	4.14
<2	9	-1.59	0.83	-2.53	+0.02	2.55
2 - 3.99	39	-2.12	1.10	-5.36	-0.44	4.92
4 - 5.99	44	-1.72	1.22	-4.97	+2.50	7.47
≥6	35	-1.32	1.76	-4.99	+3.21	8.20

TABLE B-19. CORNEAL SPHERICAL EQUIVALENT CHANGES: 180 days postexposure

<u>Exposure (W)</u>	<u>Number of eyes</u>	<u>Mean (D.)</u>	<u>Standard deviation</u>	<u>Maximum decrease (D.)</u>	<u>Maximum increase (D.)</u>	<u>Range (D.)</u>
Control	36	-1.23	0.93	-2.87	+0.76	3.62
<2	9	-1.66	0.62	-2.27	-0.50	1.77
2 - 3.99	39	-2.01	1.10	-5.55	-0.30	5.25
4 - 5.99	44	-1.69	1.03	-4.70	+0.31	5.00
≥6	35	-1.55	1.76	-6.64	+1.62	8.26

TABLE B-20. CORNEAL TORICITY CHANGES: 180 days postexposure

<u>Exposure (W)</u>	<u>Number of eyes</u>	<u>Mean (D.)</u>	<u>Standard deviation</u>	<u>Minimum (D.)</u>	<u>Maximum (D.)</u>	<u>Range (D.)</u>
Control	36	0.38	0.33	0.01	1.40	1.39
<2	9	0.37	0.31	0.01	1.03	1.02
2 - 3.99	39	0.44	0.32	0.00	1.43	1.43
4 - 5.99	44	0.70	1.05	0.01	4.62	4.61
≥6	35	1.37	1.77	0.05	7.09	7.04

TABLE B-21. CORNEAL CURVATURE CHANGES IN HORIZONTAL MERIDIAN:
270 days postexposure

<u>Exposure (W)</u>	<u>Number of eyes</u>	<u>Mean (D.)</u>	<u>Standard deviation</u>	<u>Maximum decrease (D.)</u>	<u>Maximum increase (D.)</u>	<u>Range (D.)</u>
Control	34	-1.30	1.20	-3.93	+1.57	5.50
<2	9	-2.01	0.68	-2.80	-0.50	2.30
2 - 3.99	36	-2.06	1.29	-6.22	-0.09	6.13
4 - 5.99	40	-1.78	1.82	-5.41	+6.13	11.54
≥6	33	-2.61	2.73	-12.49	+2.03	14.52

TABLE B-22. CORNEAL CURVATURE CHANGES IN VERTICAL MERIDIAN:
270 days postexposure

<u>Exposure (W)</u>	<u>Number of eyes</u>	<u>Mean (D.)</u>	<u>Standard deviation</u>	<u>Maximum decrease (D.)</u>	<u>Maximum increase (D.)</u>	<u>Range (D.)</u>
Control	34	-1.32	1.27	-3.57	+1.46	5.03
<2	9	-1.96	0.89	-2.97	-0.36	2.61
2 - 3.99	36	-2.21	1.11	-5.17	0.00	5.17
4 - 5.99	40	-2.13	1.09	-5.06	-0.29	4.77
≥6	33	-2.18	2.89	-13.17	+2.60	15.77

TABLE B-23. CORNEAL SPHERICAL EQUIVALENT CHANGES: 270 days postexposure

<u>Exposure (W)</u>	<u>Number of eyes</u>	<u>Mean (D.)</u>	<u>Standard deviation</u>	<u>Maximum decrease (D.)</u>	<u>Maximum increase (D.)</u>	<u>Range (D.)</u>
Control	34	-1.31	1.22	-3.75	+1.52	5.27
<2	9	-1.99	0.76	-2.69	-0.43	2.26
2 - 3.99	36	-2.14	1.18	-5.70	-0.05	5.65
4 - 5.99	40	-1.95	1.22	-4.77	+1.41	6.17
≥6	33	-2.39	2.49	-10.32	+1.32	11.64

TABLE B-24. CORNEAL TORICITY CHANGES: 270 days postexposure

<u>Exposure (W)</u>	<u>Number of eyes</u>	<u>Mean (D.)</u>	<u>Standard deviation</u>	<u>Minimum (D.)</u>	<u>Maximum (D.)</u>	<u>Range (D.)</u>
Control	34	0.31	0.29	0.00	1.03	1.03
<2	9	0.34	0.25	0.04	0.80	0.76
2 - 3.99	36	0.47	0.29	0.05	1.11	1.06
4 - 5.99	40	0.93	1.51	0.00	9.45	9.45
≥6	33	1.62	2.07	0.01	8.85	8.84

TABLE B-25. CORNEAL CURVATURE CHANGES IN HORIZONTAL MERIDIAN:
365 days postexposure

<u>Exposure (W)</u>	<u>Number of eyes</u>	<u>Mean (D.)</u>	<u>Standard deviation</u>	<u>Maximum decrease (D.)</u>	<u>Maximum increase (D.)</u>	<u>Range (D.)</u>
Control	32	-1.50	1.42	-4.78	+1.07	5.85
<2	9	-2.35	0.90	-3.16	-0.43	2.73
2 - 3.99	36	-2.64	1.52	-6.94	-0.63	6.31
4 - 5.99	40	-2.38	1.73	-5.73	+2.24	7.97
<u>>6</u>	33	-2.78	3.37	-12.01	+8.88	20.89

TABLE B-26. CORNEAL CURVATURE CHANGES IN VERTICAL MERIDIAN:
365 days postexposure

<u>Exposure (W)</u>	<u>Number of eyes</u>	<u>Mean (D.)</u>	<u>Standard deviation</u>	<u>Maximum decrease (D.)</u>	<u>Maximum increase (D.)</u>	<u>Range (D.)</u>
Control	32	-1.50	1.42	-4.25	+1.36	5.61
<2	9	-2.42	0.95	-3.39	-0.72	2.67
2 - 3.99	36	-2.82	1.45	-6.47	-0.29	6.18
4 - 5.99	40	-2.90	1.35	-6.84	-0.06	6.78
<u>>6</u>	33	-3.33	3.01	-12.88	+1.43	14.31

TABLE B-27. CORNEAL SPHERICAL EQUIVALENT CHANGES: 365 days postexposure

<u>Exposure (W)</u>	<u>Number of eyes</u>	<u>Mean (D.)</u>	<u>Standard deviation</u>	<u>Maximum decrease (D.)</u>	<u>Maximum increase (D.)</u>	<u>Range (D.)</u>
Control	32	-1.50	1.41	-4.50	+1.22	5.71
<2	9	-2.38	0.91	-3.23	-0.58	2.66
2 - 3.99	36	-2.73	1.42	-6.71	-0.46	6.25
4 - 5.99	40	-2.64	1.43	-5.71	+0.22	5.93
<u>>6</u>	33	-3.06	2.93	-12.45	+3.74	16.18

TABLE B-28. CORNEAL TORICITY CHANGES: 365 days postexposure

<u>Exposure (W)</u>	<u>Number of eyes</u>	<u>Mean (D.)</u>	<u>Standard deviation</u>	<u>Minimum (D.)</u>	<u>Maximum (D.)</u>	<u>Range (D.)</u>
Control	32	0.35	0.25	0.01	0.96	0.95
<2	9	0.26	0.19	0.03	0.60	0.57
2 - 3.99	36	0.56	0.66	0.01	3.73	3.72
4 - 5.99	40	0.85	1.03	0.01	5.87	5.86
<u>>6</u>	33	1.56	2.06	0.00	10.29	10.29

APPENDIX C

STATISTICS FOR CORNEAL CURVATURE CHANGES AS MEASURED WITH THE PHOTOKERATOSCOPE

The format of Tables C-1 through C-7 in this Appendix follows that of the meridional tables of Appendix B with the exception that the tables are expanded to include data from each of the photokeratoscope rings. Table C-8 provides a summary of horizontal meridian mean changes from ring II of the photokeratoscope and that of the keratometer. All changes in corneal curvature are in diopters (D.). For radiant exposures see Appendix E.

Exposure (W)	Mean of area (D.)	Standard deviation (D.)	Minimum (D.)	Maximum (D.)	Range (D.)
Control	0.35	0.25	0.00	0.95	0.95
5	0.50	0.19	0.03	0.90	0.87
5 - 3.92	0.56	0.06	0.01	0.73	0.72
4 - 2.50	0.62	0.03	0.01	0.67	0.66
3	0.70	0.03	0.00	0.93	0.93

TABLE C-1. CORNEAL CURVATURE CHANGES: 30 minutes postexposure

Exposure (W)	Ring	Number of eyes	Mean (D.)	Standard deviation	Maximum decrease (D.)	Maximum increase (D.)	Range (D.)
Nonirradiated	I	8	-0.07	0.27	-0.41	+0.46	0.87
	II	8	+0.06	0.37	-0.57	+0.53	1.10
	III	8	0.00	0.33	-0.55	+0.59	1.14
	IV	8	+0.08	0.34	-0.26	+0.77	1.03
	V	8	+0.02	0.37	-0.34	+0.89	1.23
<2	I	11	+0.04	1.24	-3.12	+1.75	4.87
	II	11	-0.24	1.02	-3.02	+0.49	3.51
	III	11	-0.12	0.99	-2.88	+0.75	3.63
	IV	11	-0.37	0.96	-3.04	+0.31	3.35
	V	11	-0.29	0.87	-2.85	+0.28	3.13
2-3.99	I	26	-0.49	1.79	-4.89	+2.63	7.52
	II	27	-0.34	1.54	-5.14	+2.06	7.20
	III	27	-0.34	1.22	-4.30	+2.01	6.31
	IV	28	-0.12	1.10	-3.91	+2.29	6.20
	V	29	-0.09	1.44	-3.69	+5.05	8.74
4-5.99	I	16	-0.47	1.21	-3.25	+1.42	4.67
	II	16	+0.03	1.02	-1.93	+1.47	3.40
	III	16	-0.01	0.78	-1.45	+1.72	3.17
	IV	17	-0.04	0.82	-1.41	+0.80	2.21
	V	17	-0.09	0.75	-1.46	+0.59	2.05
>6	I	5	+0.62	1.22	-0.70	+2.42	3.12
	II	5	+0.52	1.31	-0.62	+1.94	2.56
	III	7	-0.16	1.46	-1.94	+2.25	4.19
	IV	7	-1.55	1.85	-5.34	+0.12	5.46
	V	7	-0.97	1.22	-2.78	+0.24	3.02
Keratometer control			0.00	0.31	-0.75	+0.59	1.34

TABLE C-2. CORNEAL CURVATURE CHANGES: 7 days postexposure

Exposure (W)	Ring	Number of eyes	Mean (D.)	Standard deviation	Maximum decrease (D.)	Maximum increase (D.)	Range (D.)
Nonirradiated	I	8	+0.41	0.33	-0.05	+0.89	0.94
	II	8	+0.43	0.48	-0.28	+1.12	1.40
	III	8	+0.30	0.40	-0.26	+0.84	1.10
	IV	8	+0.16	0.45	-0.60	+0.78	1.38
	V	8	+0.17	0.51	-0.72	+0.89	1.61
<2	I	5	+0.56	1.31	-0.38	+2.85	3.23
	II	5	+0.27	0.64	-0.54	+1.24	1.78
	III	5	-0.17	0.33	-0.48	+0.22	0.70
	IV	5	-0.35	0.36	-0.75	+0.04	0.79
	V	5	-0.43	0.46	-1.16	+0.10	1.26
2-3.99	I	36	-0.13	1.31	-2.84	+3.16	6.00
	II	36	-0.07	0.99	-2.26	+1.46	3.72
	III	36	-0.27	0.96	-3.64	+1.05	4.69
	IV	36	-0.14	0.68	-1.49	+0.99	2.48
	V	36	-0.12	0.61	-1.68	+0.83	2.51
4-5.99	I	42	-0.01	2.04	-7.74	+6.06	13.80
	II	43	-0.07	1.24	-4.59	+3.81	8.40
	III	44	+0.04	0.81	-1.80	+2.50	4.30
	IV	44	-0.12	0.73	-2.64	+1.55	4.19
	V	41	-0.18	0.78	-2.47	+1.19	3.66
>6	I	34	+0.09	2.23	-5.34	+6.48	11.82
	II	35	-0.12	1.21	-2.64	+2.32	4.96
	III	36	-0.21	1.05	-2.46	+2.38	4.84
	IV	35	-0.22	0.95	-2.15	+1.54	3.69
	V	35	-0.10	0.89	-1.78	+1.47	3.25
Keratometer control		38	-0.04	0.33	-0.86	+0.70	1.56

TABLE C-3. CORNEAL CURVATURE CHANGES: 30 days postexposure

Exposure (W)	Ring	Number of eyes	Mean (D.)	Standard deviation	Maximum decrease (D.)	Maximum increase (D.)	Range (D.)
Nonirradiated	I	8	+0.08	0.84	-1.73	+1.01	2.74
	II	8	+0.02	0.78	-1.49	+1.03	2.52
	III	8	-0.10	0.59	-1.37	+0.50	1.87
	IV	8	-0.09	0.63	-1.17	+0.70	1.87
	V	8	-0.11	0.68	-1.20	+0.87	2.07
<2	I	5	-0.78	0.43	-1.18	-0.16	1.02
	II	5	-0.74	0.56	-1.51	-0.01	1.50
	III	5	-0.82	0.42	-1.27	-0.29	0.98
	IV	5	-0.77	0.40	-1.33	-0.38	0.95
	V	5	-0.78	0.75	-1.78	+0.26	2.04
2-3.99	I	38	-0.53	1.26	-3.05	+2.27	5.32
	II	39	-0.49	0.98	-2.13	+2.01	4.14
	III	39	-0.56	0.73	-1.82	+1.25	3.07
	IV	39	-0.62	0.75	-1.98	+0.90	2.88
	V	39	-0.57	0.79	-2.09	+1.41	3.50
4-5.99	I	45	-0.64	1.54	-8.14	+2.95	11.09
	II	45	-0.63	1.43	-5.62	+5.28	10.90
	III	45	-0.51	1.11	-2.90	+3.56	6.46
	IV	44	-0.41	0.93	-2.92	+1.50	4.42
	V	42	-0.47	0.95	-3.64	+1.99	5.63
>6	I	33	-0.22	4.04	-13.35	+8.84	22.19
	II	34	-0.29	2.60	-7.76	+5.44	13.20
	III	34	-0.40	1.62	-4.72	+3.71	8.43
	IV	33	-0.28	1.26	-2.29	+2.49	4.78
	V	33	-0.18	1.21	-3.48	+2.10	5.58
Keratometer control		38	-0.22	0.43	-1.13	+1.00	2.13

TABLE C-4. CORNEAL CURVATURE CHANGES: 90 days postexposure

Exposure (W)	Ring	Number of eyes	Mean (D.)	Standard deviation	Maximum decrease (D.)	Maximum increase (D.)	Range (D.)
Nonirradiated	I	8	-0.47	1.10	-2.53	+0.66	3.19
	II	8	-0.64	1.16	-2.69	+0.65	3.34
	III	8	-0.80	1.04	-2.62	+0.25	2.87
	IV	8	-0.84	1.10	-2.61	+0.66	3.27
	V	8	-0.92	1.18	-2.81	+0.49	3.30
<2	I	9	-1.32	0.68	-1.96	-0.94	1.02
	II	9	-1.43	0.74	-2.44	-0.47	1.97
	III	9	-1.34	0.65	-2.69	-0.75	1.94
	IV	9	-1.44	0.87	-2.87	-0.48	2.39
	V	9	-1.53	0.69	-2.66	-0.38	2.28
2-3.99	I	38	-1.04	2.11	-6.67	+6.34	13.01
	II	37	-0.94	1.68	-4.13	+4.50	8.63
	III	37	-1.21	1.54	-5.41	+3.33	8.74
	IV	38	-1.18	1.36	-4.54	+2.88	7.42
	V	38	-1.26	1.10	-3.44	+2.14	5.58
4-5.99	I	44	-1.05	1.94	-9.35	+2.59	11.94
	II	45	-1.05	1.22	-6.36	+1.68	8.04
	III	45	-1.16	0.98	-3.84	+1.60	5.44
	IV	45	-1.09	0.92	-3.31	+1.75	5.06
	V	44	-1.10	0.83	-3.74	+1.81	5.55
>6	I	32	-1.22	2.60	-5.90	+7.20	13.10
	II	35	-1.36	2.55	-8.46	+6.76	15.22
	III	35	-1.53	1.94	-6.55	+2.91	9.46
	IV	33	-1.45	1.78	-6.59	+1.17	7.76
	V	33	-1.25	1.80	-6.64	+1.88	8.52
Keratometer control		36	-0.65	0.71	-2.63	+0.93	3.56

TABLE C-5. CORNEAL CURVATURE CHANGES: 180 days postexposure

Exposure (W)	Ring	Number of eyes	Mean (D.)	Standard deviation	Maximum decrease (D.)	Maximum increase (D.)	Range (D.)
Nonirradiated	I	8	-1.14	1.41	-3.17	+0.85	4.02
	II	8	-1.04	1.38	-3.16	+0.47	3.63
	III	8	-1.23	1.09	-2.79	-0.03	2.76
	IV	8	-1.32	1.16	-2.99	-0.05	2.94
	V	8	-1.41	1.31	-3.30	-0.05	3.25
<2	I	6	-2.13	0.76	-2.84	-1.14	1.70
	II	6	-1.95	0.69	-2.68	-1.13	1.55
	III	6	-2.04	0.57	-2.74	-1.41	1.33
	IV	6	-1.89	0.66	-2.85	-1.17	1.68
	V	6	-1.98	0.60	-2.57	-1.09	1.48
2-3.99	I	37	-1.71	2.05	-5.00	+6.56	11.56
	II	37	-1.94	1.49	-4.62	+3.61	8.23
	III	37	-1.96	1.21	-4.36	+1.72	6.08
	IV	37	-2.02	1.31	-4.40	+1.73	6.13
	V	37	-2.15	1.35	-4.44	+1.64	6.08
4-5.99	I	42	-2.01	2.39	-12.13	+1.85	13.98
	II	43	-1.66	1.78	-8.46	+2.32	10.78
	III	43	-1.45	1.51	-5.32	+2.86	8.18
	IV	43	-1.63	1.27	-4.69	+2.77	7.46
	V	42	-1.74	1.07	-4.51	+0.82	5.33
>6	I	29	-1.30	3.40	-10.30	+8.60	18.90
	II	30	-1.48	2.15	-6.19	+2.22	8.41
	III	29	-1.80	1.44	-4.40	+1.05	5.45
	IV	26	-1.85	1.24	-4.15	+1.02	5.17
	V	26	-1.70	1.21	-3.78	+0.80	4.58
Keratometer control		36	-1.27	0.96	-3.31	+0.50	3.81

TABLE C-6. CORNEAL CURVATURE CHANGES: 270 days postexposure

Exposure (W)	Ring	Number of eyes	Mean (D.)	Standard deviation	Maximum decrease (D.)	Maximum increase (D.)	Range (D.)
Nonirradiated	I	6	-1.01	1.32	-3.04	+0.34	3.38
	II	6	-1.29	1.75	-4.24	+0.74	4.98
	III	6	-1.47	1.46	-3.82	-0.20	3.62
	IV	6	-1.68	1.53	-4.13	-0.34	3.79
	V	6	-1.56	1.61	-4.13	+0.14	4.27
<2	I	8	-2.38	0.93	-4.04	-0.93	3.11
	II	8	-2.34	0.47	-2.98	-1.82	1.16
	III	8	-2.39	0.49	-3.08	-1.78	1.30
	IV	8	-2.43	0.58	-3.29	-1.77	1.52
	V	8	-2.51	0.49	-3.19	-1.80	1.39
2-3.99	I	35	-2.40	1.71	-5.61	+1.67	7.28
	II	34	-2.31	1.59	-4.89	+2.32	7.21
	III	34	-2.52	1.41	-4.86	+0.63	5.49
	IV	34	-2.58	1.37	-5.13	-0.23	4.90
	V	35	-2.55	1.49	-5.18	+0.35	5.53
4-5.99	I	39	-2.11	2.56	-9.21	+6.81	16.02
	II	39	-2.33	2.40	-11.35	+2.84	14.19
	III	39	-2.10	1.73	-6.93	+1.89	8.82
	IV	39	-2.07	1.55	-5.43	+1.70	7.13
	V	39	-2.09	1.41	-5.32	+1.22	6.54
>6	I	27	-1.70	3.42	-8.58	+8.76	17.34
	II	29	-2.35	2.29	-8.53	+0.78	9.31
	III	29	-2.17	1.91	-5.49	+1.97	7.46
	IV	27	-2.15	1.64	-4.98	+0.91	5.89
	V	26	-1.91	1.43	-4.71	+0.76	5.47
Keratometer control		34	-1.30	1.20	-3.93	+1.57	5.50

TABLE C-7. CORNEAL CURVATURE CHANGES: 365 days postexposure

Exposure (W)	Ring	Number of eyes	Mean (D.)	Standard deviation	Maximum decrease (D.)	Maximum increase (D.)	Range (D.)
Nonirradiated	I	8	-2.04	1.81	-5.20	+0.17	5.37
	II	8	-1.55	1.75	-4.89	+0.43	5.32
	III	8	-2.06	1.85	-5.01	-0.31	4.70
	IV	8	-2.25	1.93	-5.30	-0.33	4.97
	V	8	-2.26	2.01	-5.55	-0.09	5.46
<2	I	8	-2.54	0.69	-3.45	-1.56	1.89
	II	8	-2.38	0.84	-3.73	-1.05	2.68
	III	8	-2.50	0.63	-3.66	-1.82	1.84
	IV	8	-2.68	0.62	-3.67	-1.91	1.76
	V	8	-2.60	0.62	-3.42	-1.80	1.62
2-3.99	I	34	-3.16	2.15	-8.23	+0.56	8.79
	II	34	-3.09	1.58	-6.00	+0.25	6.25
	III	34	-2.90	1.44	-5.23	+0.58	5.81
	IV	34	-2.81	1.44	-5.47	+0.48	5.95
	V	34	-2.93	1.45	-5.81	+0.69	6.50
4-5.99	I	38	-2.50	2.38	-9.96	+4.28	14.24
	II	38	-2.61	1.84	-7.19	+3.04	10.23
	III	37	-2.54	1.25	-4.89	+0.11	5.00
	IV	38	-2.67	1.13	-5.00	-0.32	4.68
	V	38	-2.74	1.14	-5.35	-0.50	4.85
>6	I	28	-2.92	3.06	-12.79	+1.56	14.35
	II	29	-2.58	2.29	-7.83	+3.82	11.65
	III	29	-2.51	1.79	-5.67	+1.45	7.12
	IV	27	-2.36	1.68	-5.53	+0.46	5.99
	V	26	-2.27	1.74	-5.64	+0.60	6.24
Keratometer control		32	-1.50	1.42	-4.78	+1.07	5.85

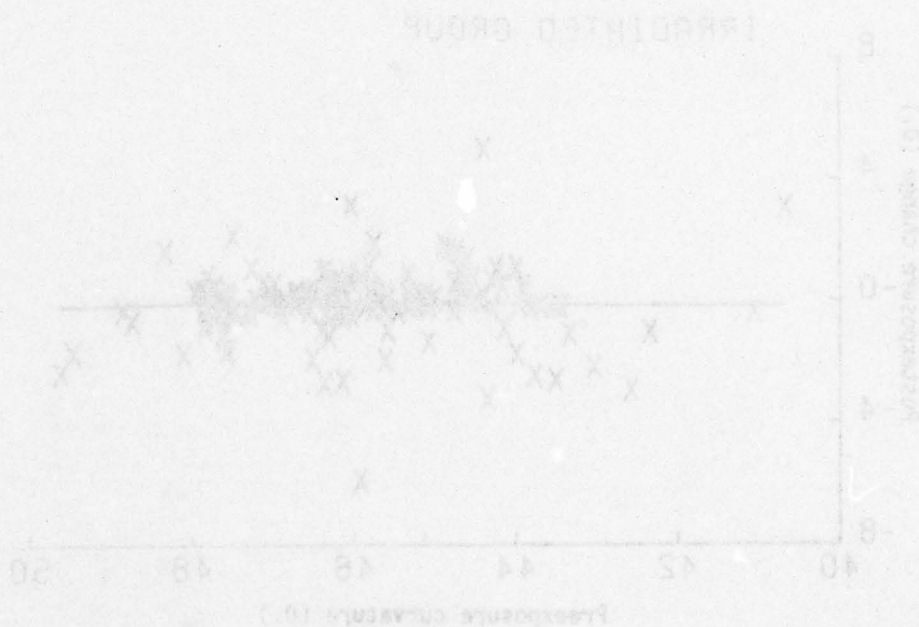
TABLE C-8. MEAN POSTEXPOSURE CURVATURE CHANGES. A SUMMARY OF HORIZONTAL MERIDIAN DATA FROM RING II OF THE PHOTOKERATOSCOPE AND THE KERATOMETER RING (THE NUMBERS OF EYES COMPRISING EACH MEAN CHANGE ARE IN PARENTHESES).

Exposure (W)	Instrument	30 Minutes postexposure	Day 7	Day 30	Day 90	Day 180	Day 270	Day 365
Nonirradiated controls	Photokeratoscope	+0.06 (8)	+0.43 (8)	+0.02 (8)	-0.64 (8)	-1.04 (8)	-1.29 (6)	-1.55 (8)
	Keratometer	0.00 (38)	-0.04 (38)	-0.22 (38)	-0.65 (36)	-1.27 (36)	-1.30 (34)	-1.50 (32)
<2	Photokeratoscope	-0.24 (11)	+0.27 (5)	-0.74 (5)	-1.43 (9)	-1.95 (6)	-2.34 (8)	-2.38 (8)
	Keratometer	-0.24 (13)	-0.12 (11)	-0.58 (11)	-0.90 (9)	-1.72 (9)	-2.01 (9)	-2.35 (9)
2 - 3.99	Photokeratoscope	-0.34 (27)	-0.07 (36)	-0.49 (39)	-0.94 (37)	-1.94 (37)	-2.31 (34)	-3.09 (34)
	Keratometer	-0.19 (26)	-0.03 (39)	-0.50 (39)	-1.12 (39)	-1.89 (39)	-2.06 (36)	-2.64 (36)
4 - 5.99	Photokeratoscope	+0.03 (16)	-0.07 (43)	-0.53 (45)	-1.05 (45)	-1.66 (43)	-2.33 (39)	-2.61 (38)
	Keratometer	+0.14 (10)	+0.04 (45)	-0.22 (47)	-0.93 (46)	-1.66 (44)	-1.78 (40)	-2.38 (40)
>6	Photokeratoscope	+0.52 (5)	-0.12 (35)	-0.29 (34)	-1.36 (35)	-1.48 (30)	-2.35 (29)	-2.58 (29)
	Keratometer	-3.89 (4)	-0.57 (39)	-0.59 (35)	-1.66 (37)	-1.79 (35)	-2.61 (33)	-2.78 (33)

APPENDIX D

CURVATURE CHANGE AS A FUNCTION OF INITIAL CURVATURE

The figures in this appendix show the postexposure change in curvature or the toricity as a function of the preexposure curvature or toricity. They are presented in the sequence horizontal meridian, vertical meridian, spherical equivalent, and toricity for both the control and the irradiated groups for each measurement. On each page, the figure for the control group is paired with its corresponding irradiated group for ease of comparison. In the meridional and spherical equivalent figures, positive and negative values on the ordinate scale indicate, respectively, corneal curvature increases and decreases. In the figures for toricity, positive values indicate toricity with the horizontal curvature greater than the vertical, and negative values show toricity with the vertical curvature greater than the horizontal. In all figures, linear or quadratic curves have been fitted to the data. When a quadratic curve did not fit better than a linear, the linear was used. When the linear curve did not fit better than a line with zero slope drawn through the mean, the latter was used.



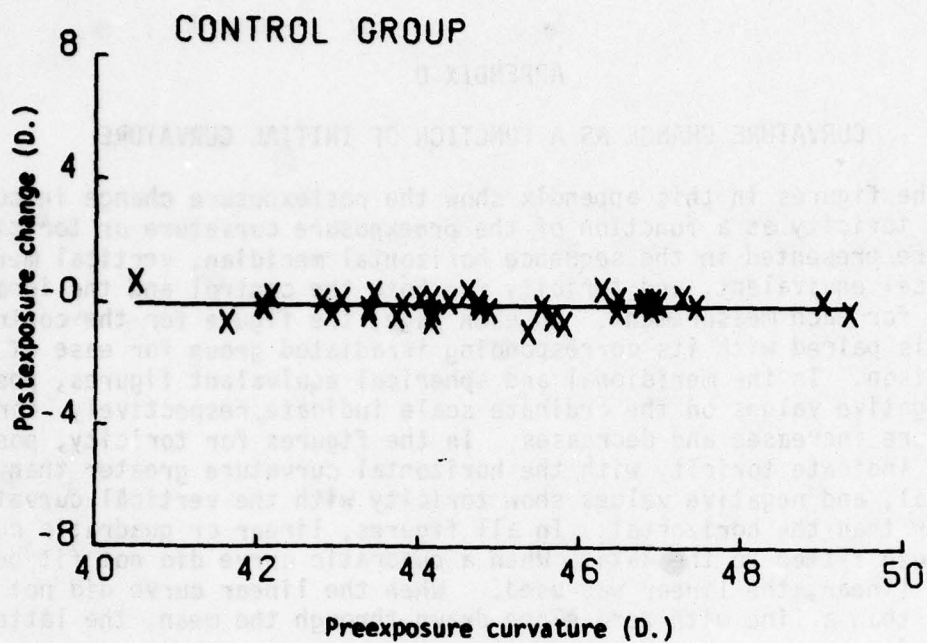


Figure D-1. Horizontal meridian change: Day 7.

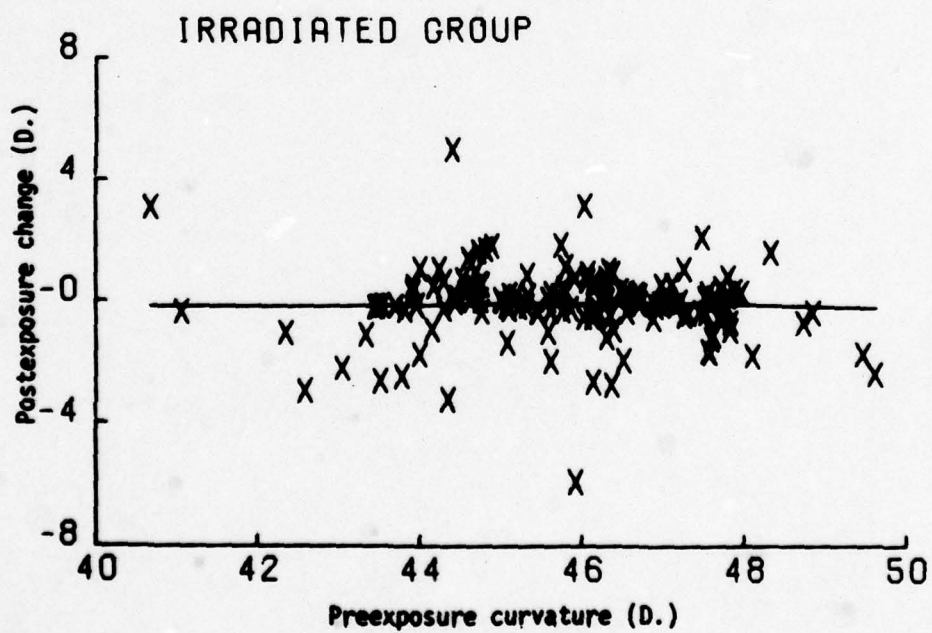


Figure D-2. Horizontal meridian change: Day 7.

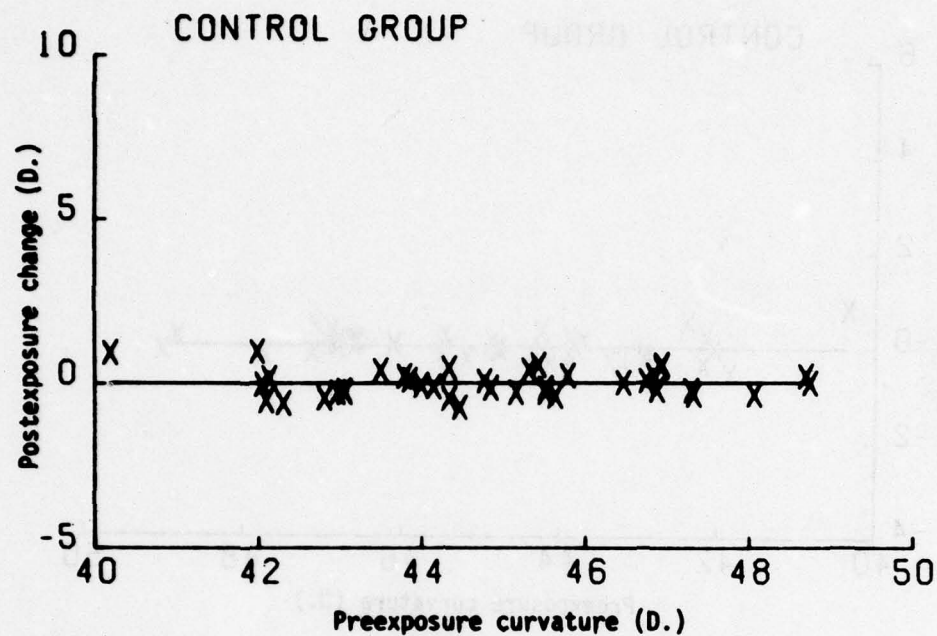


Figure D-3. Vertical meridian change: Day 7.

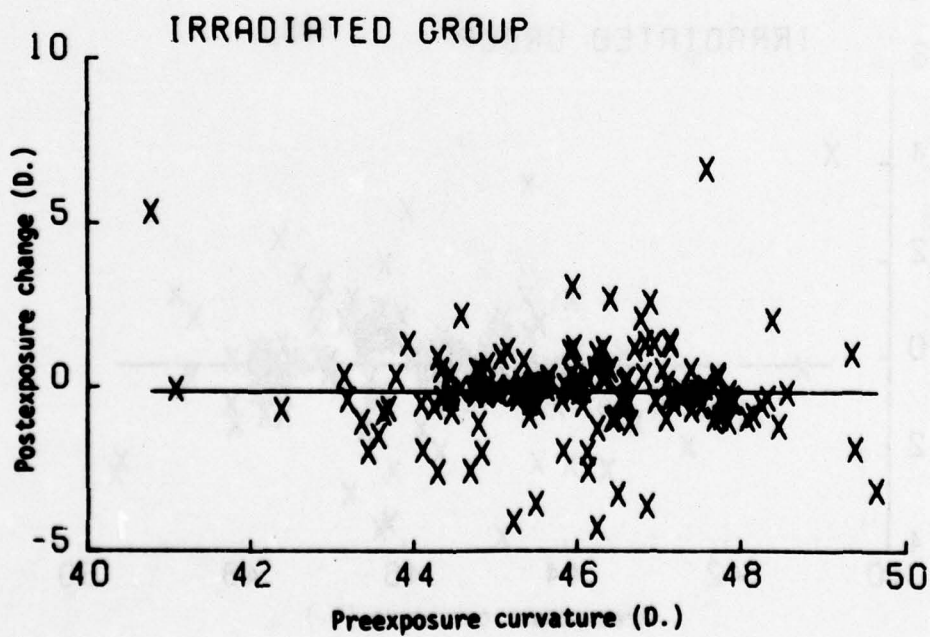


Figure D-4. Vertical meridian change: Day 7.

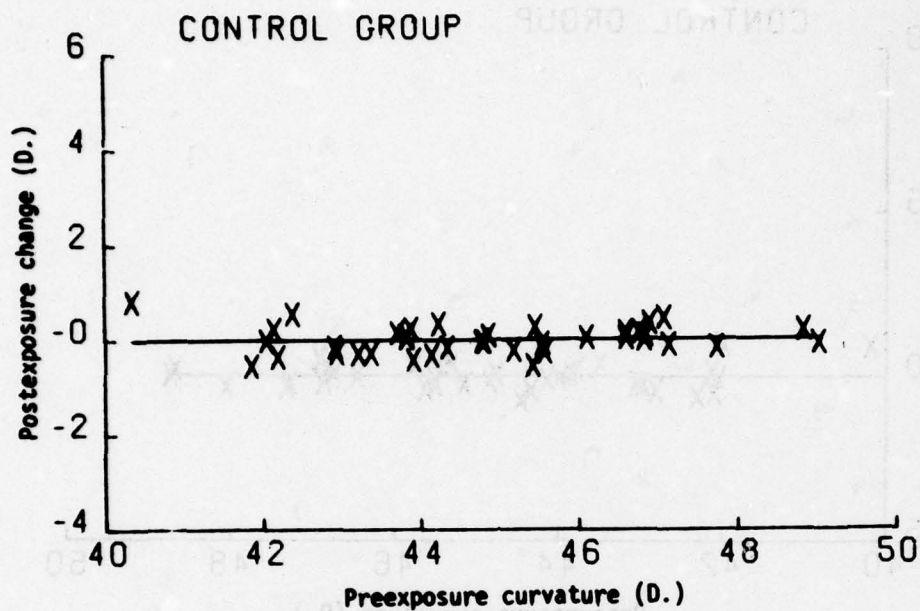


Figure D-5. Spherical equivalent change: Day 7.

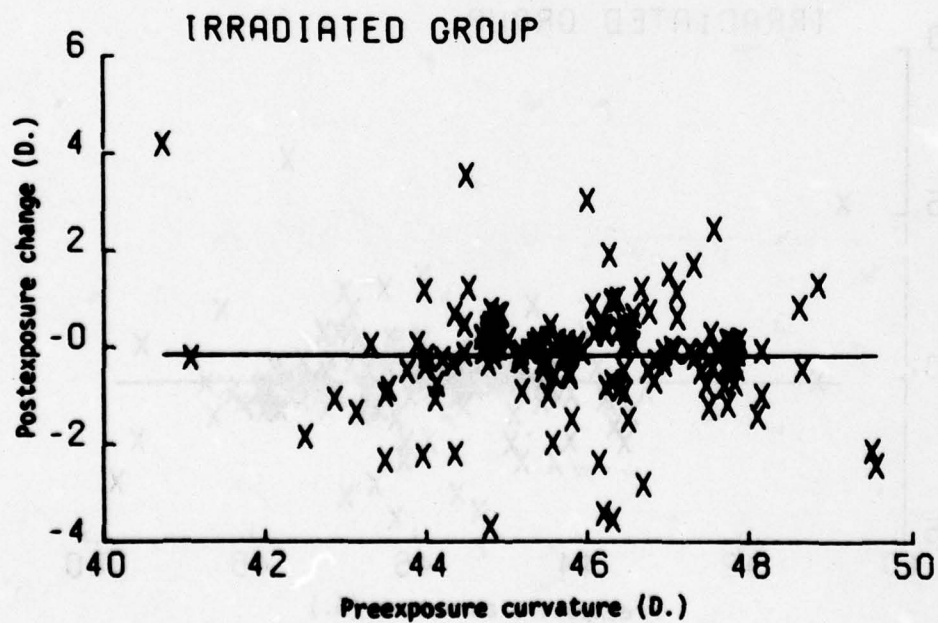


Figure D-6. Spherical equivalent change: Day 7.

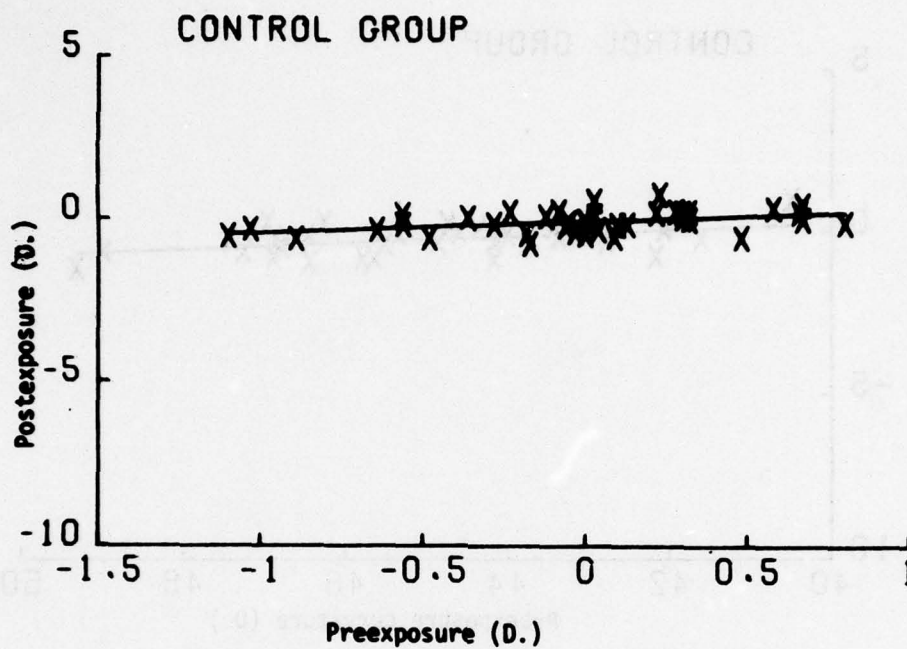


Figure D-7. Toricity: Day 7.

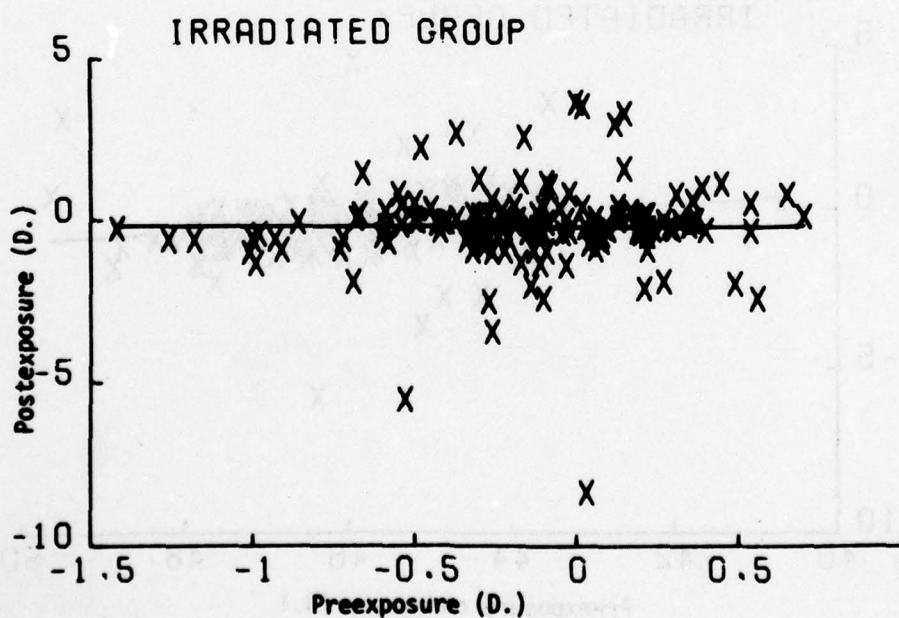


Figure D-8. Toricity: Day 7.

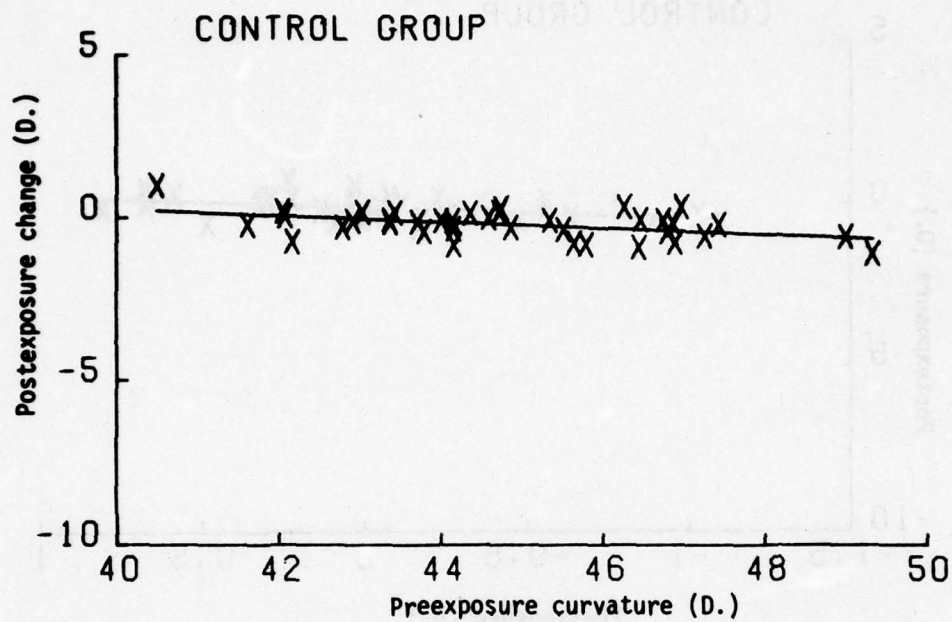


Figure D-9. Horizontal meridian change: Day 30.

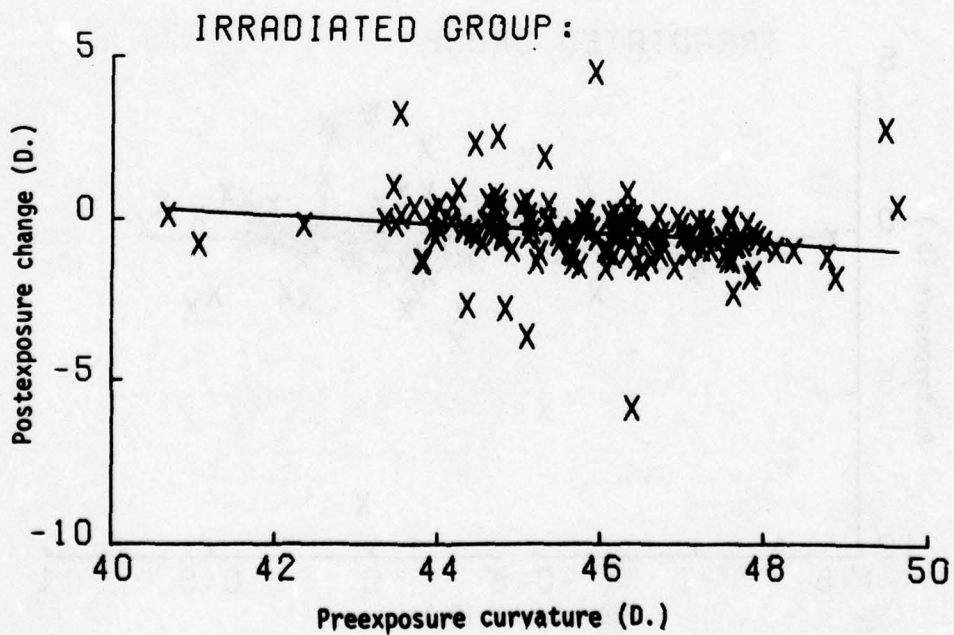


Figure D-10. Horizontal meridian change: Day 30.

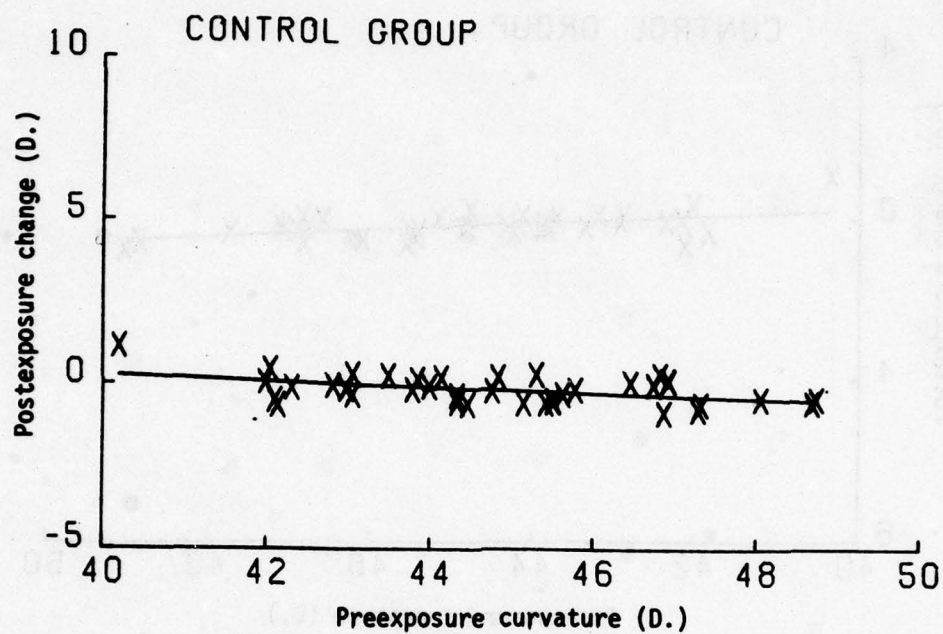


Figure D-11. Vertical meridian change: Day 30.

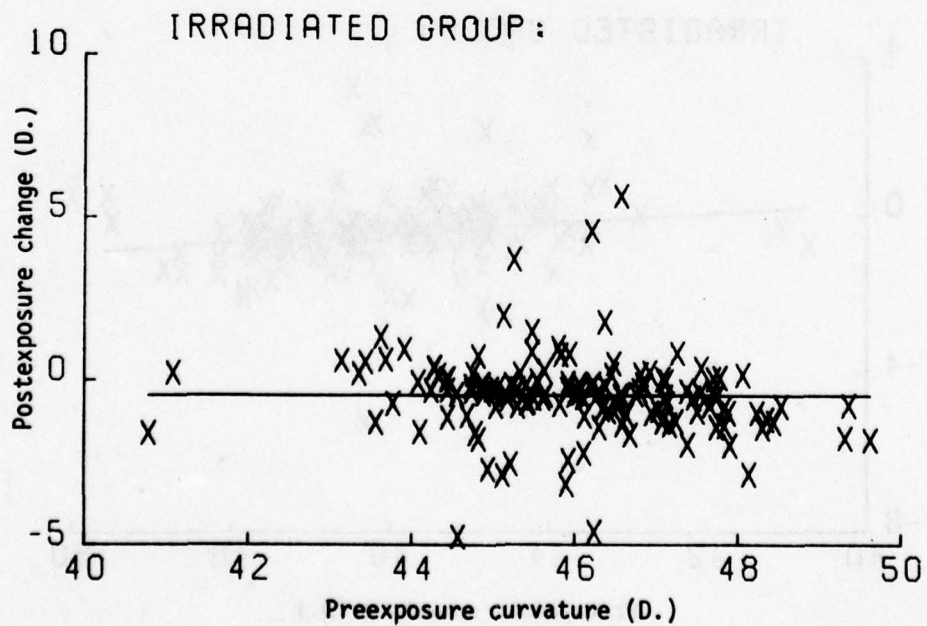


Figure D-12. Vertical meridian change: Day 30.

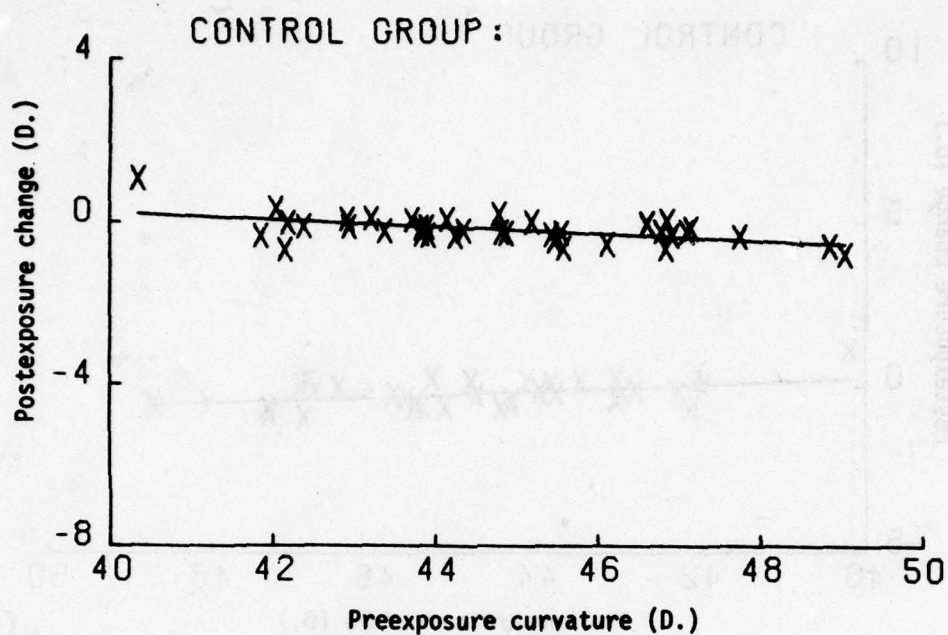


Figure D-13. Spherical equivalent change: Day 30.

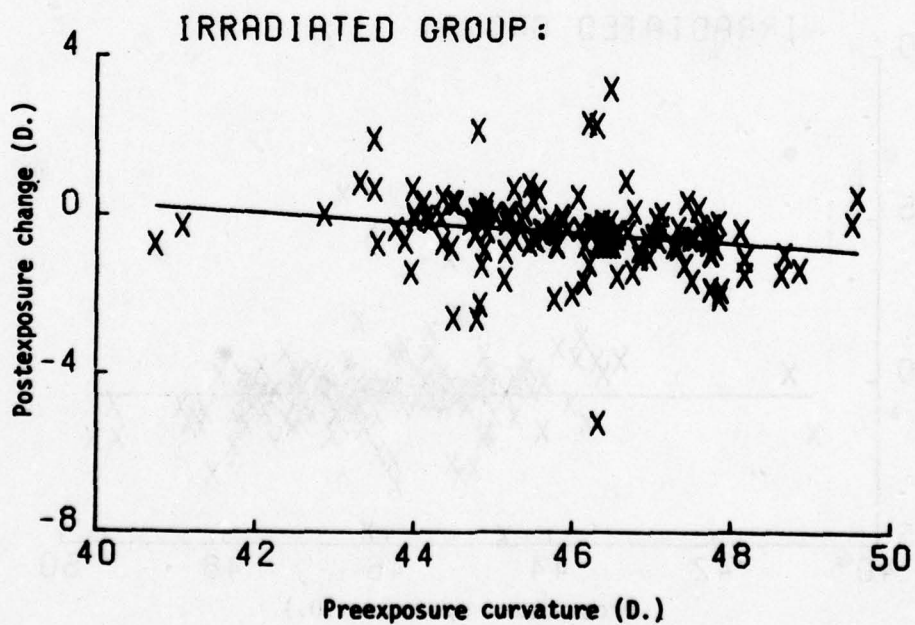


Figure D-14. Spherical equivalent change: Day 30.

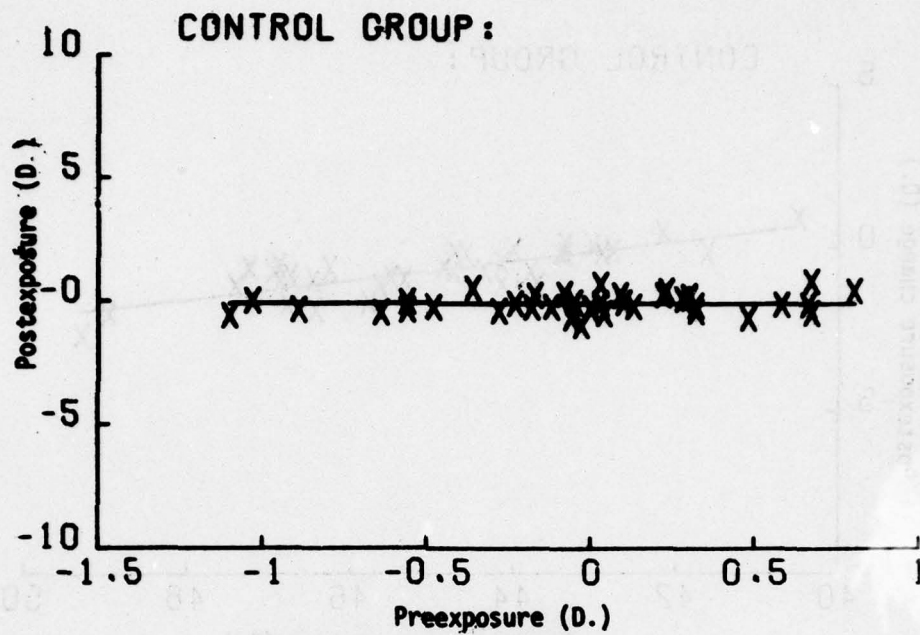


Figure D-15. Toricity: Day 30.

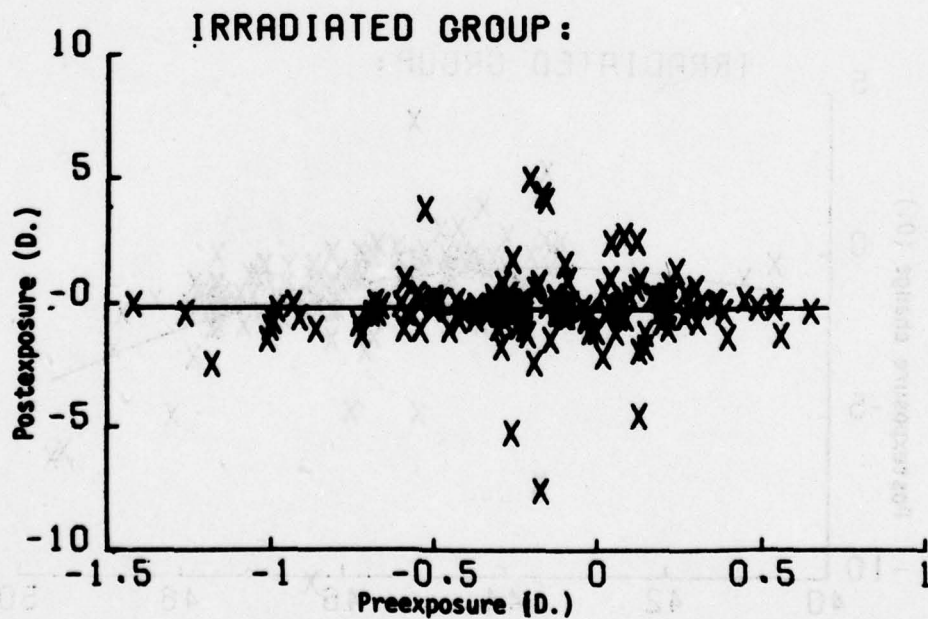


Figure D-16. Toricity: Day 30.

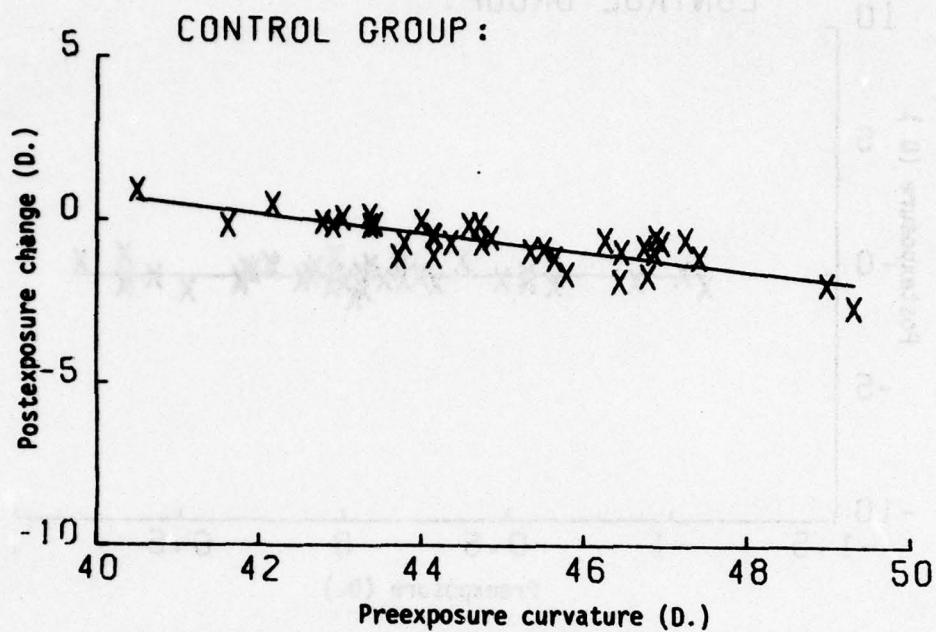


Figure D-17. Horizontal meridian change: Day 90.

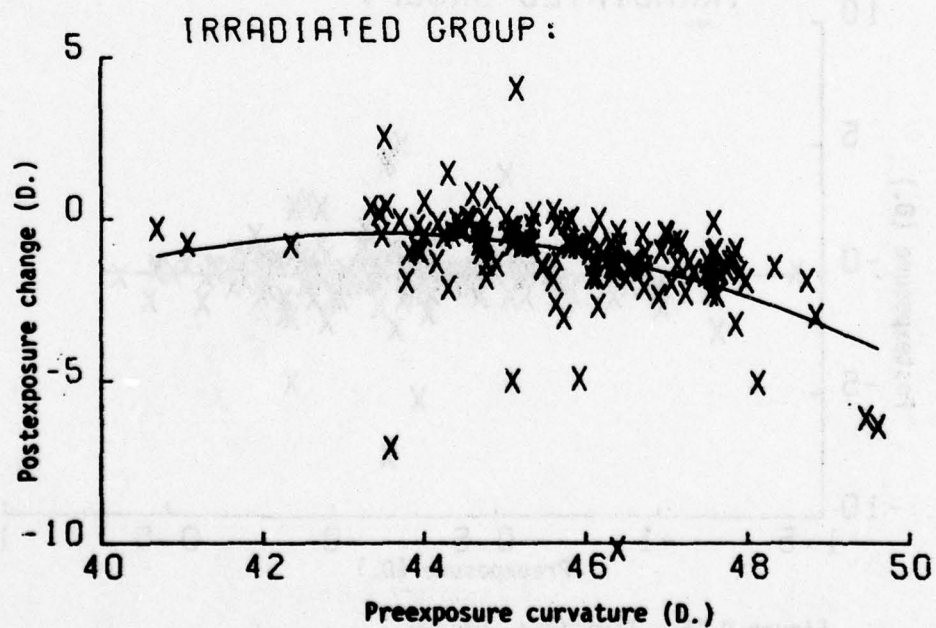


Figure D-18. Horizontal meridian change: Day 90.

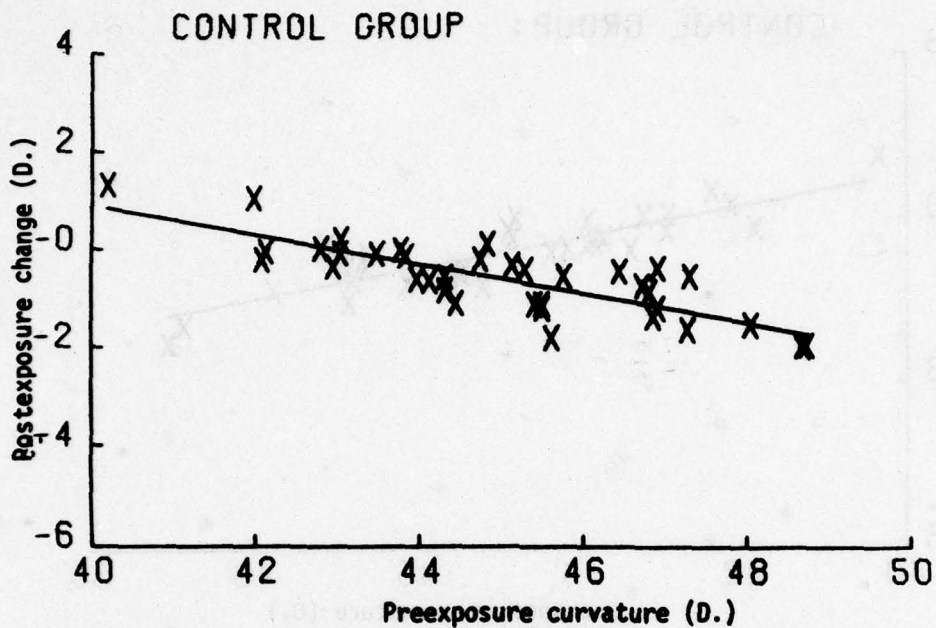


Figure D-19. Vertical meridian change: Day 90.

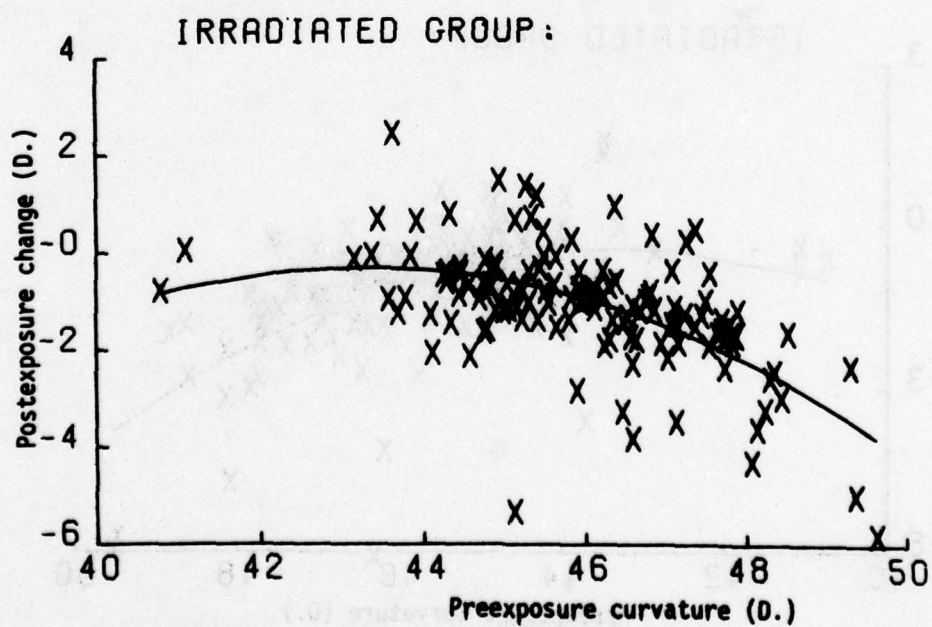


Figure D-20. Vertical meridian change: Day 90.

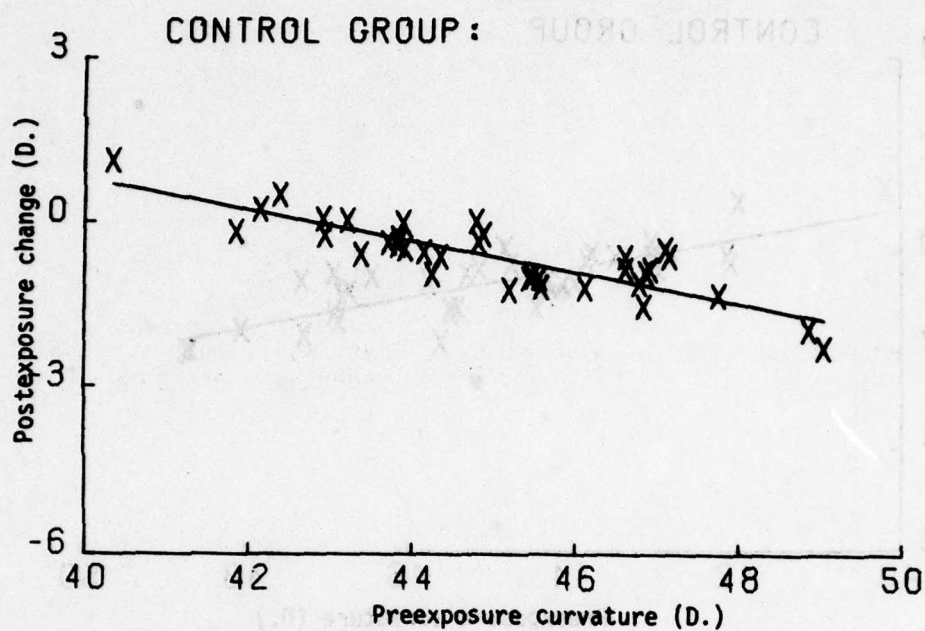


Figure D-21. Spherical equivalent change: Day 90.

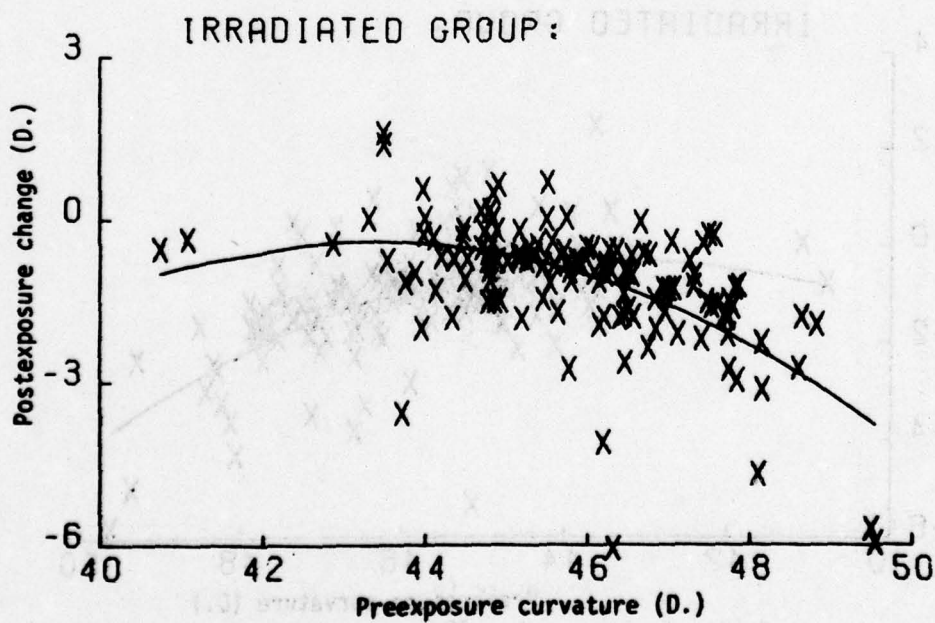


Figure D-22. Spherical equivalent change: Day 90.

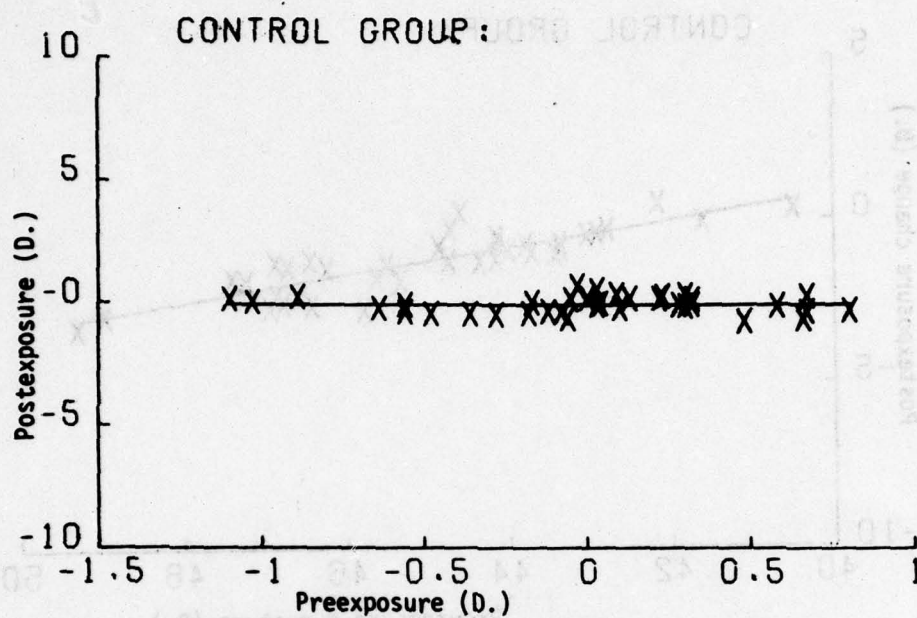


Figure D-23. Toricity: Day 90.

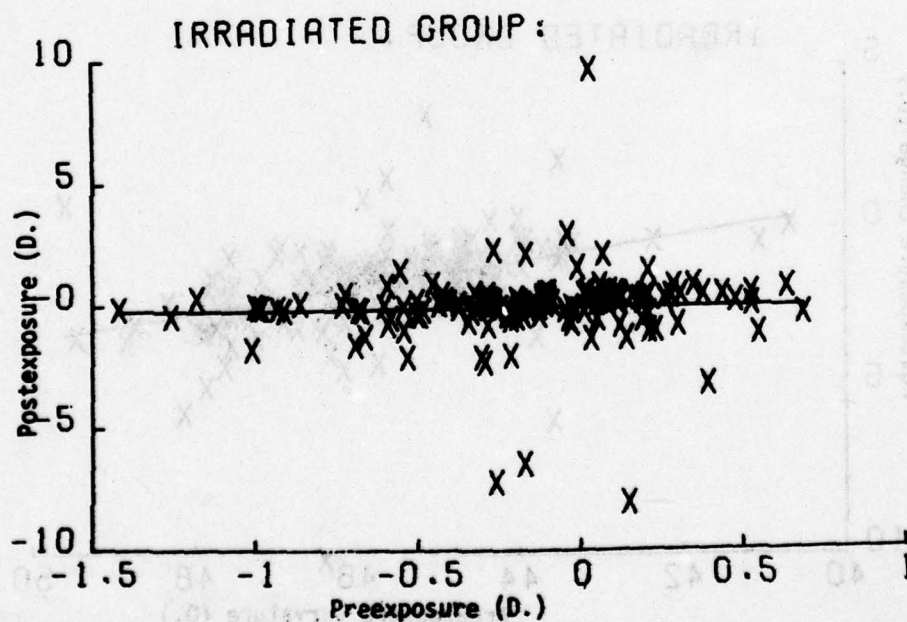


Figure D-24. Toricity: Day 90.

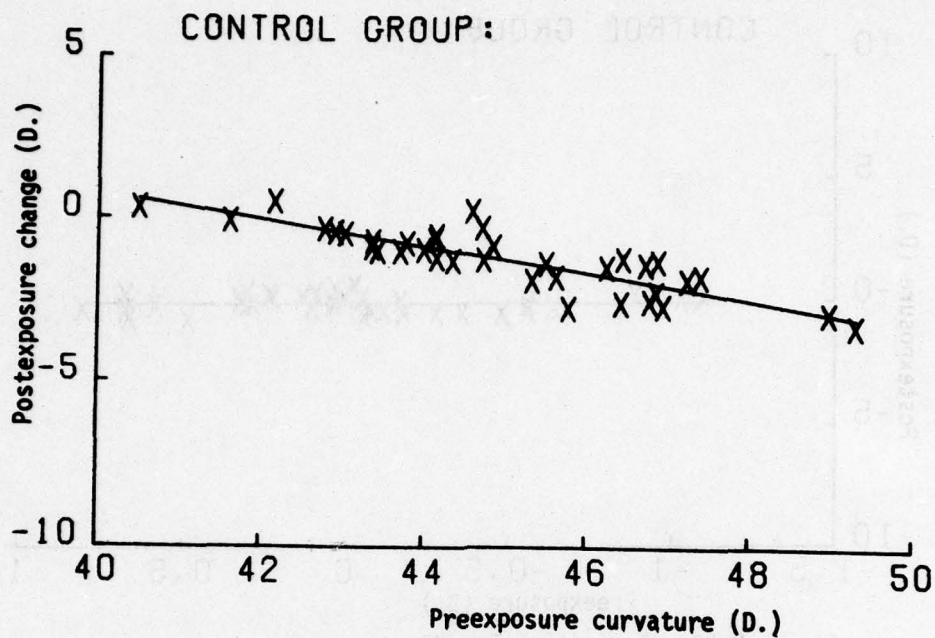


Figure D-25. Horizontal meridian change: Day 180.

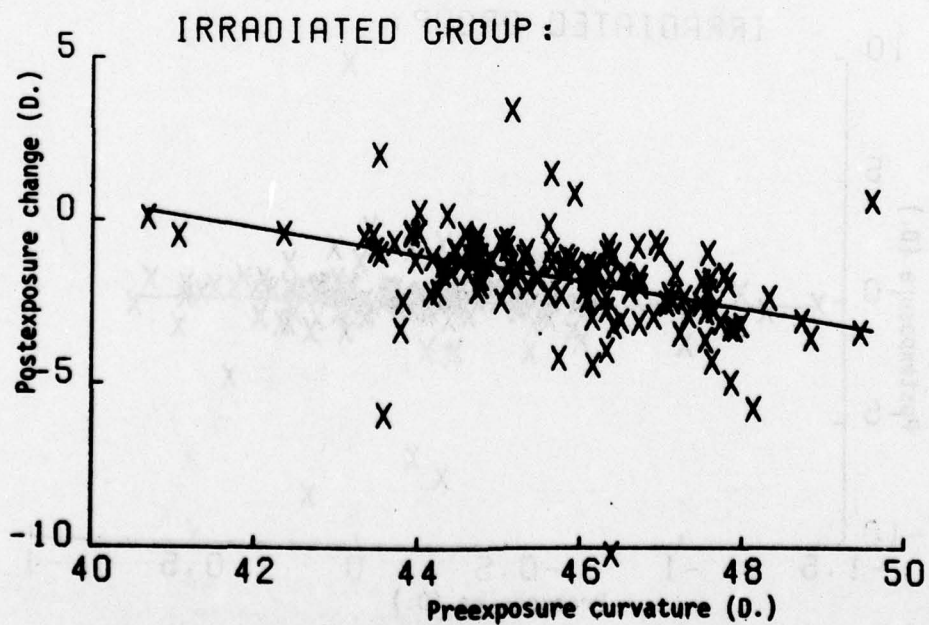


Figure D-26. Horizontal meridian change: Day 180.

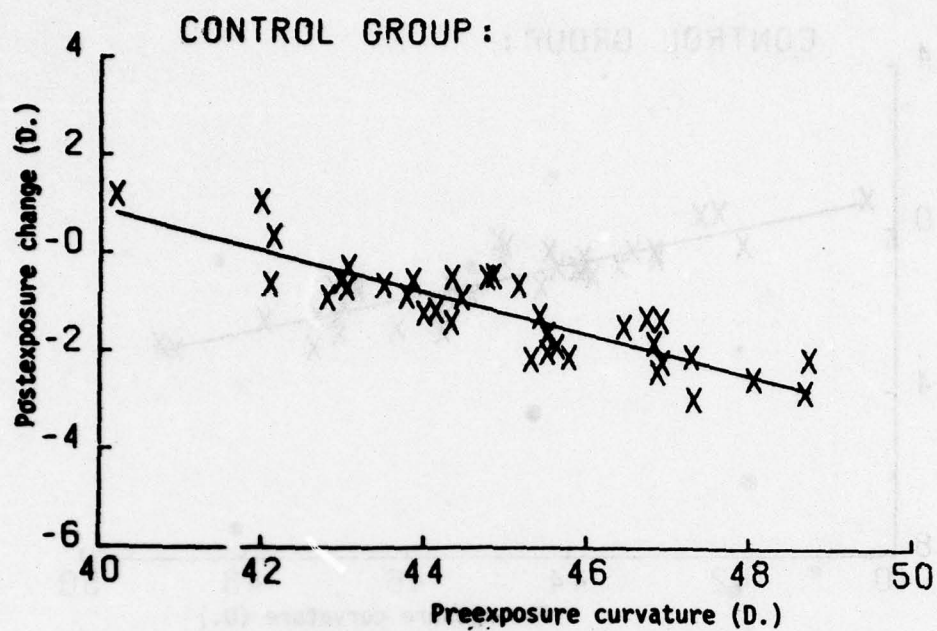


Figure D-27. Vertical meridian change: Day 180.

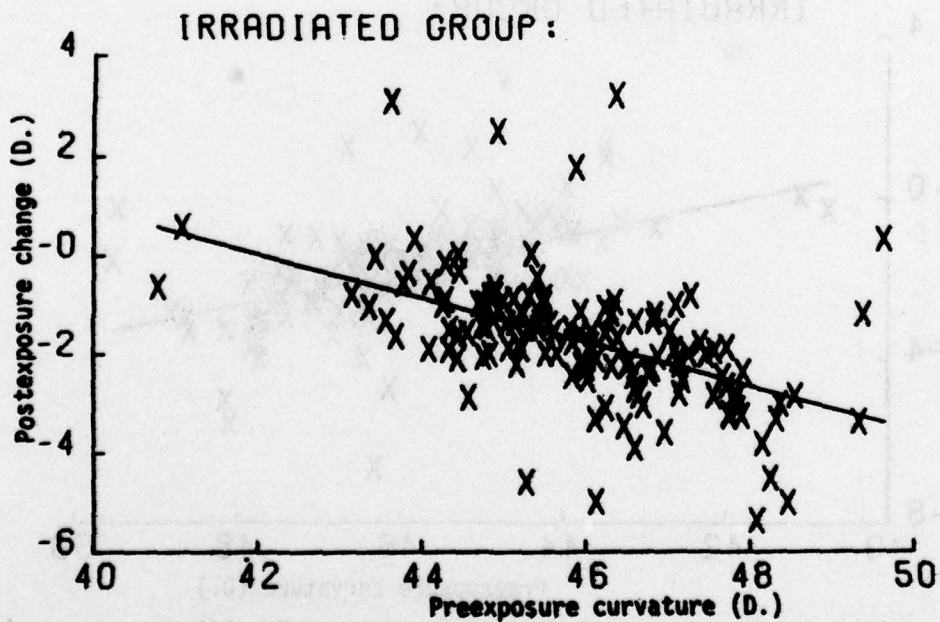


Figure D-28. Vertical meridian change: Day 180.

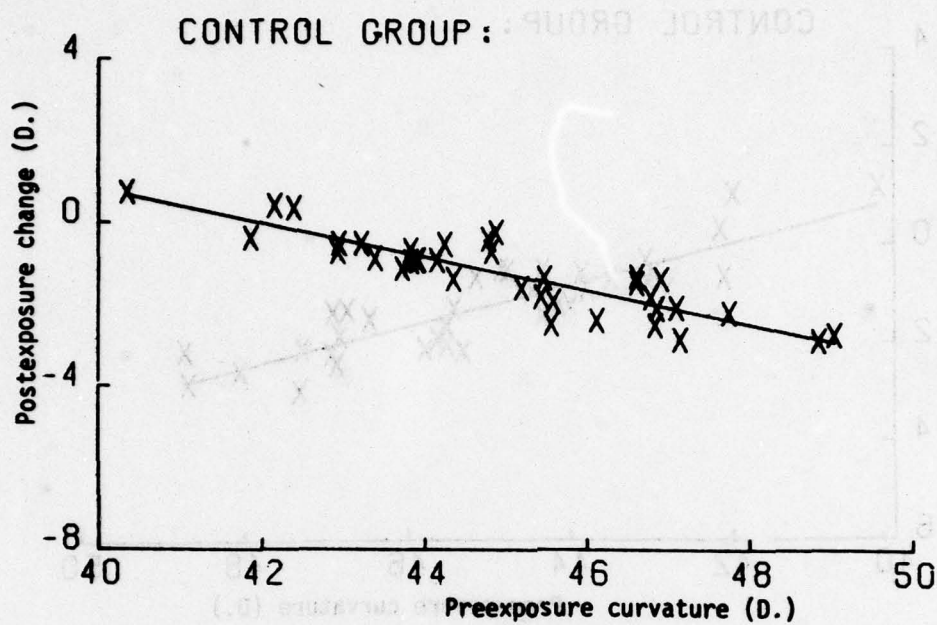


Figure D-29. Spherical equivalent change: Day 180.

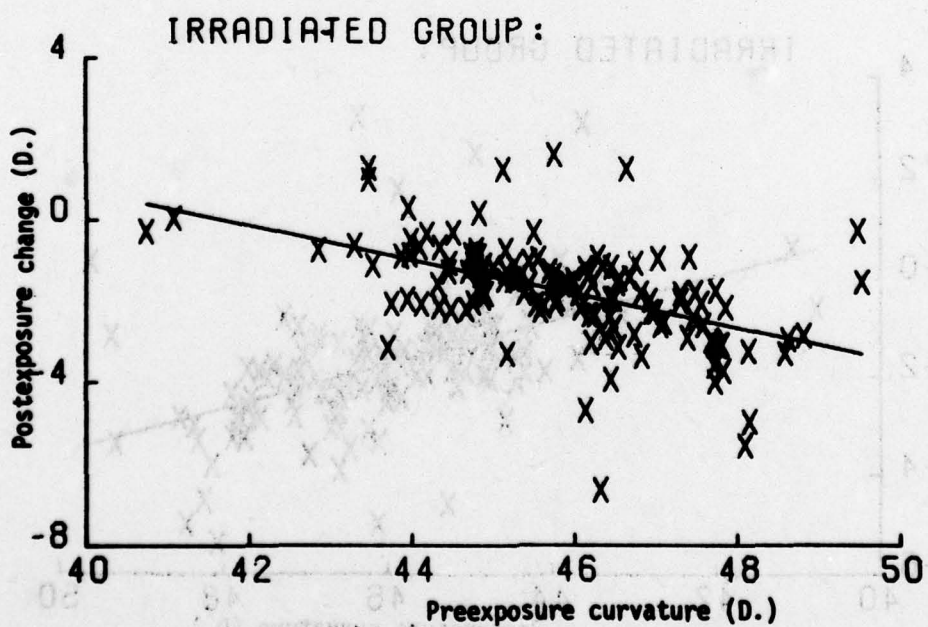


Figure D-30. Spherical equivalent change: Day 180.

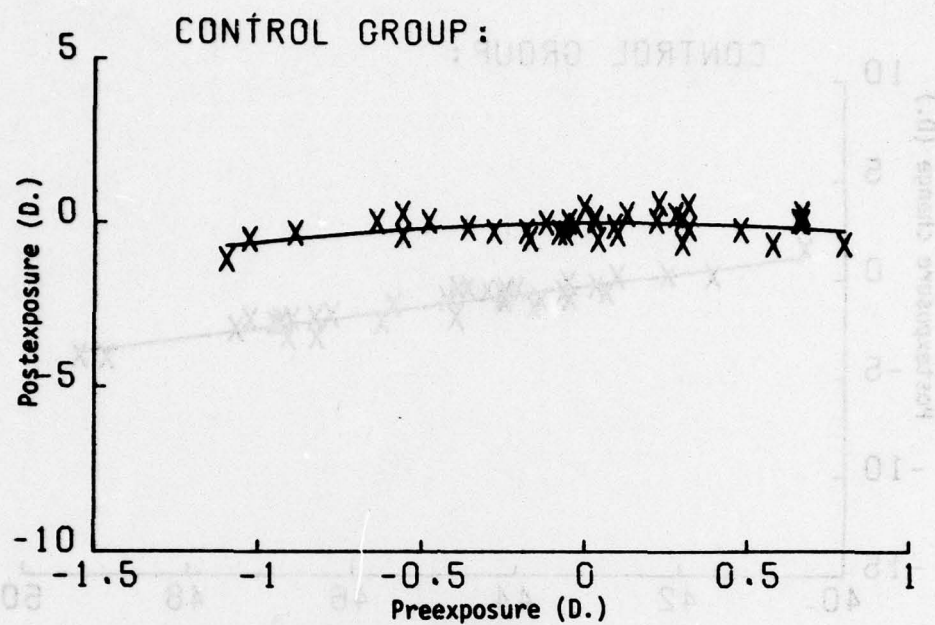


Figure D-31. Toricity: Day 180.

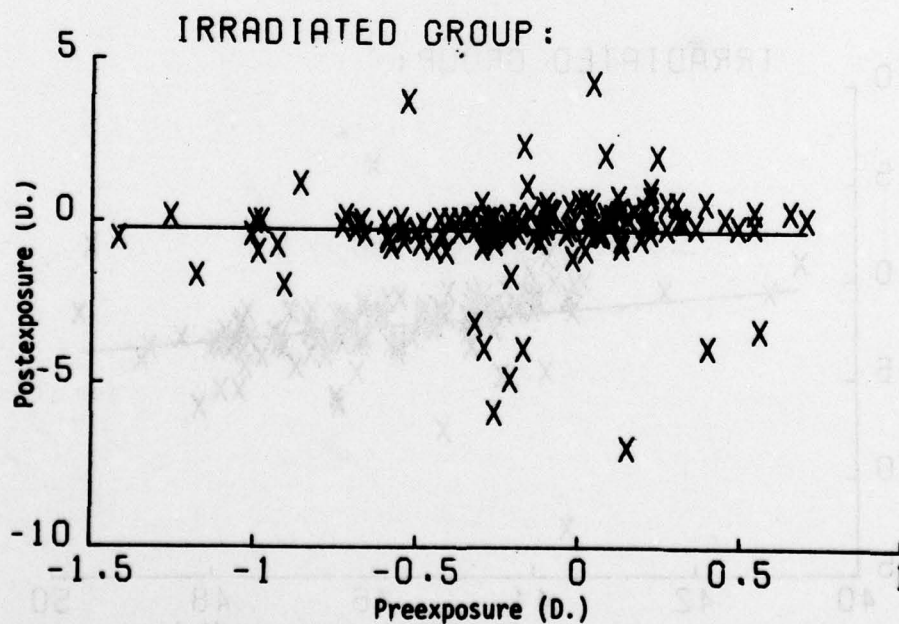


Figure D-32. Toricity: Day 180.

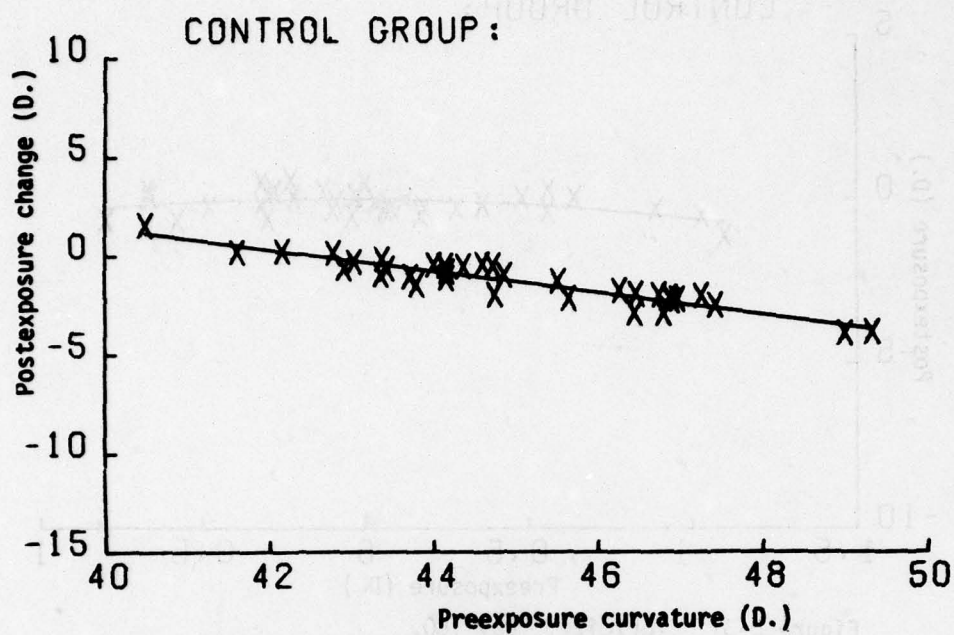


Figure D-33. Horizontal meridian change: Day 270.

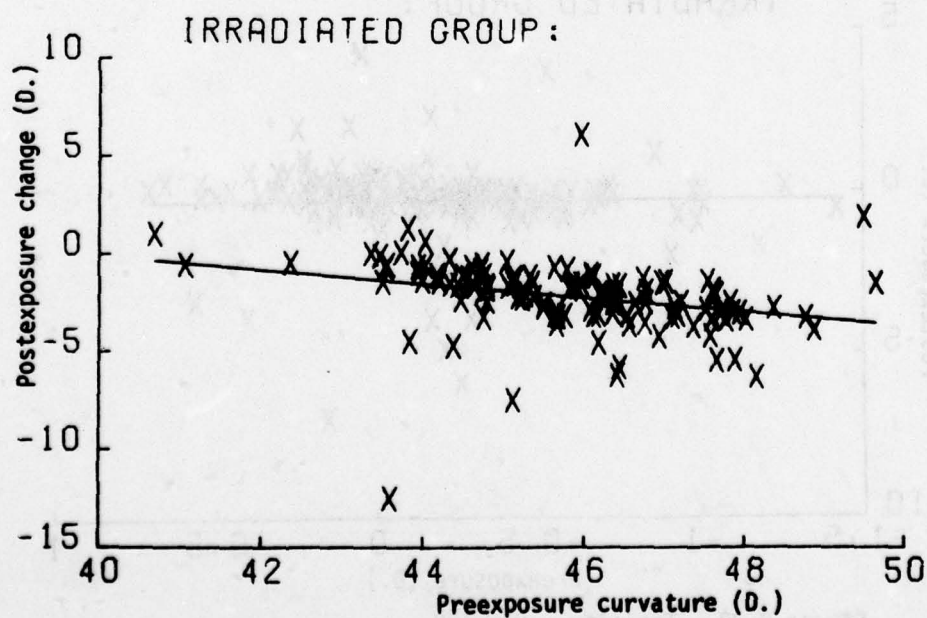


Figure D-34. Horizontal meridian change: Day 270.

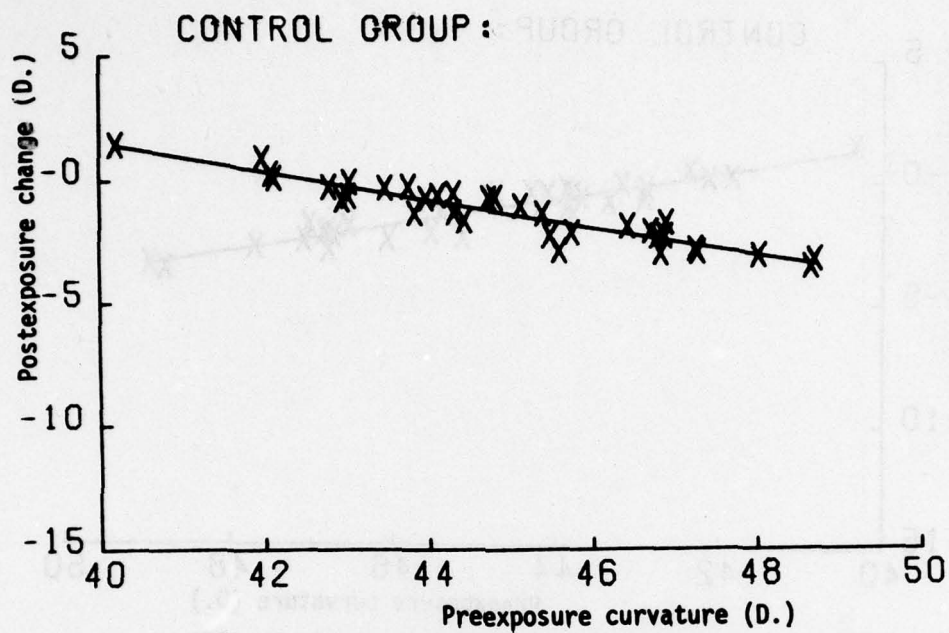


Figure D-35. Vertical meridian change: Day 270.

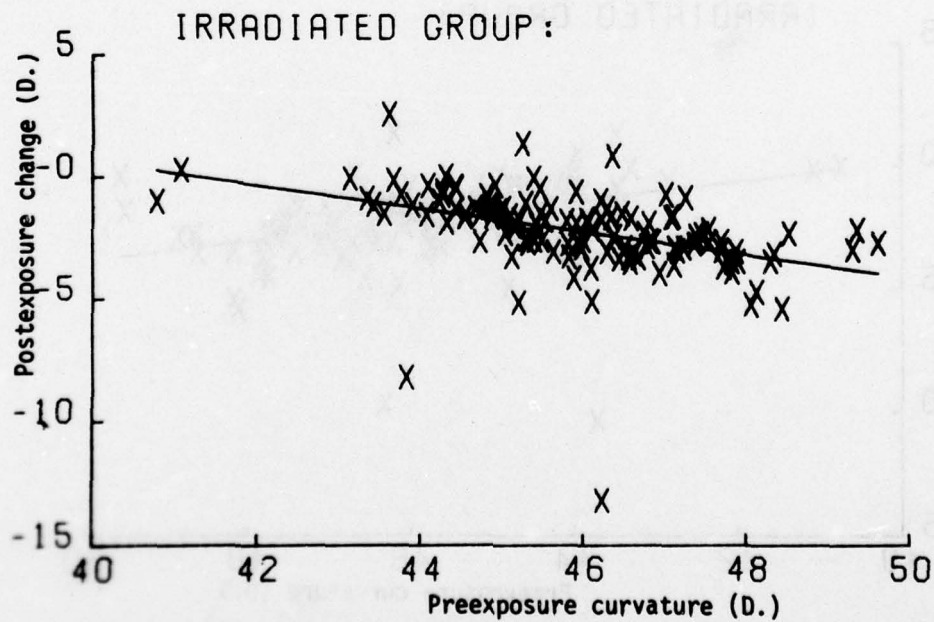


Figure D-36. Vertical meridian change: Day 270.

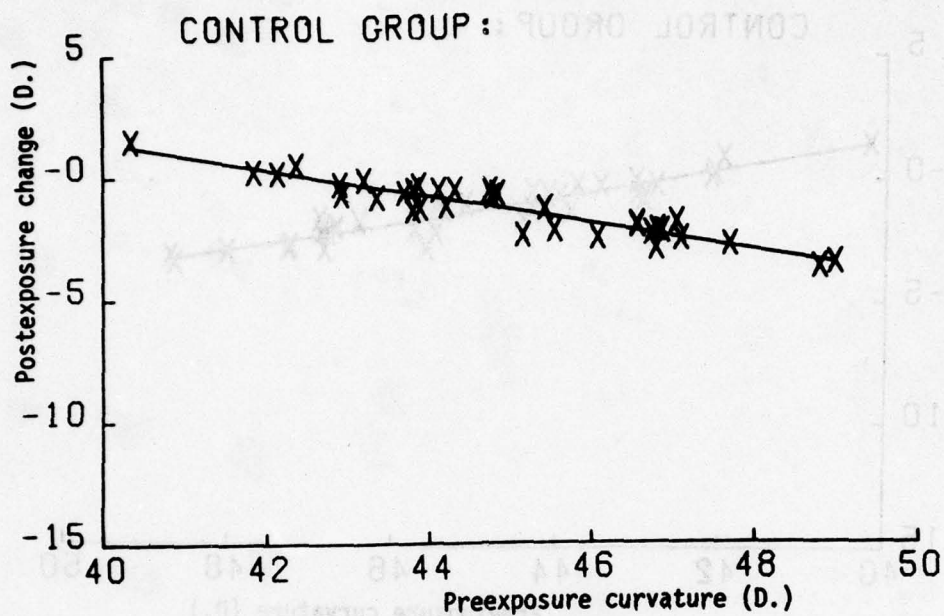


Figure D-37. Spherical equivalent change: Day 270.

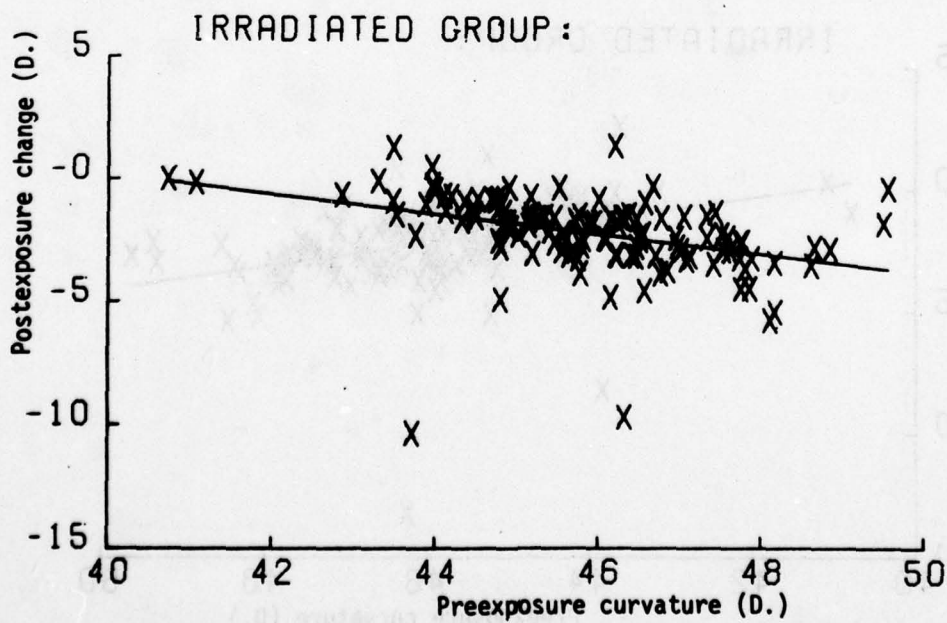


Figure D-38. Spherical equivalent change: Day 270.

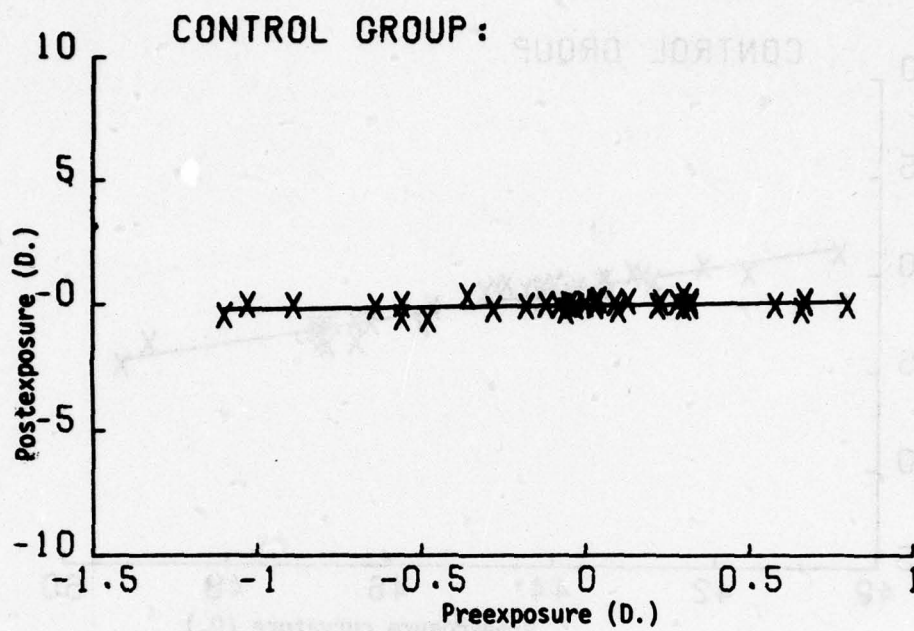


Figure D-39. Toricity: Day 270.

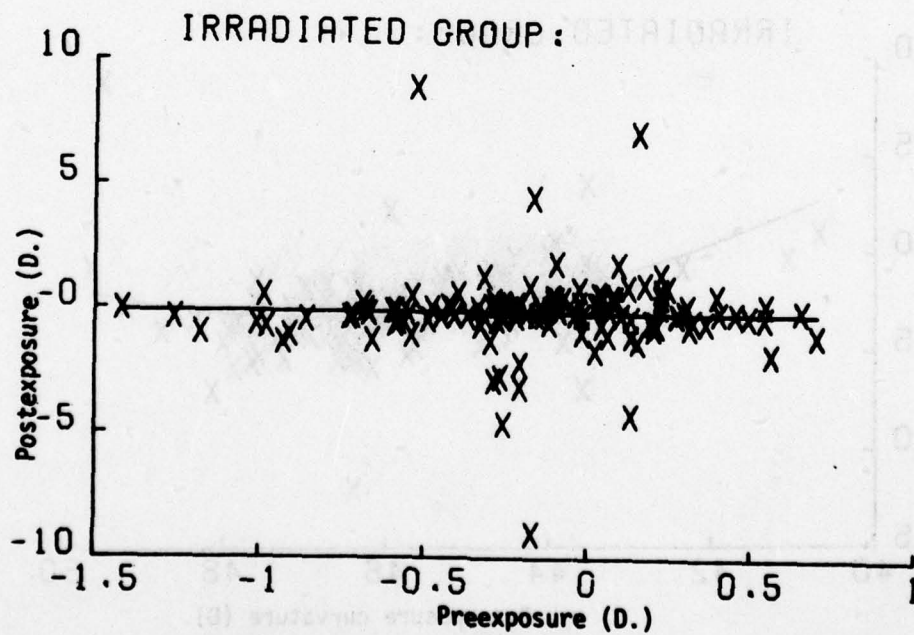


Figure D-40. Toricity: Day 270.

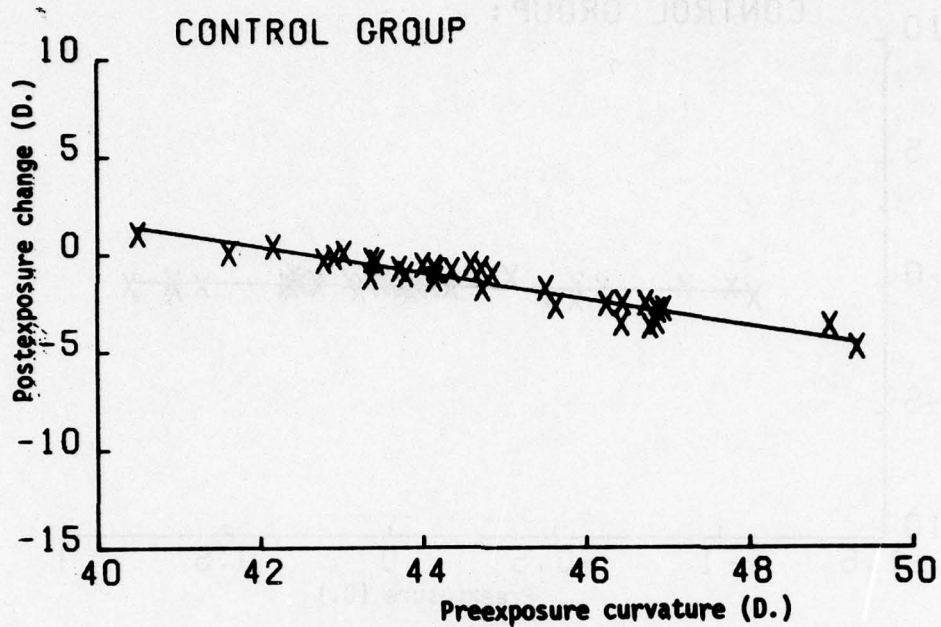


Figure D-41. Horizontal meridian change: Day 365.

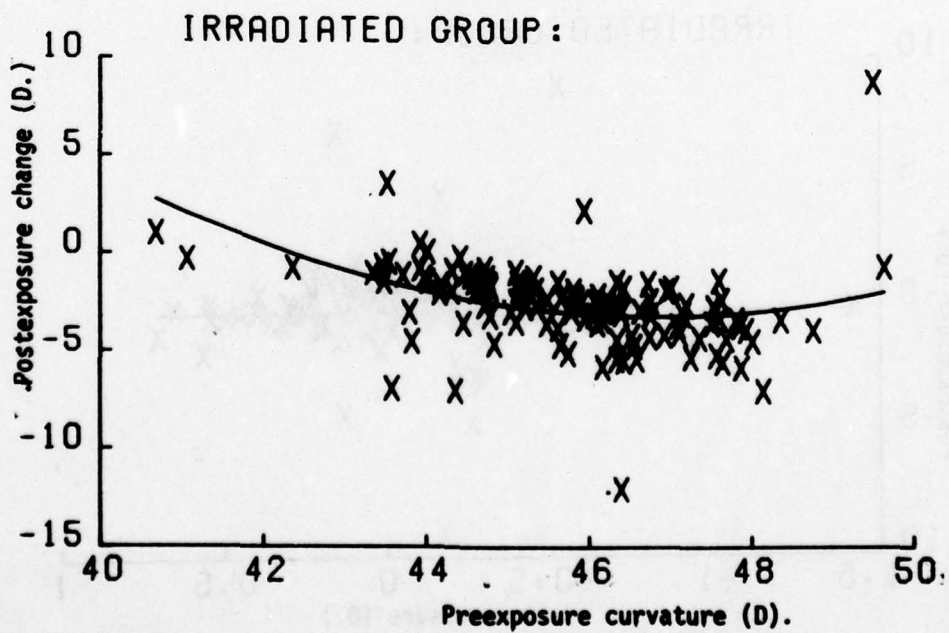


Figure D-42. Horizontal meridian change: Day 365.

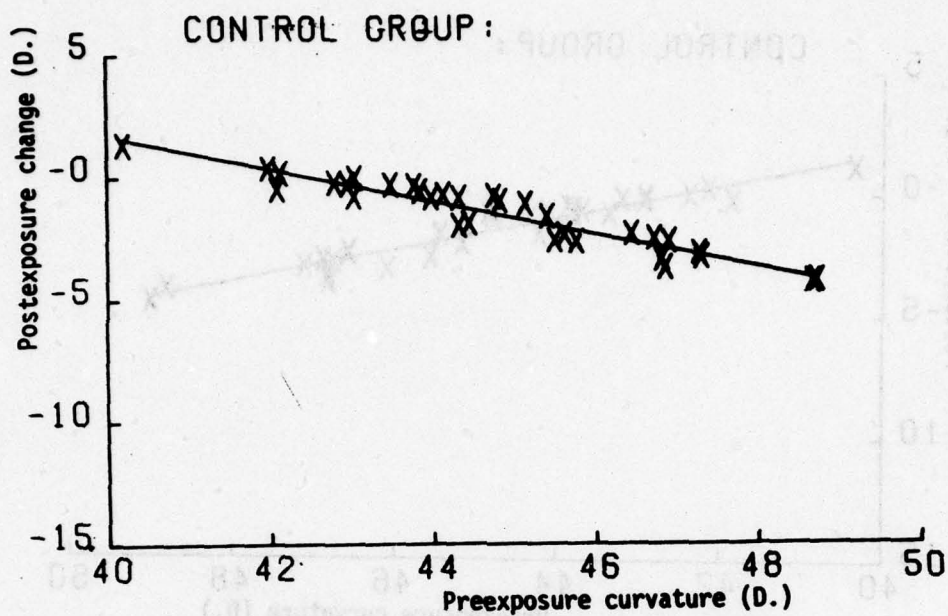


Figure D-43. Vertical meridian change: Day 365.

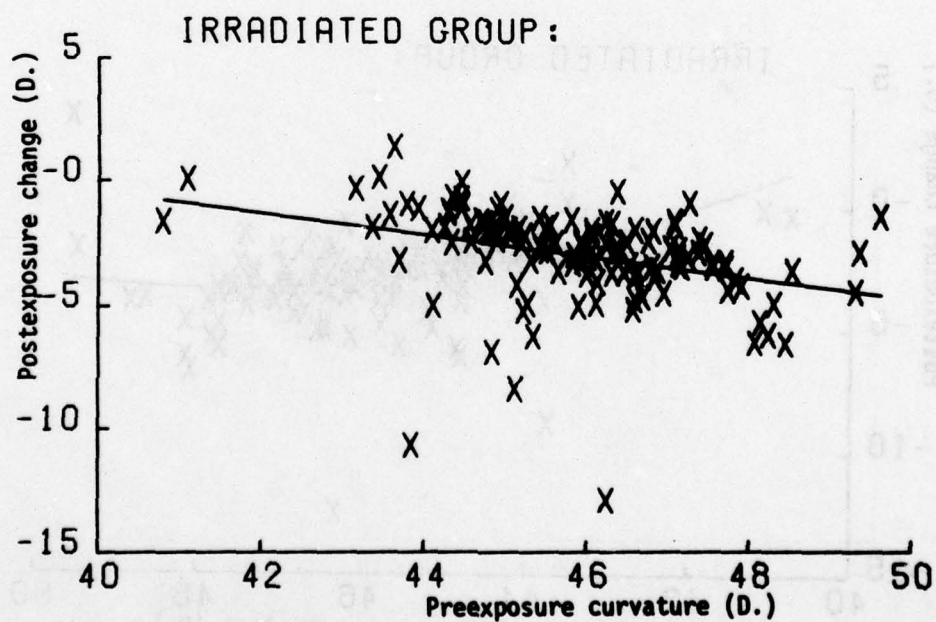


Figure D-44. Vertical meridian change: Day 365.

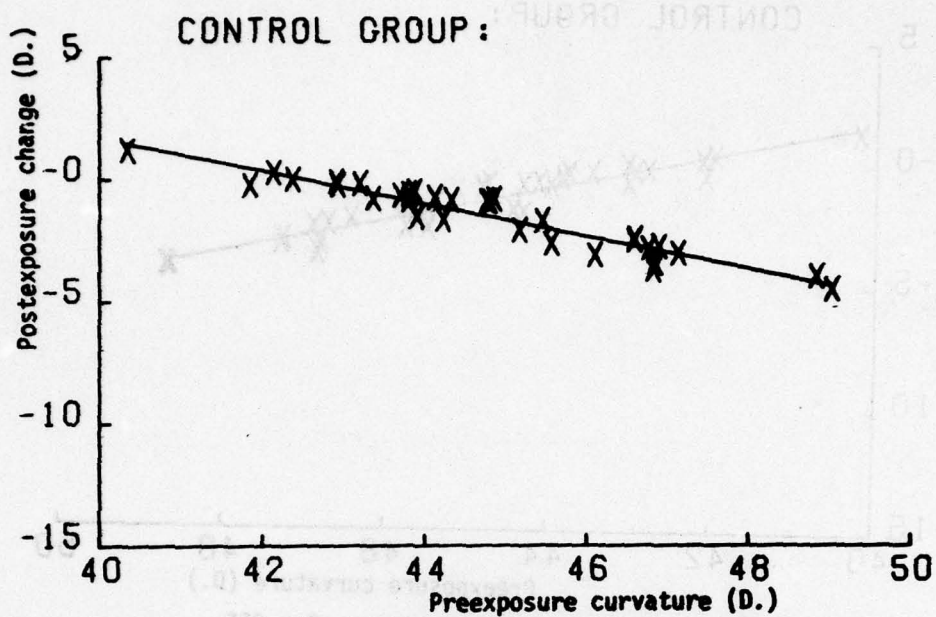


Figure D-45. Spherical equivalent change: Day 365.

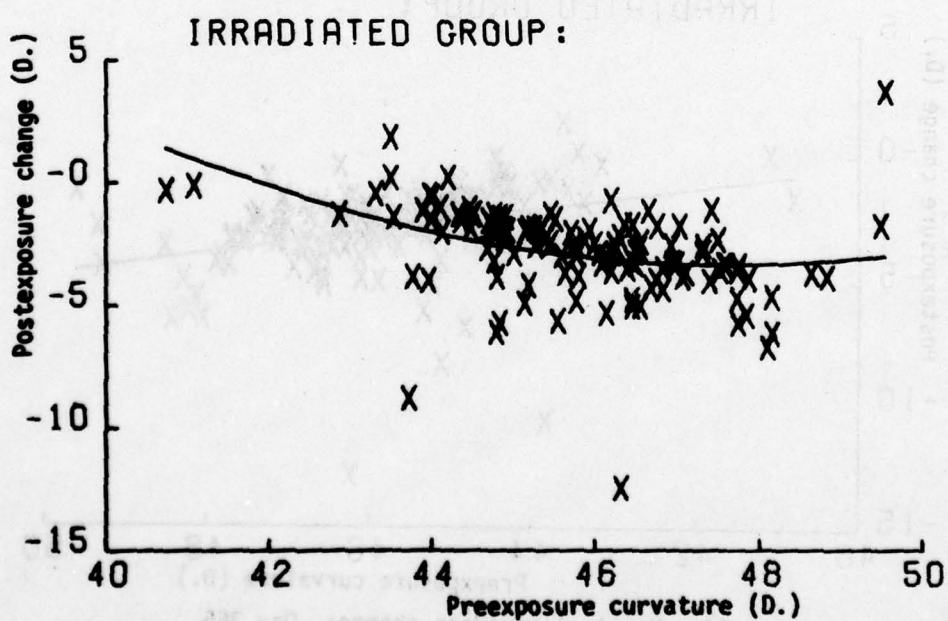


Figure D-46. Spherical equivalent change: Day 365.

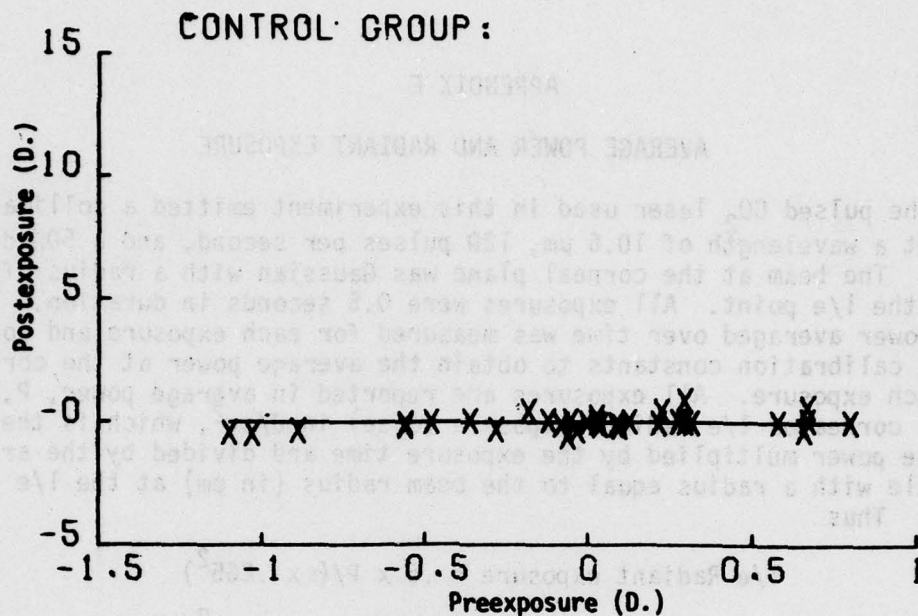


Figure D-47. Toxicity: Day 365.

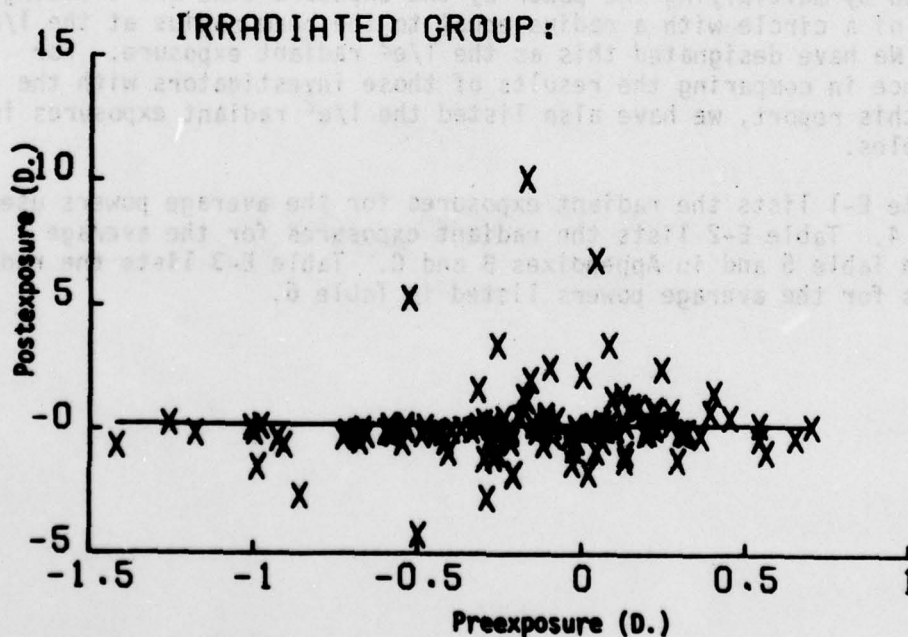


Figure D-48. Toxicity: Day 365.

APPENDIX E

AVERAGE POWER AND RADIANT EXPOSURE

The pulsed CO₂ laser used in this experiment emitted a collimated beam at a wavelength of 10.6 μm , 120 pulses per second, and a 50% duty cycle. The beam at the corneal plane was Gaussian with a radius of 2.65 mm at the 1/e point. All exposures were 0.5 seconds in duration. The beam power averaged over time was measured for each exposure and corrected by the calibration constants to obtain the average power at the cornea for each exposure. All exposures are reported in average power, P, in W at the cornea or 1/e radiant exposure (dose) in J/cm², which is the average power multiplied by the exposure time and divided by the area of a circle with a radius equal to the beam radius (in cm) at the 1/e point. Thus

$$\begin{aligned} 1/e \text{ Radiant exposure} &= .5 \times P / (\pi \times .265^2) \\ &= 2.266 \times P \text{ J/cm}^2 \end{aligned}$$

For convenience the results of this calculation are listed in the following tables for the average powers used in this report.

Some investigators report radiant exposures for a Gaussian beam calculated by multiplying the power by the exposure time and dividing by the area of a circle with a radius equal to the beam radius at the 1/e² point. We have designated this as the 1/e² radiant exposure. For convenience in comparing the results of those investigators with the data in this report, we have also listed the 1/e² radiant exposures in these tables.

Table E-1 lists the radiant exposures for the average powers used in Table 4. Table E-2 lists the radiant exposures for the average powers in Table 5 and in Appendixes B and C. Table E-3 lists the radiant exposures for the average powers listed in Table 6.

TABLE E-1. RADIANT EXPOSURE VALUES FOR THE AVERAGE POWERS IN TABLE 4.

<u>Postexposure time</u>	<u>ED₅₀ W</u>	<u>1/e Radiant exposure J/cm² (95% CL)</u>	<u>1/e² Radiant exposure J/cm² (95% CL)</u>
30 min	2.08	4.71 (4.06 - 5.26)	2.35 (2.02 - 2.63)
Day 1	2.30	5.21 (4.33 - 5.89)	2.60 (2.16 - 2.94)
Day 7	2.77	6.28 (5.15 - 7.19)	3.13 (2.57 - 3.59)
Day 30	4.85	10.99 (9.52 - 12.74)	5.49 (4.75 - 6.36)
Day 90	8.58	19.45 (15.48 - 34.52)	9.71 (7.73 - 17.24)
Day 180	11.06	25.07 (18.54 - 72.57)	12.52 (9.26 - 36.24)
Day 270	11.13	25.23 (18.54 - 77.09)	12.60 (9.26 - 38.49)
Day 365	9.90	22.44 (17.52 - 48.28)	11.20 (8.75 - 24.11)

TABLE E-2. RADIANT EXPOSURE VALUES FOR THE AVERAGE POWERS IN TABLE 5 APPENDIXES B AND C.

<u>Exposure group (W)</u>	<u>1/e Radiant Exposure J/cm²</u>	<u>1/e² Radiant Exposure J/cm²</u>
<2	<4.53	<2.26
2 - 3.99	4.53 - 9.04	2.26 - 4.52
4 - 5.99	9.07 - 13.58	4.53 - 6.78
≥6	≥13.60	≥6.79

TABLE E-3. RADIANT EXPOSURE VALUES FOR THE AVERAGE POWER IN TABLE 6.

<u>ED₅₀ W</u>	<u>1/e Radiant exposure J/cm² (95% CL)</u>	<u>1/e² Radiant exposure J/cm² (95% CL)</u>
3.2	7.25 (4.58 - 9.13)	3.62 (2.29 - 4.56)